University of Pretoria

STABILIZATION OF Cr(VI) FROM FINE FERROCHROME DUST USING EXFOLIATED VERMICULITE

By

Delphin MULANGE WA MULANGE

Dissertation submitted in fulfilment of the requirements for the degree

MASTER OF APPLIED SCIENCES (METALLURGY)

Department of Materials Science and Metallurgical Engineering

FACULTY OF ENGINEERING, BUILT ENVIRONMENT AND INFORMATION TECHNOLOGY, UNIVERSITY OF PRETORIA, SOUTH AFRICA

June 2011

TITLE:	STABILIZATION OF Cr(VI) FROM FINE FERROCHROME DUST USING EXFOLIATED VERMICULITE
STUDENT:	DELPHIN MULANGE WA MULANGE
NUMBER:	27631835
DEGREE:	MASTER OF APPLIED SCIENCES (METALLURGY)
DEPARTMENT:	DEPARTMENT OF MATERIALS SCIENCE AND METALLURGICAL ENGINEERING
FACULTY:	FACULTY OF ENGINEERING, BUILT ENVIRONMENT AND INFORMATION TECHNOLOGY
UNIVERSITY:	UNIVERSITY OF PRETORIA, SOUTH AFRICA
SUPERVISOR:	PROF. ANDRIE M. GARBERS–CRAIG
STUDY YEAR:	2009-2011

AKNOWLEDGEMENTS

First of all, none of this would be possible without the grace of our Almighty God and heavenly Father Jesus Christ.

I would like to express my sincere gratitude to Prof Andrie M. Garbers–Craig for her valuable guidance, suggestions, care and encouragement she has taken to bring this thesis into this form.

I would also like to express my gratitude to professors and personnel of the Department of Materials Science and Metallurgical Engineering, especially Prof. Johan de Villiers for his valuable suggestions and advice in all stages of work.

Special thanks extended to Prof. P.C. Pistorius for giving me the opportunity to begin this work.

I wish to acknowledge the help from Dr. Etienne Balan (Université Paris VI), Dr. John F. Papp (USSG), Sheraz Neffati (ICDA) and all my colleagues and friends who were directly or indirectly involved in successful completion of the work.

Finally I would like to express my heartfelt thanks to my wife, Laetitia Yafu and children Carlse Mulange and Daniella Mulange; my mother, sister, brothers and aunts for their support and encouragement given to complete my masters program.

June 15, 2011

ABSTRACT

It was been reported that untreated wastes from ferrochrome plants release heavy metals including lead, chromium, copper, cadmium, zinc and nickel in the environment. Some of these metals such as hexavalent chromium are potentially toxic and carcinogenic, and can cause a serious threat to human health. The contamination of terrestrial and aquatic ecosystems by hexavalent chromium is worldwide of major environmental concern, especially in South Africa which is the largest producer of chromite and ferrochrome. Therefore, the pre-treatment of these wastes before landfill is of great importance to prevent the contamination of the ecosystems. In the present study, vermiculite, a natural occurring mineral, has been tested for its adsorption effectiveness in removing Cr(VI) from ferrochrome dust leachate. Batch adsorption studies have been carried out to determine the effect of pH, contact time and adsorbent dose on the removal of Cr(VI). The process was found to be highly pH dependent. The optimum conditions for the removal were found to be at pH 1.5, contact time 2 hours and adsorbent dose 10 $g.L^{-1}$. According to kinetic and isotherm studies, the process is best fitted by the pseudo-second order kinetic model, and to both Langmuir and Freundlich isotherms. The maximum adsorption capacity was found to be 23.25 $mg.g^{-1}$. Thermodynamic parameters show the spontaneous and endothermic nature of Cr(VI) adsorption onto vermiculite.

Keywords: Adsorption, Ferrochrome, Chromium (VI), Vermiculite, Isotherms.

TABLE OF CONTENTS

LIST OF FIGURES

LIST OF TABLES

ABBREVIATIONS

AA	Atomic Absorption
AEC	Anionic Exchange Capacity
ASTM	American Society for Testing and Materials
ATSDR	Agency for Toxic Substances and Disease Registry
CEC	Cationic Exchange Capacity
Cr(III)	Trivalent chromium
Cr(VI)	Hexavalent chromium
DG	Directorates General
EU	European Union
FCD	Ferrochrome Dust
HCGFCD	High Carbon Charge Grade Ferrochrome Dust
ICDA	International Chromium Development Association
IETEG	Independent Environmental Technical Evaluation Group
FT-IR	Fourier Transform Infrared
LOI	Loss On Ignition
MSWI	Municipal Solid Waste Incineration
PSD	Particle Size Distributions
SAF	Submerged Arc Furnace
SEM	Scanning Electron Microscopy
SM	Stabilized Matrix
TCLP	Toxicity Characteristic Leaching Procedure
USA	United States of America
USEPA	United States Environmental Protection Agency
USGS	United States Geological Survey
XRD	X-Ray Diffraction

CHAPTER 1: INTRODUCTION

1.1 Background

Chromium is one of the world's most used elements. It is used in the manufacture of many diverse products including alloys, chemicals, and refractories [1,2]. In 2008, world chromite ore production was about 24.0 million metric tons gross weight, of which approximately 94.5% was produced for metallurgical purposes such as the manufacture of ferrous and nonferrous alloys; 2.0% for the chemical industry such as pigments, electroplating, leather tanning, wood preservation (fungicides), corrosion inhibitors in cooling water; 2.8% for the foundry industry; and 0.7% for the refractory industry such as the production of chrome-magnesite bricks [3]. However, ferrochrome and stainless steel production are the most important with an estimated 4,780 and 5,214 thousand metric tons of contained chromium in 2008, respectively [3,4]. There is no substitute for Cr in stainless steel [4,5].

Chromium occurs in various oxidation states, of which trivalent chromium (Cr(III)) is an essential trace element for human health. But some chromium compounds, especially the hexavalent state (Cr(VI)), are acutely toxic, mobile, carcinogenic, and have potential adverse environmental effects [1,2,6]. Leakage, poor storage, and improper disposal practices at manufacturing and ore processing facilities can release hexavalent chromium to the environment causing contamination of soils, surface water and groundwater directly by infiltration of leachate derived from land disposal [1,2]. Cr(VI) can enter the environment by several natural processes, but Cr(VI) contamination by human activities has become a worldwide and regulatory concern [5].

South Africa is the world's largest producer of both chromite and ferrochrome, and accounts respectively for approximately 39 and 42% of global chromite and ferrochrome production [3,4]. The ferrochrome industry plays an important role in the South African economy by not only earning foreign exchange, but also employing about 28,000 people [7]. Dusts arising from ferrochromium and stainless steelmaking plants have been mentioned among the greatest contributors to atmospheric emission of hexavalent chromium and other hazardous materials [5]. Due to its high

solubility in aquatic environments, hexavalent chromium can be absorbed by living organisms, posing a potential threat to the environment and human health [8,9]. Efforts have been made to minimize these emissions into the atmosphere. Therefore, dusts are cooled down in the off-gas duct and gathered by cyclones and bag house filters [8]. Landfill and stockpiling on waste sites are the most commonly used methods of getting rid of these wastes. However, the management of waste products from industrial processes is generally considered problematic due to the potential spillage or leakage of pollutants into the environment.

Worldwide regulatory agencies have listed chromium among the 20th top hazardous substances, and set drastic regulation limits for safe discharge of effluent containing Cr(VI) [5,8]. In order to comply with this limit, it is essential for industries to treat their effluents before landfill. Therefore, several treatment technologies including chemical reduction and precipitation, adsorption, ion exchange, electrokinetics, physical separation, and bioremediation have been explored for removing heavy metals from solution [1,2,5,6,10]. Economic and environmental considerations, availability of remedial materials, and long-term remediation, have also been investigated. However, most of these processes have considerable disadvantages, such as incomplete metal removal, expensive equipment, regular monitoring, reagent and high energy costs or the production of a toxic sludge [11,12].

Adsorption emerges as one of the most versatile, low cost and effective methods for removing heavy metals from aqueous solutions [12]. Several researches demonstrated that some natural materials or wastes products from certain industries have a great potential for adsorbing heavy metals such as chromium, lead, nickel, zinc, copper, and cadmium from their solution, and have been widely used in water treatment for centuries [11,12,14,15,16]. The removal efficiency of these materials is mainly influenced by their crystalline structure and also by their chemical and physical properties.

In this regard, several studies have examined the potential of vermiculite, a 2:1 layered clay mineral, as ion exchanger for hazardous cations [11,17,18]. Since, vermiculite is widely available in South Africa where the largest mines in the world are located, it was decided to examine the potential use of South African vermiculite to stabilize Cr(VI) from fine ferrochrome dust in aqueous solution.

1.2 Objectives of the project

In the present work, Cr(VI) removal from ferrochrome dust in aqueous solution by a batch adsorption method as a function of initial pH of the solution, contact time, temperature, adsorbent concentration and particle size distribution was examined using South African vermiculite. Additionally, isotherms, kinetic and thermodynamic parameters were determined to interpret and elucidate the mechanism of hexavalent chromium adsorption onto South African vermiculite.

1.3 Structure of the thesis

This thesis is subdivided into five main parts:

- Literature review, presented in Chapter 2, provides more background information on chromium contamination and chemistry. It also reports on work done in the field of adsorption of Cr(VI).
- The characterization of ferrochrome dust and exfoliated vermiculite is covered in Chapter 3, which gives a summary of the physical and chemical properties of ferrochrome dust and exfoliated vermiculite. This chapter also provides information on the formation of dust and also on the origin and production of exfoliated vermiculite.
- The mechanism of adsorption, which is described in Chapter 4, presents a consolidated summary and description of the fundamental principles associated with adsorption phenomena. It provides the theoretical framework for the analysis and interpretation of the experimental data.
- The experimental work that was performed is covered in Chapter 5, which deals with a batch adsorption method.
- Results and discussion are covered in Chapter 6, where the experimental data is interpreted through the use of the fundamental principles and theories discussed in Chapter 4.
- Conclusions drawn from the current research and recommendations for future studies are summarized in Chapter 7.

CHAPTER 2: LITERATURE REVIEW

2.1. Overview of chromium in the environment

2.1.1 Occurrence

Chromium is the 21st most abundant element in the earth's crust with an average concentration of 100 ppm. It is one of the world's most strategic and critical materials having a wide range of uses in the metals and chemical industries [5,19]. Chromium occurs in nature in combination with various elements to form minerals such as chromite ($FeCr_2O_4$), chromatite ($CaCrO_4$), eskolaite (Cr_2O_3), crocoite ($PbCrO_4$), etc. However, chromite is the sole commercial source of Cr which is obtained through reduction and electrolysis [5].

2.1.2 Resources and world production

Approximately 95% of the worldwide chromium resources are geographically concentrated in Southern Africa and Kazakhstan, and the remainder is located in China, Russia, Brazil, and selected other countries [4]. Chromium ore is mined in over 20 countries, but 88% of the production are concentrated in seven countries: South Africa accounts for 42% of the world total, 33% of the world total are accounted for by Kazakhstan and India, and the remainder by Russia, Brazil, Turkey, and Zimbabwe. An overview of the world production capacity of chromite ore, ferrochromium, chromium metal, chromium chemicals, and stainless steel in 2008 is given in Table 2–1. World production of chromite ore and ferrochromium in 2008, calculated from Table 2–1, are shown in Figures 2–1 and 2–2, respectively [3,4].

Table 2–1 World production capacity of chromite ore, ferrochromium, chromium metal, chromium chemicals, and stainless steel in 2008 [3,4].

Country	Production capacity (Thousand metric tons of contained Cr)				
	Ore	Ferrochrome	Stainless steel	Chemicals	Metal
Albania	90	21	–	–	–
Argentina	–	–	–	13	–
Australia	80	–	–	–	–
Austria	–	–	11	–	–
Belgium	–	–	259	–	–
Brazil	230	117	105	–	–
China	60	770	1,294	70	6
Cuba	10	–	–	–	–
Finland	174	145	222	–	--
France	–	–	51	–	7
Germany	–	15	293	–	1
India	1,170	421	315	4	–
Iran	74	4	–	2	–
Italy	–	–	311	–	–
Japan	1	8	695	17	1
Kazakhstan	1,110	660	–	37	2
Korea, Republic of	–	–	389	–	–
Madagascar	42	–	–	–	–
Oman	122	–	–	–	–
Pakistan	97	–	–	3	–
Philippines	14	–	–	–	–
Russia	290	360	19	31	16
Slovenia	–	–	15	–	–
South Africa	2,910	1,960	117	23	–
Spain	–	–	214	–	–
Sudan	10	–	–	–	–
Sweden	–	75	116	–	–
Taiwan	–	–	279	–	–
Turkey	210	38	–	17	–
Ukraine	–	–	21	–	–
United Arab Emirates	10	–	–	–	–
United Kingdom	–	–	69	17	7
United States	–	20	418	38	3
Vietnam	58	–	–	–	–
Zimbabwe	240	135	–	–	–
Total	**6,951**	**4,780**	**5,214**	**272**	**43**

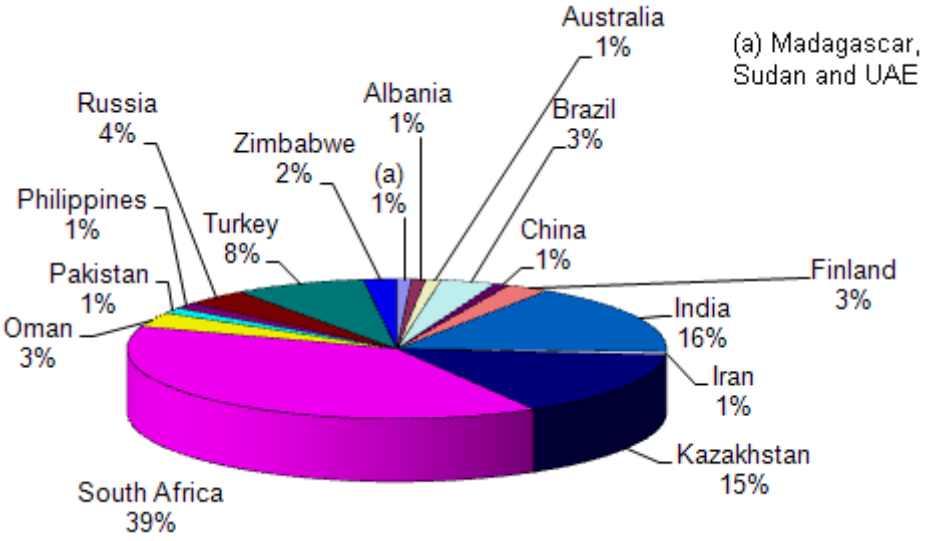

Figure 2–1 World chromite ore production in 2008 [3,4].

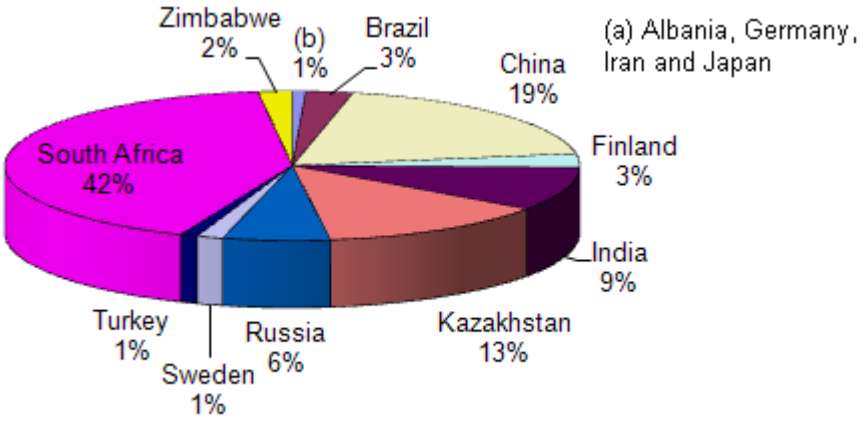

Figure 2–2 World Ferrochromium Production in 2008 [3,4].

2.1.3 Consumption and use of chromium

The primary uses of chromium relate to the production of nonferrous and ferrous alloys in which it enhances metal resistance to impact, corrosion, and oxidation [5]. Of the world's 2008 total production of chromite, approximately 95% of chromite consumption was for metallurgical use where it was smelted into ferrochromium alloys. 2% was used in the chemical industry for pigments in paints, electroplating, plastics and ceramics, leather tanning, wood preservation (fungicides), corrosion inhibitors in cooling water and magnetic tapes. Production of chromite for foundry sands was about 2.8% of word production, and the remainder was for the refractory industry such as the production of chrome-magnesite bricks [3]. Chromite ore production by end use sector in 2008 is shown in Table 2–2.

Table 2–2 Chromite ore production by end use sector in 2008 [3].

End uses	Metric ton	Percentage (%)
Metallurgical	22,684,810	94.5
Chemical	485,577	2.0
Refractory	166,050	0.7
Foundry Sands	666,567	2.8
Total	**24,003,004**	**100**

2.2. Chemistry of chromium

Chromium is a hard, shiny, and bluish-silvery metallic element with an atomic number and molar mass of 24 and 52 g.mol^{-1}, respectively. It has high melting and boiling points of 1907 and 2672 °C, respectively [5]. It is also odourless, tasteless, and malleable; and was discovered by Louis-Nicolas Vauquelin in the mineral crocoites ($PbCrO_4$) in 1797 [5].

Pourbaix or Eh–pH diagrams are important tools to illustrate the leaching behaviour of chromium species in the aquifer environment. Figure 2–3 shows the distribution of Cr(VI) species as a function of pH while Figure 2–4 represents the Eh–pH stability field for chromium species in aqueous systems. Referring to these diagrams, concentration, pressure, pH, temperature, and the absence or presence of other aqueous ions can all affect which chromium species will be stable.

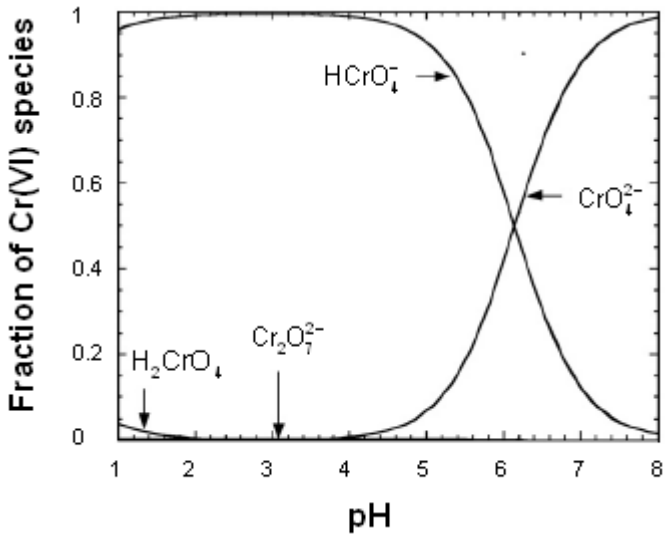

Figure 2–3 Distribution diagram of Cr(VI) species as function of pH [11,21].

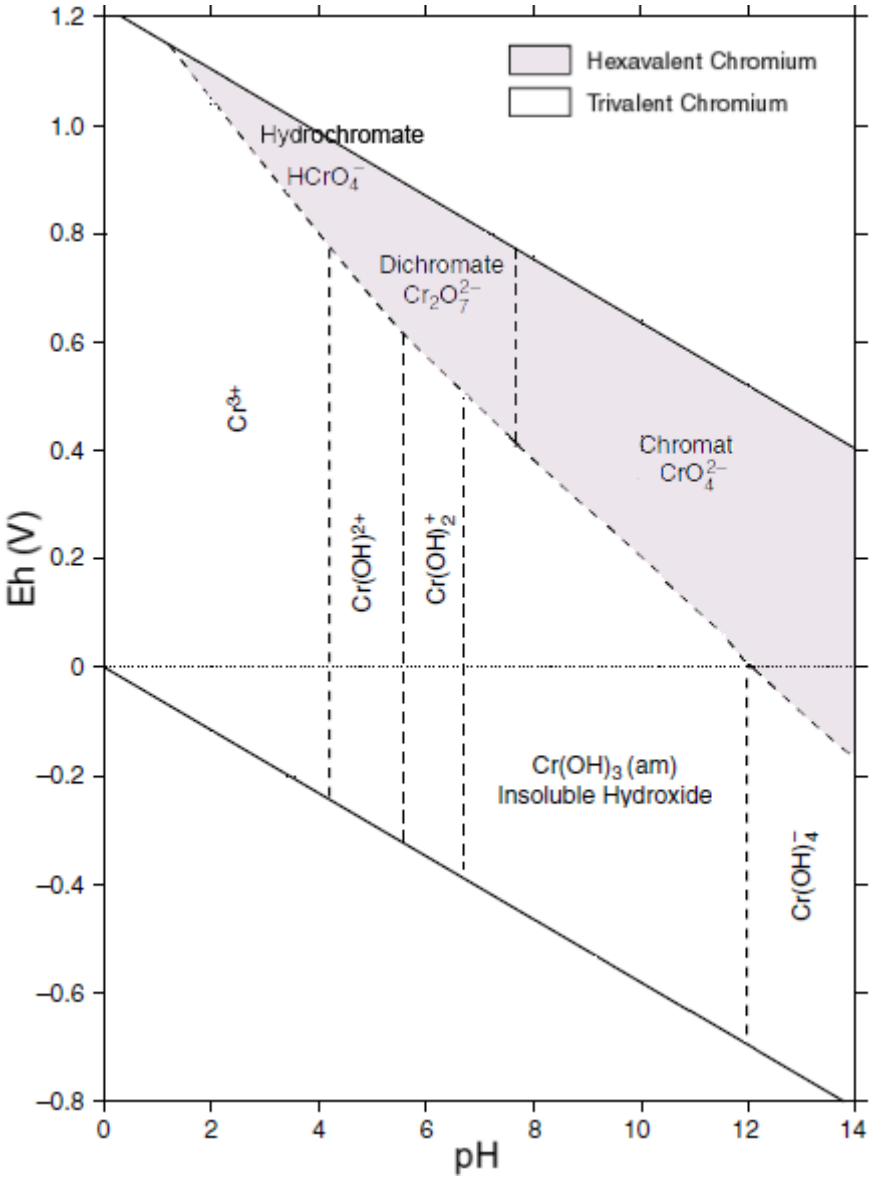

Figure 2–4 Pourbaix diagram for chromium species in aqueous systems [2].

Chromium can exist in a wide range of possible oxidation states, from –2 to +6. Except for the rarely-found, elemental Cr with an oxidation state of zero, the most prevalent and stable forms found in the natural environment are the trivalent (Cr(III)) and hexavalent (Cr(VI)) oxidation states [5]. Oxidation states –2, –1 and +1 occur at specific conditions of concentration and pH in synthetic organic-chromium compounds [5], while the oxidation states +4 and +5 are the intermediate states that influence the rate of reduction of the hexavalent form [2]. The oxidation state of chromium has a significant effect on the transport and fate of chromium [19]. Based on the distribution diagram of Cr(VI) shown in Figure 2–3, the predominant form of hexavalent chromium at acidic pH is $HCrO_4^-$ which is the product of the hydrolysis

reaction of $Cr_2O_7^{2-}$. Increasing pH shifts the concentration of $HCrO_4^-$ to $Cr_2O_7^{2-}$ and CrO_4^{2-} [11,20,21]. According to Calder [20], the leaching behaviour of chromium species by groundwater is related to the pH of the environment and the redox potential of the aqueous solution as shown in Figure 2–4. He also reported that Cr(III) is thermodynamically stable under reducing potentials (low Eh values), and with respect to the pH of the ambient environment, Cr(III) may form cationic, neutral and rarely anionic hydroxy complexes, specifically Cr^{3+}, $Cr(OH)^{2+}$, $Cr(OH)_2^+$, $Cr(OH)_3$, and $Cr(OH)_4^-$. Cr(VI) is stable under oxidizing potentials (high Eh values) and may exist, depending on the pH of the ambient environment, as anions, specifically hydrochromate ($HCrO_4^-$), dichromate ($Cr_2O_7^{2-}$) and chromate (CrO_4^{2-}) [2].

The two chromium oxidation states, Cr(III) and Cr(VI), have very different mobilities in the environment owing to differing solubility and adsorption characteristics. Cr(III) tends to be immobile because it is a cation that is sorbed to the negatively charged soil surfaces in the environment. While Cr(VI), an oxyanion, is poorly sorbed by the negatively charged soil particles due to repulsive electrostatic interactions, hence, it is more mobile in groundwater and can transfer freely in aqueous environments [22]. Cr(VI) sorption in soil is limited to positively charged surface exchange sites, the number of which decrease with increasing pH.

The concerns related to Cr(III) are less stringent since it has a much lower human toxicity rating. Hexavalent chromium is highly toxic, mutagenic, allergenic, carcinogenic, soluble in water, and is likely to be transported over long distances. The effects of hexavalent chromium in human health and in the environment are harmful. Therefore, pretreatment of Cr(VI)-loaded wastes before landfill is of great importance [6].

2.3. Regulation limits

There are extensive rules governing the supply, transport, consigning and disposal of hazardous materials and wastes in most countries. Worldwide regulatory agencies such as USEPA and ATSDR within the USA, and the DG III, V, XI in the EU are responsible for setting regulations to protect health, safety, and the environment. In South Africa, all work-related matters fall under the Department of Water Affairs and Forestry, Department of Environmental Affairs and Tourism, Department of Minerals

and Energy Affairs, and the Department of Labour [5,6]. Guidelines of the regulatory agencies require that the concentration of Cr(VI) in leachates be measured down to regulation limits. The maximum acceptable concentrations of Cr species in leachate from the wastes and the regulation limits of Cr species for different water sources specified by different countries are presented in Tables 2–3 and 2–4, respectively.

Table 2–3 The maximum acceptable concentration of Cr species in leachate from wastes specified by different countries [6].

Country	Leachate	Regulation limits (mg/l)	
		Cr(III)	Cr(VI)
Spain	DIN † leachate	4	0.5
Germany	Leachate	–	0.5
Italy	TCLP leachate	2	0.2
USA	TCLP leachate	5	–
South Africa	ARL (Acceptable Risk Levels)	4.7	0.02

† Deutches Institutes für Normung

Table 2–4 The regulation limites of Cr species for different water sources specified by different countries [6].

Country	Type of water	Regulation limits (mg/l)	
		Cr(VI)	Cr(Tot)
France	General water	0.1	0.5
	Drinking water	0.05	–
Germany	Metal/Chemical industry	0.1	0.5
	Leather Industry	0.05	1
USA	Drinking water	0.015	0.1
UK	Drinking water	–	0.05
South Africa	Effluent discharge	–	0.5
	Drinking water	0.05	0.1

It can be seen from Tables 2–3 and 2–4 that the regulation limits for Cr(VI) are stringent. Hence the remediation of Cr(VI)-contaminated sites is a challenge. The initial stages of such decontamination or clean up can often be accomplished in a relatively short period of time by removing potential contaminant sources, removing highly contaminated shallow soils, and in some cases installing a low permeability cap. In contrast, remediation of the subsurface is often an inexact process that can take many years and may be very expensive [2,8,22]. It is therefore recommended

that the hexavalent chromium content in waste should be removed or stabilized before landfill.

2.4. Sources of chromium contamination

Cr(VI) can enter the environment by several geogenic or natural processes (volcanic activity and weathering of rocks) as well as from human activities such as metal extraction, metal fabrication, leather tanning facilities, electroplating, surface finishing, paints, pigments and manufacture of batteries [2,10].

2.4.1 Geogenic sources

Chromium compounds are found in the environment, most notably in its most concentrated forms as an ore mineral derived from erosion of chromium-containing rocks and can be distributed by volcanic eruptions [19]. Native chromium deposits are rare, and generally found in reducing environments. Naturally occurring Cr(VI) has been reported in several environments, soil, sediments, and groundwater associated with serpentine bedrocks [$Mg_3Si_2O_5(OH)_4$] [5,23,24]. King and Rytuba [25] reported that the occurrence of Cr(VI) in these areas could be explained by the possible geochemical processes that transform Cr(III) to Cr(VI) in the presence of MnO_2 including hydrothermal alteration of the country rock containing chromite and Cr-bearing minerals. In surface water, the predominant form is Cr(III), however, Kaczynski and Kleber [26] reported the presence of Cr(VI) in oxygenated fresh water and estuaries.

2.4.2 Anthropogenic sources

Cr(VI) in the environment has generally been assumed to be anthropogenic (manmade) contamination, since it is used in numerous and varied applications. According to the Independent Environmental Technical Evaluation Group [5], soil, air and groundwater can become contaminated with Cr(VI) by:

- Direct infiltration of leachate from landfill disposal of solid waste, sewage sludge;
- Leachate from mining wastes;
- Seepage from industrial lagoons;
- Spills and leaks from industrial metal processing or wood preserving (H_2CrO_4) and insecticide facilities ($Na_2Cr_2O_7$), and other industrial operations;

- Suspended particles and exhaust emission from metallurgical and chemical manufacturing industries, cement-producing plants, and combustion of natural gas, oil, and coal.

2.4.3 The Chromium cycle in the environment

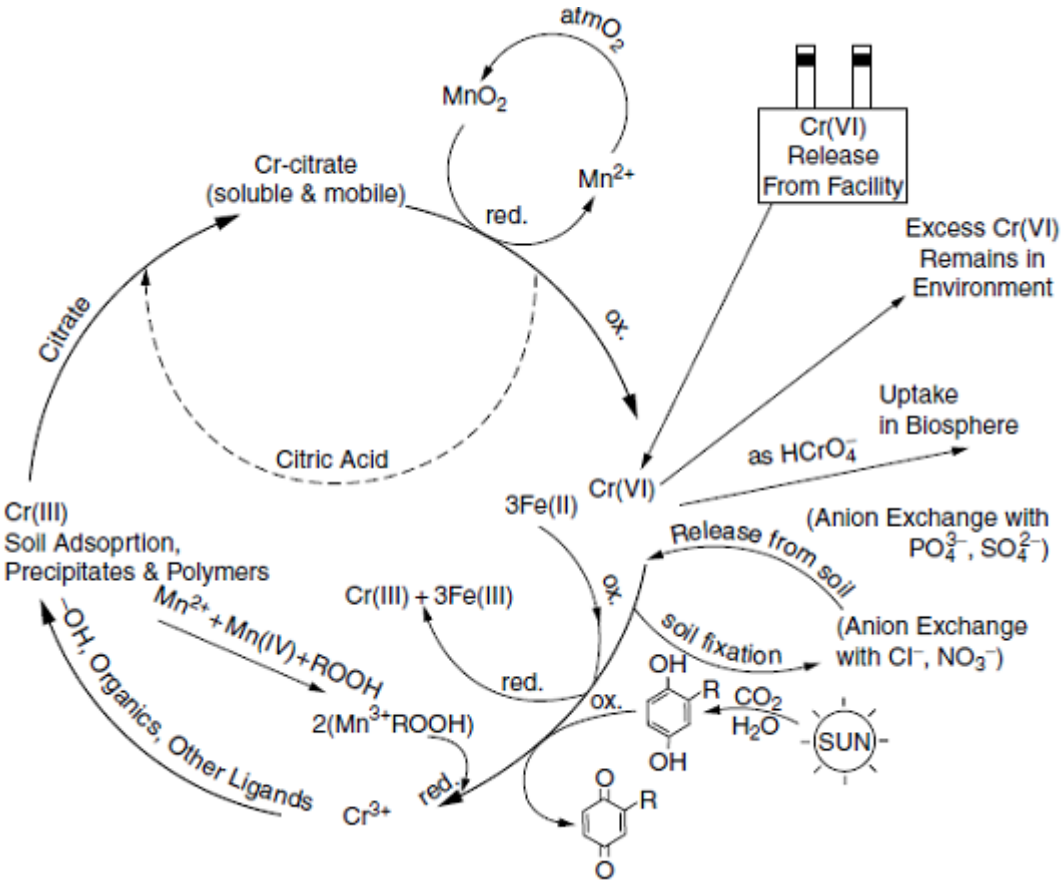

Figure 2–5 The chromium cycle in the environment [23].

The chromium cycle in the environment is illustrated in Figure 2–5 which describes the apparent paradox of simultaneous oxidation and reduction of chromium [5,17,23]. A fraction of hexavalent chromium released from the chromium facility plants remains in the biosphere, while the remaining fraction is subject to adsorption/desorption and oxidation/reduction activity by soil components. Clay minerals are responsible for the adsorption/desorption activity, while Fe(II)/Fe(III) and Mn(II)/Mn(III) are responsible for the oxidation/reduction activity, and soil organic matter (including humic acid and fulvic acid) for reduction only [17,23].

2.5. Effects of chromium on the environment and health

Chromium in its trivalent form is considered essential for good health in moderate intake not only for humans but also for all mammals. Trivalent chromium is essential in glucose metabolism by promoting the action of insulin in the body tissues so that the body can use sugar protein [5,15]. In its hexavalent state, chromium is considered harmful, even in small quantities. Ingestion (eating or drinking contaminated water or food), dermal contact with contaminated soil or liquid (skin penetration), and inhalation of contaminated vapour or particulates are the common exposure routes [5].

Health effects are categorized as mutagenic (capable of inducing mutations and allied effects such as chromosomal aberrations), carcinogenic (causing cancer) and non-carcinogenic which include skin irritation resulting in ulcer formation, asthma, nasal septum ulcers, stomach ulcers, liver damage, pulmonary congestion, dizziness, headache, weakness, and oedema [5]. Exposure to low concentrations of chromium in any form is unlikely to cause significant effects to ecological species. Therefore, the level of chromium in final effluent has to be reduced by the application of appropriate technology. Below is an overview of some low-cost sorbents used in adsorption processes.

2.6. A review of potentially low-cost sorbents for chromium

Several sorbents have been explored for the removal of heavy metals from industrial wastes before landfill. Hence, various organic and inorganic materials, and some biomasses have been tested in the past. These include fly ash, tamarind seeds, sawdust, peat moss, coconut coir pith, chitins, calcined bauxite, activated carbon, clay minerals, riverbed sand, microorganisms, and plants [16,17]. Crucial aspects such as cost effectiveness, environmental impact, availability, and long term remediation must be taken into account before selecting an effective sorbent. However, cost information is seldom reported, and the expense of individual sorbents varies depending on the degree of processing required and local availability. In general, a sorbent can be assumed as “low cost" if it requires little processing, is abundant in nature, or is a by-product or waste material from another industry. Of course improved sorption capacity may compensate for the cost of

additional processing [16]. A summary of some of the alternative sorbent materials is provided in the rest section.

2.6.1 Organic sorbents

a. Chitosan

Babel and Kurniawan [27] observed that chitosan, a polysaccharide derived from chitin (the principal component found in the exoskeletons of crabs, shrimp, etc. and other arthropods and in the cell walls of some fungi) exert sorption capacity for heavy metals due to their large surface area and the presence of amino groups in their crystalline structure. An adsorption capacity of 27.3 mg of Cr(VI) per unit gram of chitosan was achieved at pH 4.0. The use of chitosan is mainly limited by its solubility in acidic solutions, and also its lack of porosity [16].

b. Coconut coir pith

Namasivayam and Sureshkumar [22] reported that coconut coir pith, an agricultural solid waste was used as biosorbent for the removal of chromium(VI) after modification with a cationic surfactant, hexadecyltrimethylammonium bromide. Adsorption capacity of 76.3 $mg.g^{-1}$ was found at pH 2. Reduction of Cr(VI) to Cr(III) occurred to a slight extent during the removal. This technology is very effective both on the basis of cost of the preparation of adsorbent and waste recycling.

c. Fly ash

Rao *et al*. [28] reported that fly ash, a waste product from thermal power plants, has some adsorption capabilities for Cr(VI). An adsorption capacity of 15.58 $mg.g^{-1}$ was observed at pH 6.0–7.0. Cr(VI) loaded-fly ash readily forms cementitious calcium-silicate hydrates, sets and solidifies due to the presence of pozzolanic particles that react with lime in the presence of water. Qian *et al.* [29] also reported the effectiveness of the MSWI fly ash-based Friedel matrices with a small addition of active aluminium. Moreover, leaching tests carried out on the aforementioned fly ash confirm that the stabilization process makes it possible to obtain materials without major risks to the environment.

d. Peat moss

Peat is a complex soil material with organic matter in various stages of decomposition and contains lignin and cellulose as major constituents [16]. These

constituents contain polar functional groups with a high cation exchange capacity that can be involved in chemical bonding with heavy metals. Peat moss has an adsorption capacity of 43 $mg.g^{-1}$ at optimum conditions, pH < 2 and T = 35ºC. Sharma and Forster [30] found that peat becomes unstable and little desorption occurs in low caustic solutions. This is the major drawback of this material.

e. Tamarind seeds

Gupa and Babu [31] recently investigated the removal of Cr(VI) from aqueous solutions by means of waste material such as activated tamarind seeds with concentrated sulfuric acid. They observed that the maximum adsorption of Cr(VI) takes place at low pH ranging between 1 and 3. The major drawbacks of tamarind seeds are time to reach equilibrium, which is found to be considerably long (50 hours), and the higher desorption of Cr(VI) in alkaline environment (high pH). Hence, from a maximum adsorption capacity of 29.7 mg per unit gram of activated tamarind seeds, approximately 95% or 28.2 mg of Cr(VI) is desorbed in alkaline pH range. To tackle this problem, they suggested the precipitation of Cr(VI) from aqueous solution using barium chloride. All water or acid soluble barium compounds are extremely poisonous. At low doses, barium acts as a muscle stimulant, while higher doses affect the nervous system, causing cardiac irregularities, tremors, weakness, anxiety, dyspnea and paralysis. Therefore, the resulting matrix is not safe for disposal.

f. Treated sawdust

Experiments for removal of chromium by treated pine sawdust were carried out by Uysal and Ar [32]. Sawdust has been treated with 1,5-disodium hydrogen phosphate before the adsorption experiments. Important findings were drawn from this process: removal of chromium ion was found to be highly pH-dependent and also depends on the initial Cr(VI) concentration of the solution. Optimum conditions for adsorption were determined as T = 40°C and pH = 2. This finding is in total agreement with Baral *et al.* [33], where the experiments were carried out with sawdust collected from a sawmill and dried in sunlight. Depending on the type of sawdust, the adsorption capacity ranges from 2.7 to 39.7 $mg.g^{-1}$.

2.6.2 Inorganic sorbents

a. Clay minerals

The clay minerals are a part of an important group within the phyllosilicates that contain large percentages of water trapped between the silicate sheets [34]. Most clay minerals are generated by a combination of octahedral and tetrahedral sheets normally classified in two groups of hydrous phyllosilicates that have the inorganic structural arrangement in 1:1 or 2:1 layers. The first layered structure consists of a single tetrahedral coordinated $[Si_2O_5](OH)_2$ layer which is connected to an edge-shared octahedral $M(OH)_6$ sheet, where M is Mg^{2+} and Al^{3+} [12]. The 2:1 layered material contains one octahedral sheet sandwiched by two tetrahedral layers and in both cases the oxygen atoms are responsible to connect the sheets. However, the main inorganic layer can have the cation substituted either in the tetrahedral or octahedral sites for cations of comparable radii. Such substitution causes residual negative charges which are neutralized by the electrostatic adsorption of alkali and alkali earth cations (sodium, calcium and magnesium). Thus, the ions present in the interlayer space of clay minerals can be exchanged by other cationic ions [12,35].

Minerals within the smectite group, one of the clay mineral sub-groups, play an important role in natural and industrial processes as they can take up huge amounts of organic and inorganic molecules at solid–liquid or solid–gas interfaces [36]. The smectite group is composed of several 2:1 layered minerals including saponite, vermiculite and montmorillonite [34,36]. These minerals, especially vermiculite and montmorillonite show a large propensity for adsorbing and immobilizing cationic and anionic species due to their high values of cation exchange capacity (CEC) [36]. The cation and anion exchange capacity (CEC, AEC) of a soil for trace elements is closely associated with the specific surface area of the soil particles [36,37]. Generally, clay minerals exhibit a large surface area due to their lamellar structure [16]. Therefore, optimization of adsorption properties and swelling behaviour has opened prospects of using clay minerals, especially 2:1 phyllosilicates such as smectite, montmorillonite and vermiculite, for pollution control and environmental protection [36].

Kraepiel *et al*. [38] studied the adsorption of heavy metals onto expanding 2:1 layer montmorillonite. They found that heavy metals can be adsorbed by clay minerals via

two pH dependent mechanisms: (1) ion exchange in the interlayers resulting from the interactions between ions and negative permanent charges, and (2) formation of inner-sphere complexes through Si–O^- and Al–O^- groups at the clay particle edges. Similar adsorption mechanisms were also observed by Abollino et *al*. [39] during the adsorption of heavy metals using Na-montmorillonite. Krishna *et al*. [40] demonstrated a maximum uptake of 41.34 mg of Cr(VI) per g of surfactant-modified montmorillonite at pH lower than 3.

Several works have applied vermiculite, a clay mineral formed by the alteration of mica under natural conditions via hydration and weathering, as ion exchanger for hazardous cations [12,17,18]. Vermiculite exhibits high adsorption propensity for heavy metals due to its high CEC and high specific surface area [41]. A study done by Fonseca *et al*. [12] reported that vermiculite demonstrates strong affinity for heavy metals. An investigation done on Cr(VI) leachability from Cr(VI)-loaded vermiculite showed that vermiculite could be used for chromium removal and subsequently disposed of as nonhazardous waste. Many experimental factors can influence exchange processes, such as time of reaction, concentrations of ions, and medium pH. Vermiculite has several advantages such as wide availability in South Africa, low cost adsorbent, expansibility upon hydration, harmlessness to the environment, easy handling [18]. More details on vermiculite and surface charge will be discussed in Chapter 3. The CECs and specific surface for various clay minerals are listed in Table 2–5.

Table 2–5 CEC and specific surface area for various clay minerals.

Clay minerals	**CEC (meq/100g)**	**Specific surface area (m^2/g)**	**Reference**
Chlorite	10 – 40	25 – 0	[17]
Illite	10 – 40	50 – 100	[36]
Kaolinite	3 – 15	7 – 30	[36]
Montmorillonite	70 – 120	10 – 800[†]	[36]
Oxides and Oxhydroxides	3 – 25	25 – 40	[36]
Saponite	80 – 120	20 – 45	[17]
Vermiculite	130 – 210	1 – 800[†]	[36]

[†] Depending on the participation of internal surfaces; lowest value represents the external specific surface area.

b. Activated carbon

Schneider *et al.* [42] investigated the uptake of chromium ions in activated carbon (a highly porous, amorphous solid consisting of microcrystallites with a graphite lattice).

A prior reduction of hexavalent to trivalent form is required, and the uptake is enhanced in the acidic range of pH. Activated carbon has high adsorption capacity for Cr(VI) ranging between 186 and 315 $mg.g^{-1}$. Khezami *et al.* [43] showed that chemical activation using KOH increases the surface area of activated carbon by giving a microporous product. High cost, high combustibility, and lack of long–term stabilization are the main drawbacks of activated carbon.

c. Calcined bauxite

Baral *et al.* [44], found that calcined bauxite is effective in removing Cr(VI) from aqueous solutions having low initial concentration (10 $mg.L^{-1}$). The percentage adsorption increased from 60.7 to 88.7 for an adsorbent dose increasing from 20 to 100 $g.L^{-1}$. They also found that time has very little effect on percentage adsorption and immediate adsorption takes place, which is one of the advantages of using bauxite. The adsorption capacity of 2 $mg.g^{-1}$ was found at optimum conditions (pH 3.8, 46ºC and 10 minutes of contact time).

d. Riverbed sand

On the basis of the investigation done by Sharma *et al.* [45] on the removal of Cr(VI) with riverbed sand, a natural and activated sediment collected from shallow waters near the bank of the river, it was observed that higher removal occurs at low concentration with maximum removal (74.3%) at 10^{-5} M of Cr(VI) concentration. Removal decreased with increasing temperature with maximum removal (74.3%) at 25°C, and higher removal of chromium was obtained in acidic pH ranges. Parameters such as contact time and particle size also have a pronounced effect on removal efficiency.

e. Zeolites

Barros *et al.* [46] reported that Zeolites, natural or synthetic aluminosilicate minerals consisting of a framework of tetrahedral molecules, linked with each other by shared oxygen atoms, show a strong cation-framework interaction with heavy metals. The adsorption properties of zeolites result from their ion-exchange capabilities. The three-dimensional structure of zeolite possesses large channels containing negatively charged sites resulting from Al^{3+} replacement of Si^{4+} in the tetrahedra. Sodium, calcium, potassium and other positively charged exchangeable ions occupy

the channels within the structure, and can be replaced with heavy metals. Zeolites exhibit an adsorption capacity that ranges between 0.4 and 0.7 $mg.g^{-1}$.

2.6.3 Biomass

a. Microorganisms

Microorganisms such as *Thiobacillus sp. Bacteria*, *Cynobacterium, Alcaligenes eutrophus, Pseudomonas aeruginosa* respond to metals by several processes, including transport, biosorption to cell biomass, entrapment in extracellular capsules, precipitation, and oxidation-reduction reactions [16,17]. The sorption capacity of biomass is due to the presence of ionized groups in the cell wall polymers, causing the cell to attract metal cations [16]. Bioremediation is a biological treatment method which involves the adsorption of metals into biomass such as algal or bacterial cells [47]. The major drawbacks of bioremediation are longer time frames required to achieve objectives, cost generated by sites characterization, and long-term monitoring [17].

b. Plants

Some plants including *Chenopodium, Urtica, Polygonum, Thlaspi, Alyssim*, *Mucor rouxii*, etc. have the ability to store large amounts of heavy metals by immobilizing them at the interface of roots and soil [48]. Phytoremediation encompasses a variety of *in situ* strategies involving the use of plants to remove or render environmental pollutants harmless by taking advantage of their ability to take up, accumulate, and degrade inorganic and organic constituents [17,49]. Groundwater contaminated with metals can be treated through the use of deep-rooted trees such as poplars to capture groundwater, uptake the metals, and retard contaminant migration. Phytoremediation technologies are applicable to sites with low to moderate soil contamination over large areas, and to sites with large volumes of groundwater with low levels of contamination that have to be cleaned to low standards [17]. They are most effective if soil contamination is limited to within 3 feet of the surface, and if groundwater is within 10 feet of the surface [48,50]. The major disadvantage of this process is the amount of time that is required to achieve treatment to clean-up levels [17]. This technology may be used as a follow-up technique after areas having high concentration of pollutants have been mitigated, or in conjunction with other remediation technologies [17].

2.6.4 Summary

Prior treatment of industrial wastes before disposal is of paramount importance when dealing with risk and ecological assessment. Economic considerations and availability of remedial materials are of great importance in choosing the most appropriate remediation method. Therefore, adsorption using vermiculite is the most promising and one of the least expensive approaches since this process is inexpensive and vermiculite is widely available in South Africa. The adsorption capacities and average prices of some alternative sorbent materials are listed in Table 2–6.

Table 2–6 Summary of reported adsorption capacities for Cr(VI).

Sorbent material	Adsorption Capacity (mg/g)	Price ($/ton)	Reference
Organic sorbents			
Chitosan	27.3	15 – 20	[27,51]
Coconut coir pith	76.3	130 – 200	[16,51]
Fly ash	4.3 – 15.58	25 – 60	[16,51]
Peat moss	43.0	100 - 200	[16,51]
Sawdust	2.7 – 39.7	110 – 125	[11,33,51]
Tamarind seeds	29.7	350 – 400	[31,51]
Inorganic Sorbents			
Activated carbon	186 – 315	>300	[16,43,51]
Calcined bauxite	2.0	100 – 500	[44,51]
Riverbed sand	0.2	–	[45]
Zeolite	0.4 – 0.7	50 – 200	[5,51]
Soil clays			
Bentonite		30 – 45 †	[52]
Montmorillonite	41.34	40 – 120 †	[27]
Vermiculite		95 – 400 †	[53]
Biosorbents			
Microorganismes	1.5 – 3.1		[50]
Plants	N/A		

† Depends on sized grades

N/A: Not available

CHAPTER 3: THE CHARACTERISTICS OF FERROCHROME DUST AND VERMICULITE

3.1 Introduction

Each material has a unique set of characteristics and properties derived from its origin and processing. Understanding the physical and chemical properties of a material is of paramount importance to explain its behaviour in the environment. Ferrochrome dust contains valuable components (e.g. iron, chromium, zinc and manganese) as well as significant levels of hazardous substances (e.g. hexavalent chromium and lead), which pose a potential threat to the environment and human health [8,9]. Vermiculite has a wide range of applications such as lightweight aggregate for concrete and also for insulative concrete, insulation in steelworks and foundries, additive to fireproof and adsorbent for water treatment [54]. The present chapter gives a summary of the physical and chemical properties of ferrochrome dust and exfoliated vermiculite. It also provides information not only on the formation of dust but also on the origin and production of exfoliated vermiculite.

3.2 Ferrochrome dust

3.2.1 Origin

Dusts arising from ferrochromium production are cooled down in the off-gas duct and gathered by cyclones and bag house filters [8]. The coarse dusts are collected by a cyclone separator, while the fine dusts are gathered in the bag house filters (Figure 3–1). Due to the reducing atmosphere that prevails during ferrochrome production, chromium (VI) cannot from in the furnace. It can therefore be assumed that chromium (VI) is formed at the top of the furnace or in the off-gas duct, where higher oxygen potentials prevail [55–58].

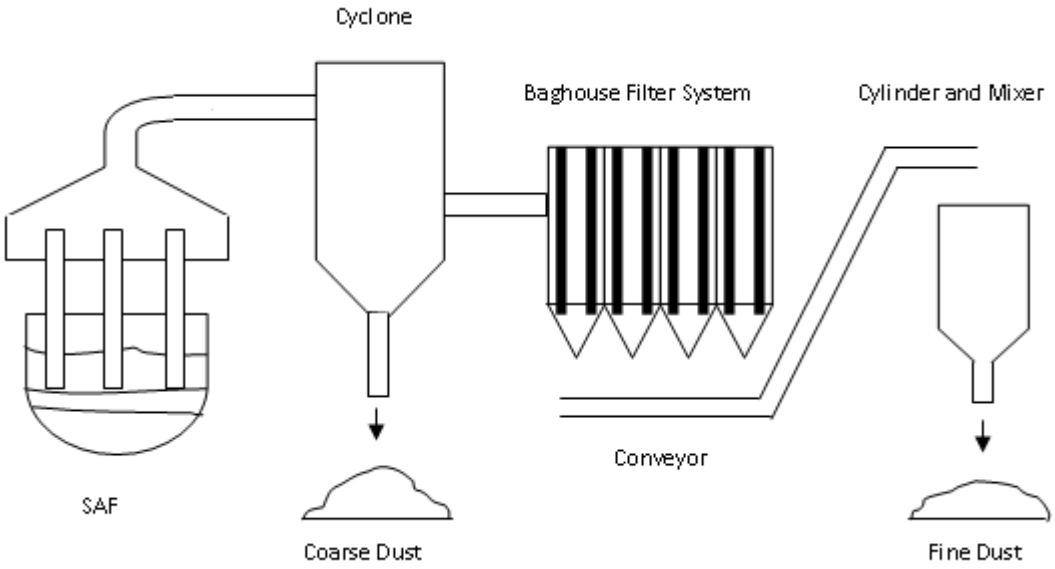

Figure 3–1 Schematic diagram of off-gas treatment systems in ferrochrome plant [8].

3.2.2 Chemical composition and phases

Ferrochrome dusts are fine, light powders and mainly consist of silica, alumina, magnesia, chromium and iron oxides. These dusts also contain some calcium and zinc oxides, sulphur, chlorine and fluorine [7,8]. The $(Mg,Fe,Al,Mn,Cr)_3O_4$ spinel phase, quartz, and forsterite are major phases that are present in ferrochrome dusts. Some fluorite, chromite and carbon particles are also present in ferrochrome dusts [7,8]. The typical elemental composition and crystalline phases present in ferrochrome dusts are presented in Table 3–1, composed from a number of publications.

Table 3–1 Typical elemental composition of ferrochrome dust [8].

Element	Composition range of element (*wt %*)		Phases that contain the element
	Coarse dust	Fine dust	
Cr	13.14-17.11 (0.4)[a]	1.92-7.4 (21)	Chromite ($FeCr_2O_4$), $(Mg,Fe)(Cr,Fe,Al)_2O_4$ spinel
Cr (VI)	0.0005-0.0017	0.035-0.122	–
Si	9.15-13.86	16.45-34.2	Quartz (SiO_2), Cristobalite (SiO_2), Mullite ($3Al_2O_3.2SiO_2$), and fayalite (Fe_2SiO_4)
Al	5.61-13.86	1.06-5.62	$(Ca,Na)(Si,Al)_4O_8$, Alumina (Al_2O_3), and Mullite ($3Al_2O_3{\cdot}2SiO_2$)
Ca	0.71-1.72	0.14-0.57 (65.6)	Lime (CaO), fluorite (CaF_2) and $Ca(OH)_2$
Zn	0.59-0.64 (0.1)	1.37-12.13 (65.3-1109)	Zincite (ZnO), Gordaite ($NaZn_4(SO_4)Cl(OH)_6.6H_2O$), $Zn_4SO_4(OH)_6.5H_2O$ and $ZnCl_2$
Fe	5.37-10.58	0.61-3.01 (1.0)	Iron alpha (Fe), Forsterite ($Mg_2Fe)(SiO_4$), chromite ($FeCr_2O_4$) and $(Mg,Fe,Mn,Cr)_3O_4$ spinel
Mn	0.11-0.18 (0.2)	0.23-0.58 (12-17)	$(Mg,Fe,Mn,Cr)_3O_4$ spinel
Mg	4.14-7.16	1.01-13.92 (434)	Mg_2SiO_4, $CaMg(CO_3)_2$, Enstatite ($Mg_2Si_2O_6$), $MgCr_2O_4$, $(Mg,Fe,Mn,Cr)_3O_4$ spinel and periclase (MgO)
Mo	–	0.008 (12)	–
Pb	0.007-0.009 (0.3)	0.06-0.123 (0.01-0.03)	Lead oxide (PbO), lead chloride ($PbCl_2$) and lead sulphate ($PbSO_4$)
S	0.28-0.76	0.96-3.4	Calsium sulfate ($CaSO_4$)
Cl	0.89	0.95-3.32	Potassium chloride (KCl), sodium chloride (NaCl) and $ZnCl_2$
Na	1.32-1.89	1.71-5.94 (2848-22400)	Sodium chloride (NaCl)
K	0.84-0.91	1.0-7.58 (632-1919)	Potassium chloride (KCl)
Ti	0.31-0.4	0.03-0.12	–
P	0.013-0.044	0.013-0.044	–
C	9.97-15.5	1.1-1.58	Graphite
Cu	0.024	0.008-0.018	–
F	0.01	0.04-0.9	Fluorite (CaF_2)
Ga	0.015	0.026-0.39	–

[a] values in brackets are the elemental concentrations in ppm in the TCLP leachate

[b] The elements such as Cr, Si, Al, Ca, Fe, Mn, Mg, Na, K and Ti can also exist in the glassy slag phase that is present in the dust.

3.2.3 Mechanisms of dust formation

a. The formation mechanisms of dust in EAF

Electric Arc Furnace dust is generated by direct entrainment of the charged materials in the off-gas, by vaporization and melt explosion of volatiles metals such as lead, cadmium and zinc in the melting bath, and by splitting or bursting of gas bubbles (CO and CO_2). The solidification and oxidation reaction of these vaporized metals in the off-gas duct produce EAF dust [55,56].

b. The formation mechanisms of dust in SAF

Ejection of slag and metals droplets from the electrode hole, the entrainment of charge materials, and the vaporization and precipitation of compounds from vaporized species in the off-gas duct contribute to dust formation in Submerged Arc Furnaces [57,59].

c. The formation mechanisms of dust in semi-closed SAF

Semi-closed Submerged Arc Furnaces dust is generated by several mechanisms including the vaporization of elements or compounds from high temperature zones, ejection of slag and metal via the holes of the electrodes, charge materials captured in the off-gas, and phases and reaction products that form in the off-gas from species in the off-gas [8,58].

3.2.4 Treatment options for wastes containing Cr(VI)

To prevent the threat these Cr(VI) containing wastes pose to the environment and nature water resources, several ferrochrome industries have implemented units for the treatment of their wastes. Addition of ferrous ions is the most common treatment option for removing Cr(VI) from aqueous solutions [7]. An example of this technology, the Ecodose system, has been implemented at Xstrata Lydenberg Plant, one of the South African ferrochromium producers, to remove Cr(VI) from the fine dust. The dust is transported from bag houses in a slurry form, resulting in most of the Cr^{6+} being dissolved in water [60]. The process, therefore, focuses on treating the water. The Ecodose system consists of submerging confined metal electrodes (steel plates) in the electrolyte flow (water and $FeCl_2$) through which a current flows. When an electric direct current (DC) is passed through the electrochemical cell, electrons flow from the cathode

through the electrolyte to the anode. The conditions maintained result in Fe^{2+} being released into the water system which then acts as a reductant for the Cr^{6+}. The resultant product is then separated from the electrolyte, and is no longer a pollutant [60,61]. The major drawback of this process is the presence of chloride which is corrosive [7].

3.3 Vermiculite

3.3.1 Occurrence, resources, production and uses

Vermiculite is a naturally occurring sheet silicate mineral, usually formed by hydrothermal alteration of mica mineral [36]. It is a member of the phyllosilicates group of minerals, and contains large percentages of water trapped between the silicate sheets [36]. When heated rapidly at a temperature of 900ºC or higher; flake vermiculite loses its interlayer water, and the flakes expand into concertina-shaped granules called exfoliated vermiculite [53,62]. Vermiculite is found in various parts of the world, but currently the largest mine is located in the Phalaborwa region of North-Eastern Limpopo in South Africa. Other mines are located in China, Brazil, Zimbabwe, and the United States [53]. The world production of vermiculite in 2009 is depicted Figure 3–2.

Exfoliated vermiculite is a lightweight material which is inert, fire resistant, and has a high liquid adsorption capacity. It is used in construction (e.g. fire protection, loft insulation, floor and roof screeds), agriculture (e.g. animal feed and fertilizer), horticulture (e.g. hydroponics and blocking mixes), and industrial markets (e.g. sorbent, fixation of hazardous material, nuclear waste disposal, drilling muds, filtration, furnaces, insulation block and industrial heat insulation) [53,54].

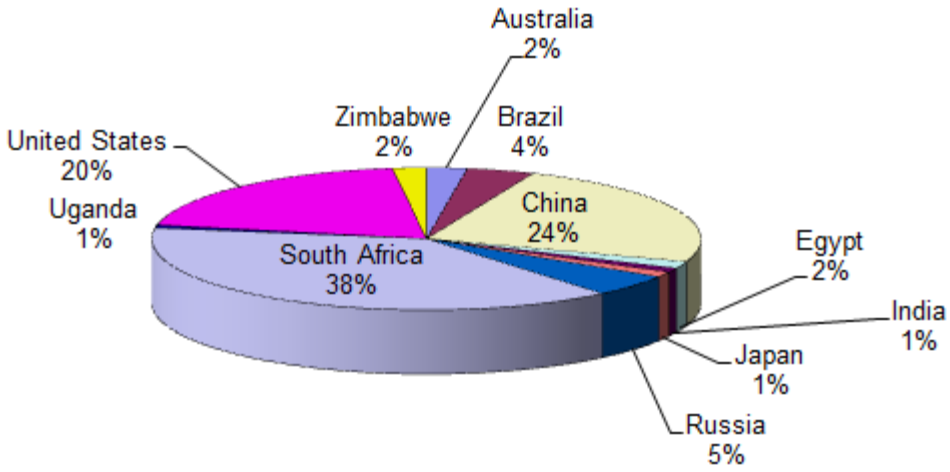

Figure 3–2 Vermiculite world production (Metric tons) in 2009 [53].

3.3.2 Crystal chemistry of vermiculite

Most clay minerals are generated by a combination of octahedral and tetrahedral sheets normally classified in two groups of hydrous phyllosilicates that have the inorganic structural arrangement in 1:1 or 2:1 layers illustrated in Figures 3–3 and 3–4, respectively [36]. The 1:1 layer structure consists of the repetition of one tetrahedral and one octahedral sheet (T:O). The tetrahedrally coordinated $[Si_2O_5](OH)_2$ layer is connected to an edge-shared octahedral $M(OH)_6$ sheet, where M is Mg^{2+}, Al^{3+} [11]. The 2:1 layer structure consists of the repetition of one octahedral sheet sandwiched between two tetrahedral sheets (T:O:T), and in both cases the oxygen atoms are responsible to connect the sheets [12,36].

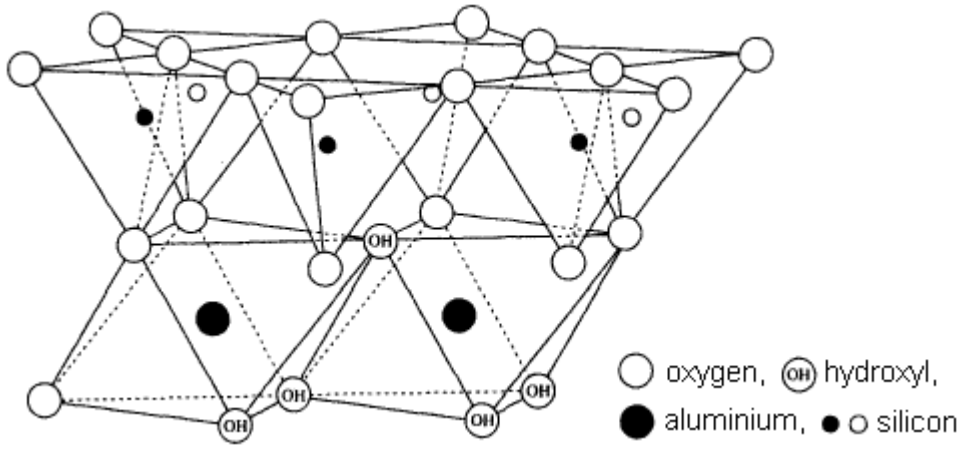

Figure 3–3 T:O or 1:1 or two-layer structure [63].

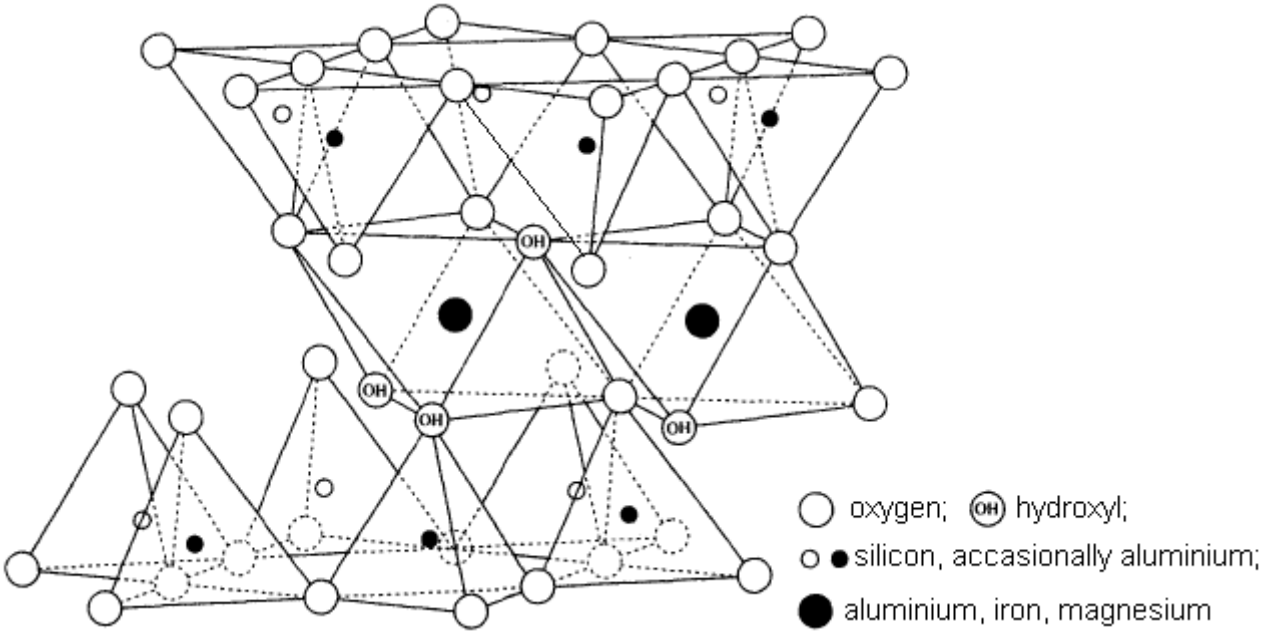

Figure 3–4 T:O:T or 2:1 or three-layer structure [63].

3.3.3 Surface charge of vermiculite

Vermiculite has two types of charges: a permanent layer charge originating from isomorphic substitutions of Al^{3+} or Fe^{3+} for Si^{4+} in the tetrahedral layer and Mg^{2+} or Ca^{2+} for Al^{3+} in the octahedral layer. This charge is balanced by the presence of exchangeable cations (Ca^{2+}, Mg^{2+}, K^{+} and Na^{+}) within the interlayers. The second

charge derived from the fracture of Si–O–Si and Al–O–Al bonds along the crystal edges which are converted into hydroxyl functional groups including silanol (Si–OH) and aluminol (Al–OH) groups. Broken bonds at crystal corners lead to the ionization of surface groups, usually due to exposed O^{2-} and OH^{-}. The resulting charge is related to the pH of the ambient solution [36,63,64]. A sorbent phase with a net negative surface charge exhibits cation exchange capacity (CEC), whereas one with a net positive surface charge has anion exchange capacity (AEC) [63]. Schematically, the structure of vermiculite may be represented as illustrated in Figure 3–5.

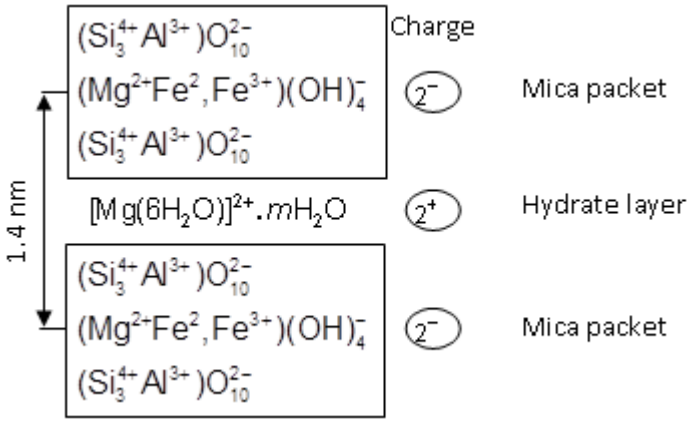

Figure 3–5 Schematic illustration of vermiculite [65].

The general formula of clay vermiculite is given below. The typical chemical composition and physical properties of commercial vermiculite are shown in Tables 3–2 and 3–3, respectively.

The general formula of clay vermiculite is [34]:

$$(Mg, Fe, Al)_3(Al, Si)_4O_{10}(OH)_2 - 4H_2O$$

Vermiculite has the highest cation exchange capacity among the clays due to its divalent interlayer cations [36,54].

Table 3–2 The typical chemical analysis of vermiculite [54].

Element	**Wt %**
SiO_2	38 – 46
Al_2O_3	10 – 16
MgO	16 – 35
CaO	1 – 5
K_2O	1 – 6
Fe_2O_3	6 – 13
H_2O	8 – 16
Other	0.2 – 1.2

Table 3–3 The typical physical properties of exfoliated vermiculite [54].

Color	Light to dark brown
Bulk density	64–160 kg/m^3
Moisture loss at 110°C	4–10%
pH (in water)	6–9
Combustibility	Non–combustible
MOH Hardness	1–2
Sintering temperature	1150–1260°C
Fusion point	1200–1320 °C
CEC	50–150 meq/100g
Specific heat	0.84–1.08 kJ/kgK or 0.20–0.26 kcal/kgK
Waterholding capacity	220–325% by wt or 20–50% by vol

CHAPTER 4: THE MECHANISM OF ADSORPTION

4.1 Introduction

According to Langmuir [63], the influence of chemical equilibrium on the progress of chemical reactions often determines the abundance, distribution, and fate of substances in the environment. Given sufficient time, chemical substances in contact with each other tend to come to chemical equilibrium. Adsorption is the adhesion of ions or molecules to the surface of a solid sorbent with which they are in contact. In more practical terms, “adsorption” relates to the existence of a higher concentration of a particular component on the surface of a solid phase than is present in bulk solution of solids and sediments [66]. Since adsorption is an equilibrium process, the mass of sorbate sorbed to the surface depends on both the concentration of sorbate in the aqueous phase and the affinity of the sorbent for the sorbate [5]. Depending on the type of bonding involved, sorption can be classified as follows [66,67]:

a) Physisorption, also called physical adsorption, is a process in which no exchange of electrons is observed. The adsorbate is held to the surface by relatively weak van der Waals forces and multiple layers may be formed with approximately the same low value of heat of adsorption (5–40 $kJ.mol^{-1}$). Therefore, this type of adsorption is generally reversible and stable only at temperatures below 150°C.

b) Chemisorption, also called chemical adsorption, is characterized by a strong interaction between an adsorbate and a substrate surface, and as a result a chemical bond is formed. The adsorbate is held to the surface by relatively strong van der Waals forces and generally, only a single molecular layer may be adsorbed. Therefore, chemisorption may be irreversible, and is stronger and stable at high temperatures due to coordinate-covalent bonds between adsorbent and adsorbate. Chemisorption is also characterized by a wide range of adsorption enthalpies related to chemical bond strengths (40–800 $kJ.mol^{-1}$).

c) Ion exchange or electrostatic adsorption involves the adsorption of ions through coulombic forces between ions and charged functional groups. Ion exchange is a stoichiometric process with small to negligible enthalpy, often less than 8 kJ.mol^{-1}. Therefore, this type of adsorption is generally weak and reversible.

The sorptive abilities of minerals are proportional to their surface areas and surface-site densities [63]. The nature of liquid-phase ion exchange as well as adsorption onto a sorbent is very complex, and in order to avoid complexity in practical applications, adsorption is usually described through isotherms [18]. These sorption isotherms are very powerful tools for the analysis of exchange processes, as they establish the relationship between the equilibrium pressure or concentration and the amount of sorbate adsorbed by the unit mass of sorbent at a constant temperature [18,68].

4.2 The sorption isotherms

An adsorption isotherm is characterized by certain constant values, which express the surface properties and affinity of the adsorbent and can also be used to compare the adsorptive capacities of the adsorbent for different pollutants [63]. The sorption isotherm may be defined as a plot that describes the amount of solute adsorbed at equilibrium per unit weight of sorbent, measured at constant temperature. Several mathematical models have been developed to quantitatively express the relationship between the extent of sorption and the residual solute concentration. In this study, Freundlich and Langmuir sorption isotherm models were selected to fit the experimental data [11,12,32,63,68].

4.2.1 The Freundlich adsorption isotherm

This model expresses a multilayer sorption with a heterogeneous energetic distribution of active sites, accompanied by interaction between adsorbed molecules [11]. The plot of this model indicates that the highest fraction of the sorbate species is observed at the lowest sorbate concentrations [63]. The general form of this model may be represented as:

$$\frac{x}{m} = K_F C_e^{1/n} = q_t = \frac{(W_i - W_r)}{m} \qquad (1)$$

where x/m is the weight of adsorbate divided by the weight of adsorbent ($mg.g^{-1}$); K_F ($L.g^{-1}$) and 1/n are constants that depend on the temperature and properties of the sorbate and sorbent, and are measures of adsorption capacity of adsorbent and measure of adsorption intensity, respectively; C_e the aqueous concentration ($mg.L^{-1}$); q_t the adsorbed amount of adsorbate per unit mass of the adsorbent ($mg.g^{-1}$) at any time (t); W_i and W_r are the initial added and residual amount remained (mg) of adsorbate in solution, respectively. The linearized form of this model is represented as:

$$\ln q_e = \ln K_F + \frac{1}{n} \ln C_e \qquad (2)$$

where q_e = x/m and n is a constant that depends on the properties of the sorbate and sorbent. According to Lyman *et al*., values of n range from about 0.6 to 3.3, but usually lie between 0.9 and 1.4 [69].

4.2.2 The Langmuir adsorption isotherm

The Langmuir isotherm was applied to estimate the adsorption capacity of adsorbents used and suggests that uptake occurs on a homogeneous surface by monolayer sorption without interaction between adsorbed molecules. Furthermore, the model assumes uniform energies of adsorption onto the adsorbent surface and no transmigration of the adsorbate, in other words, the maximum adsorption occurs when molecules adsorbed on the surface of sorbent form a saturated layer [11,63]. The general form of this model may be represented as:

$$\frac{x}{m} = \frac{q_m K_L C_e}{1 + K_L C_e} \qquad (3)$$

where x/m is the amount of sorbate adsorbed by a unit mass of sorbent at equilibrium ($mg.g^{-1}$ adsorbent), C_e ($mg.L^{-1}$) the concentration of sorbate remaining in the solution at equilibrium, K_L ($L.g^{-1}$) the constant related to adsorption net enthalpy. Constant K_L can be looked upon as a measure of the affinity of the adsorbate for the surface, while q_m ($mg.g^{-1}$) represents the amount of sorbate adsorbed by unit mass of sorbent that is required to cover the sorbent surface completely as a monolayer. Generally the linearized form of this expression is used and represented as:

$$\frac{C_e}{q_e} = \frac{1}{q_m K_L} + \frac{C_e}{q_m} \qquad \text{where} \qquad q_e = \frac{x}{m} \qquad (4)$$

or

$$\frac{1}{q_e} = \frac{1}{q_m} + \left(\frac{1}{q_m K_L} x \frac{1}{C_e} \right) \qquad (5)$$

4.3 Adsorption kinetics and thermodynamics

Adsorption of a dissolved ionic species is always part of an exchange reaction that involves a competing ionic species. The desorbing species creates the vacant site to be occupied by the adsorbing one [63]. According to Harland [70], ion exchange reactions may be defined as the reversible interchange of ions between a solid phase (the ion exchanger) and a solution phase, the ion exchanger being insoluble in the medium in which the exchange is carried out. If an ion exchanger $M^- A^+$, carrying cations A^+ as the exchanger ions, is placed in an aqueous solution phase containing B^+ cations, an ion exchange reaction takes place which may be represented by the following equation:

$$M^- A^+ + B^+ \rightleftharpoons M^- B^+ + A^+ \quad \text{(cation exchange)}$$

Anions can be exchanged:

$$M^+ A^- + B^- \rightleftharpoons M^+ B^- + A^- \quad \text{(anion exchange)}$$

According to Hamadi *et al* [57], the mechanism of batch adsorption can be given as:

$$A + X \xleftrightarrow{k_1} AX \qquad \text{(adsorption)}$$

$$B + X \xleftrightarrow{k_2} BX \qquad \text{(adsorption)}$$

$$AX + BX \longleftrightarrow CX + X \qquad \text{(surface reaction)}$$

$$CX \longleftrightarrow C + X \qquad \text{(desorption)}$$

$$A + B \longleftrightarrow C \qquad \text{(overall reaction)}$$

$$\frac{dC_B}{dt} - \frac{dC_A}{dt} = \frac{C_{A0}dX_A}{dt} = k_1C_A - k_2C_B \quad (6)$$

$$= k_1(C_{A0} - C_{A0}X_A) - k_2(C_{B0} + C_{A0}X_A) \quad (7)$$

where C_A ($mg.L^{-1}$) in this context is the concentration of chromium in solution at any time, C_B ($mg.g^{-1}$) the concentration of chromium on the sorbent, C_{A0} and C_{B0} the initial concentrations of chromium in solution and on sorbent, respectively, X_A the fractional conversion of chromium and k_1 and k_2 the first order reaction rate constants.

At equilibrium,

$$\frac{dC_B}{dt} - \frac{dC_A}{dt} = 0 \quad (8)$$

$$X_{AC} = \frac{(K_C - C_{B0}/C_{A0})}{K_C + 1} \quad (9)$$

$$K_C = \frac{C_{Be}}{C_{Ae}} = \frac{C_{B0} - C_{A0}X_{Ae}}{C_{A0} - C_{A0}X_{Ae}} = \frac{k_1}{k_2} \quad (10)$$

where K_C is the equilibrium constant, C_{Ae} and C_{Be} are the equilibrium concentrations of Cr(VI) in solution and on sorbent, respectively, and X_{Ae} the fractional conversion of chromium at equilibrium.

The adsorption free energy change ($\Delta G°$) can be evaluated as follows:

$$\Delta G° = -RT \ln K_C \quad (11)$$

where T is absolute temperature and R the ideal gas constant: 8.314 $J.mol^{-1}$ K^{-1}.
The Van't Hoff Equation:

$$\ln K_C = \frac{\Delta S^0}{R} - \frac{\Delta H^0}{RT} \quad (12)$$

The adsorption rate constant can be calculated from Lagergren equations which are used for the first and second order reactions kinetics [22,32,71].

For the adsorption process that obeys the first order rate law, the reaction rate constant is given by the following expression:

$$\frac{dq}{dt} = k_1(q_e - q) \qquad (13)$$

this becomes linear after integration for boundary conditions when t = 0 to t > 0 and q = 0 to q > 0 and further simplifications,

$$\ln(q_e - q) = \ln q_e - k_1 t \qquad (14)$$

where q_e and q are the amounts of chromium adsorbed (mg g^{-1}) at equilibrium and at time t (min), respectively, and k_1 is the Lagergren rate constant of first order adsorption (min^{-1}). Values of q_e and k_1 can be calculated from the intercept and slope of the plots of log (q_e – q) versus t.

The second order kinetic model can be represented as follows:

$$\frac{dq}{dt} = k_2(q_e - q)^2 \qquad (15)$$

this becomes linear after integration for boundary conditions when *t* = 0 to *t* > 0 and *q* = 0 to *q* > 0 and further simplifications,

$$\frac{t}{q} = \frac{1}{k_2 q_e^2} + \frac{t}{q_e} \qquad (16)$$

where k_2 is the equilibrium rate constant of second order adsorption ($g.mg^{-1}.min^{-1}$). Values of k_2 and q_e can be calculated from the intercept and slope of the plots of t/q versus t.

Adsorption reactions depend on a number of parameters such as physical and chemical properties of sorbent and sorbate, pH of the solution, temperature, concentration and the particle size distribution [63,70].

4.4 Separation factor

The essential characteristics of the Langmuir isotherm may be expressed in terms of the dimensionless constant separation factor (R_L) or equilibrium parameter [11,13,31,32]. R_L is given by the following equation:

$$R_L = \frac{1}{1 + K_L C_0} \qquad (17)$$

where K_L is the Langmuir constant and C_0 the initial adsorbate concentration ($mg.L^{-1}$). Thus, R_L is a positive number whose magnitude determines the feasibility of the adsorption process. According to the value of R_L, the process is:

- favourable: $0 \leq R_L \leq 1$
- linear adsorption: $R_L = 0$
- irreversible: $R_L = 1$
- unfavourable: $R_L \geq 1$

CHAPTER 5: MATERIALS AND EXPERIMENTAL PROCEDURE

5.1 Introduction

The extent to which clay minerals in general, and vermiculite in particular remove ions from aqueous solutions depends not only on the environmental geochemistry which includes pH, temperature, concentration and pressure, but also on the physical and chemical properties of the adsorbent and adsorbate. This chapter describes the sample preparation, sample characterization and experimental procedure used in the current work.

5.2 Sampling

Selecting a reduced sample mass from the quantity available is one of the most common procedures prior to any analysis [72]. It is therefore of the utmost importance that subsamples be representative with respect to surface area, particle size distribution, and chemical composition. An improper subsampling procedure can lead to results that have significant biases and large imprecisions [72]. Representative subsamples of ferrochrome dust and exfoliated vermiculite were obtained through splitting, in which a revolving splitter was used. This device provides a reliable method for mass reduction with reasonable speed. The lot material is poured into a hopper from where it is led to a revolving feeder which distributes the sample material equally over a number of radial chutes [73].

5.3 Analytical methods

All analyses and experiments were carried out using representative subsamples. For observation and analysis of physical as well as chemical properties, the following analytical instruments were used.

5.3.1 Physical properties

The particle size distributions of the fine ferrochrome dust and exfoliated vermiculite were measured with a Malvern Mastersizer Particle Size Distribution Analyzer (Model 2000 UM) using laser diffraction. The bulk densities as well as the pH of the dust were

determined using ASTM D 5057-90 [74] and ASTM D 4980-89 methods [75], respectively. The water soluble fraction was determined by the standard method of soil water content measurements [76]. The specific surface areas were measured by the N_2 Brunauer-Emmett-Teller (BET) method, in a NOVA 1000e Surface area and Pore Size Analyzer.

A Mettler Toledo FG2 make digital microprocessor based pH meter was used for pH measurements. Three standard buffer solutions at pH 4.0, 7.0 and 10.0 were employed for calibration. The solutions were shaken with a LABCON MSH10 thermostated magnetic shaker.

5.3.2 Chemical composition and microstructure

XRF analyses were performed as follows: The samples were ground to <75µm in a Tungsten Carbide milling vessel, roasted at 1000ºC to determine the Loss On Ignition value and after addition of 1 g sample to 9 g $Li_2B_4O_7$, fused into a glass bead. Major element analysis was executed on the fused bead using a ARL9400XP+ spectrometer. Another aliquot of the sample was pressed in a powder briquette for trace element analyses.

The samples were prepared for XRD analysis using a back loading preparation method. They were analysed with a PANalytical X'Pert Pro powder diffractometer with X'Celerator detector and variable divergence and fixed receiving slits with Fe filtered Co-Kα radiation. The phases were identified using X'Pert Highscore plus software. The relative phase amounts (weight percentage) were estimated using the Rietveld method (Autoquan Program).

The morphological characteristics were evaluated by Scanning Electron Microscope (SEM) using a Jeol JSM-6510 Scanning Microscope equipped with Energy Dispersive X-ray Spectrometry (EDS) to obtain backscatter and secondary electron images.

A Nicolet FT-IR 6700 Spectrometer was used to analyze samples in the band regions of 400-2000 cm^{-1}. The spectra were obtained after dilution and compression of approximately 1 mg of sample into 300 mg of KBr.

5.3.3 Measurement of Cr(VI) concentration in aqueous solutions

The equilibrium concentration of Cr(VI) in the solution was determined by reacting with 1.5-diphenyl carbazide as chromogenic agent, and the absorption was measured in a PerkinElmer Lambda 25 UV-Visible spectrometer at the wavelength of 540 nm. The lowest limit of this method is 0.01 $mg.L^{-1}$ and the best suitable measurement range is 0.5–5.0 $mg.L^{-1}$. Therefore, in order to obtain more reliable measurements, some of the samples were diluted before the measurements, and measured values were multiplied by the dilution factor. The stock solution was diluted to prepare 2 sets of standards ranging from 0.5 to 10.0 $mg.L^{-1}$ of Cr(VI) and 0.02 to 0.50 $mg.L^{-1}$ of Cr(VI) for standard sets 1 and 2, respectively. Two calibration curves with correlation coefficients of 0.993 and 0.995 for standard sets 1 and 2, respectively, were constructed using the measured concentrations.

5.4 Materials and sample preparation

5.4.1 Ferrochrome dust

Product and waste specifications are closely associated with the production of ferrochrome. In South Africa, chromite is generally smelted in Submerged Arc Furnaces, together with carbonaceous reductants (coke, coal and char) and fluxes (silica) to produce High Carbon Charge Grade Ferrochrome, slag, slimes and gases (SO_2, NO_2, CO_2) [77]. The ferrochrome dust used in the present study was collected from the Baghouse Filter System, and was supplied by Xstrata Lydenburg Works plant, Mpumalanga, South Africa.

The ferrochrome dust sample was prepared as follows: 10 kg of received FCD was screened through a 1000 µm sieve, and dried in electric oven at 104 ± 2°C for 24 h. The representative subsample from the dry FCD as described in section 5.2 was kept at room temperature in a closed container until it was used in the experiments.

5.4.2 Vermiculite

Three vermiculite samples mined at Palabora Mining Company, Limpopo, South Africa, and labeled VER 1, VER 2 and VER 3 were selected for the present work. The three samples correspond to an exfoliated commercial grade, and were supplied by

Vesuvius–South Africa (VER 1) and Mandoval Vermiculite (Pty) Ltd–South Africa (VER 2 and VER 3).

To ensure the purity of the adsorbent, the exfoliated vermiculite samples were washed three times with deionised water. After that, the wet vermiculite samples were heated at 900ºC for 1 hour to remove interlayer water. As a result, a porous exfoliated vermiculite was formed. The exfoliated vermiculite samples were ground and screened through a set of sieves to a particle size –1000 µm, and then kept dry under cover. Exfoliated vermiculite of particle size –75 µm was used in the present work, except for the study of the influence of particle size on the removal efficiency.

All experiments were carried out using VER 1. VER 2 and VER 3 were only used in order to investigate the impact of phase composition on Cr(VI) uptake. Vermiculite sample VER 1 was comprehensively characterized (XRF, XRD, PSD and FTIR), while samples VER 2 and VER 3 were only characterized by XRF and XRD. The CEC was determined by the $BaCl_2$ Compulsive Exchange Method developed by Gillian and Sumpter [78].

5.4.3 Reagents

All chemicals used were of analytical reagent grade. Hydrochloric acid solution, Potassium dichromate, 1.5-diphenyl carbazide, caustic soda and other necessary chemicals were purchased from Merck. The stock solution containing 100 $mg.L^{-1}$ of Cr(VI) was prepared by dissolving 0.28 g of AR grade $K_2Cr_2O_7$ in 1000 mL of distilled water. The required standard solutions were obtained by diluting the stock solution. Distilled water was used in all experimental measurements. The pH of the solution was adjusted with 0.1 M HCl and 0.1 M NaOH solutions.

5.5 Experimental methods

The experimental approach was conducted by leaching out all Cr(VI) from the dust according to ASTM D 3987–85 procedure, and subsequently to stabilize it in the leachate by adding the desired amount of exfoliated vermiculite, supplied by Vesuvius SA. Experiments were carried out with two different sets of solutions that contain Cr(VI). In the first set, ASTM D 3987–85 (Reapproved 2004) leachate from FCD was used in

order to investigate the effect of operating parameters on the removal of Cr(VI). In the second set, a pure solution of Cr(VI) at different dilutions was used in order to study the kinetics, isotherms and thermodynamics of Cr(VI) adsorption onto vermiculite. The influence of phase composition on Cr(VI) uptake was carried out by means of isotherms using VER 1, VER 2 and VER 3.

All experiments were carried out in triplicate in order to ensure reproducibility of the test results, and the averages were taken as final values.

5.5.1 Leaching tests of FCD

Ferrochrome dust was characterized for Cr(VI) leachability according to the ASTM D 3987–85 (Reapproved 2004) test method as well as the TCLP Method 1311. Their procedures are given in the next sections.

a. ASTM D 3987–85 (2004)

The ASTM D 3987–85 (Reapproved 2004) was developed by the American Society for Testing and Materials [79]. It was originally adopted in 1985, and revised in 2004. According to this procedure, 70 g of FCD were added to 1400 mL of distilled water and agitated continuously in a central axis extractor at 30 rpm for 18 hours at room temperature (~23ºC). Thereafter, the slurry was filtered through a 0.45 µm Whatman Grade NC 45 (Cellulose Nitrate Membrane) filter paper, and the pH of the filtrate was measured immediately. An aliquot sample was taken from the filtrate for determination of Cr(VI) concentration.

b. TCLP Method 1311

The TCLP method 1311 was developed by the US Environmental Protection Agency to measure the leachability of a waste material and hence the risk it poses to groundwater [80,81]. In order to determine which TCLP solution to use, preliminary evaluation was performed by adding 96.5 mL of distilled water to a 5.0 g aliquot of dry waste in a 500 mL beaker, and stirred vigorously for 5 minutes using a magnetic stirrer. As the pH of the slurry was larger than 5.0, 3.5 mL of 1M HCl was added to the mixture, and stirred briefly. The mixture was heated to 50ºC, and held at this temperature for 10 minutes. Thereafter, the mixture was cooled down to room temperature, and the measured pH

was found to be 4.1. As the pH was smaller than 5, TCLP solution No 1 was used as follows: 2000 mL of TCLP solution No 1 was added to 100 g of FCD, and the mixture was rotated at 30 rpm at room temperature (~23ºC) for 20 hours. The slurry was filtered through a 0.45 µm Whatman Grade NC 45 (Cellulose Nitrate Membrane) filter paper. An aliquot sample was taken from the filtrate and immediately acidified with nitric acid to a pH smaller than 2 prior to determination of Cr(VI) concentration. TCLP Solution No 1 consists of 5.7 mL of glacial acetic acid, 500 mL of distilled water and 64.3 mL of 1N NaOH. This mixture is diluted to a volume of 1000 mL.

5.5.2 Determination of operating parameters

Contact time, pH, adsorbent concentration, temperature and particle size distribution are important controlling parameters that strongly affect the adsorption of Cr(VI) onto vermiculite.

5.5.3 FCD leachate and pure solution of Cr(VI)

a. FCD leachate

FCD leachate was obtained by leaching the dust according to ASTM D 3987–85 (Reapproved 2004) test method described in section 5.5.1.

b. Pure solution of Cr(VI)

Pure solutions at different initial concentrations of Cr(VI) were prepared as described in sub section 5.4.3.

5.5.4 Batch adsorption experiments

a. Step 1

Batch adsorption studies were carried out using a magnetic stirrer by stirring at 1000 rpm, 100 mL of the test solution (FCD leachate) in a 200 mL beaker and the desired amount of adsorbent at different pH and contact times.

All experiments were carried out at 20 ± 2°C using adsorbent with particle size –75 µm, except in the case of temperature and particle size studies.

The operating parameters were studied in the following range:

- pH between 1 and 9;
- adsorbent concentration between 2.5 and 12.5 $mg.L^{-1}$;
- contact time between 10 and 150 minutes;
- temperature between 20 and 80°C;
- particle size: between -75 and 1000 µm.

b. Step 2

Batch experiments were performed in the same way as in the first step, however, pure solutions of Cr(VI) at different dilutions were used instead of the FCD leachate. The kinetic, isotherm and thermodynamic studies of Cr(VI) adsorption onto exfoliated vermiculite were carried out as follows:

- Kinetic experiments were conducted at two levels (10 and 20 $mg.L^{-1}$) of Cr(VI) initial concentrations with 10 $g.L^{-1}$ of adsorbent, 20°C, pH 1.5 and contact time in the range between 10 and 150 minutes;
- The adsorption isotherm study was carried out at 20°C and a pH of 1.5 for 120 minutes with different initial Cr(VI) concentrations ranging from 10 to 100 $mg.L^{-1}$and 10 $g.L^{-1}$ of adsorbent;
- Thermodynamic experiments were performed with 20 $mg.L^{-1}$ of initial Cr(VI) concentrations, 10 $g.L^{-1}$ of adsorbent, pH 1.5 and for 120 minutes of contact time by varying the temperature from 20 to 80°C.

At the end of the adsorption period, the supernatant solution was decanted and the adsorbent was filtered through a 0.45 µm Whatman Grade NC 45 (Cellulose Nitrate Membrane) filter paper. Thereafter, the filtrate was analyzed for remaining Cr(VI) content in using the 1.5–diphenylcarbazide method and a UV–Visible spectrometer.

The amount of Cr(VI) adsorbed at any time per unit mass of the adsorbent (q_t)and the removal efficiency of Cr(VI) were evaluated using equations (18) and (19), respectively.

$$q_t = \left(\frac{C_f - C_e}{W}\right) \times V \qquad (18)$$

$$\text{Removal Efficiency}\,(\%) = \left(\frac{C_i - C_f}{C_i}\right) \times 100 \qquad (19)$$

where q_t is the adsorption capacity at any time in $mg.g^{-1}$, C_i, C_f and C_e are the initial, final and equilibrium concentrations of Cr(VI) in $mg.L^{-1}$, respectively, V is the volume of the solution in mL and W is the amount of adsorbent in g.

5.5.5 Leaching behaviour of Cr(VI) after adsorption

The leaching behaviour of Cr(VI) from the treated FCD and Cr(VI)-loaded vermiculite was investigated by means of the Modified ASTM D 3987–85 (2004) [65] and TCLP Method 1311 leaching tests [80]. More details on Cr(VI) desorption are discussed in Chapter 6, section 6.11.

CHAPTER 6: RESULTS AND DISCUSSION

6.1 Characterization of FCD and exfoliated vermiculite

6.1.1 Physical properties

The particle size distributions of the fine ferrochrome dust and exfoliated vermiculite (VER 1) are shown in Figures 6–1 and 6–2. It can be seen that the particle sizes of the dust and exfoliated vermiculite are approximately 90 % below 285 and 85 µm, respectively. The mean particle diameters (d_{50}) are 79.4 and 37.7 µm for FCD and exfoliated vermiculite, respectively. It can be seen from Figures 6–1 and 6–2 that 10% of FCD and exfoliated vermiculite have particle sizes smaller than 12 and 10 µm, respectively.

The main physical properties of FCD and exfoliated vermiculite that were measured include bulk density, moisture content and pH in distilled water are presented in Table 6–1. The specific surface areas of FCD and exfoliated vermiculite (VER 1) were found to be 3.32 and 7.62 m^2/g, respectively. The low value of specific surface area of exfoliated vermiculite represented the external specific surface area of the –75 µm fraction. The moisture contents of FCD and exfoliated vermiculite were found to be 0.3 and 1.46 wt%, respectively. When leached in distilled water, FCD and exfoliated vermiculite generated basic solutions with pH of 8.5 and 9.3, respectively. According to Ma and Garbers-Craig [8], the basic pH generated by FCD was assumed to derive from the presence of lime in the dust.

Table 6–1 Physical properties of fine ferrochrome dust and exfoliated vermiculite.

Property	**FCD**	**VER 1**
Specific surface area (m^2/g)	3.32 ± 0.12	7.62 ± 0.97
Bulk density (g/cm^3)	2.11 ± 0.01	0.17 ± 0.01
Water soluble fraction (wt%)	0.30 ± 0.00	1.46 ± 0.00
pH (in distilled water)	8.54 ± 0.05	9.31 ± 0.02
CEC (meq/100g)	–	132.38 ± 0.86

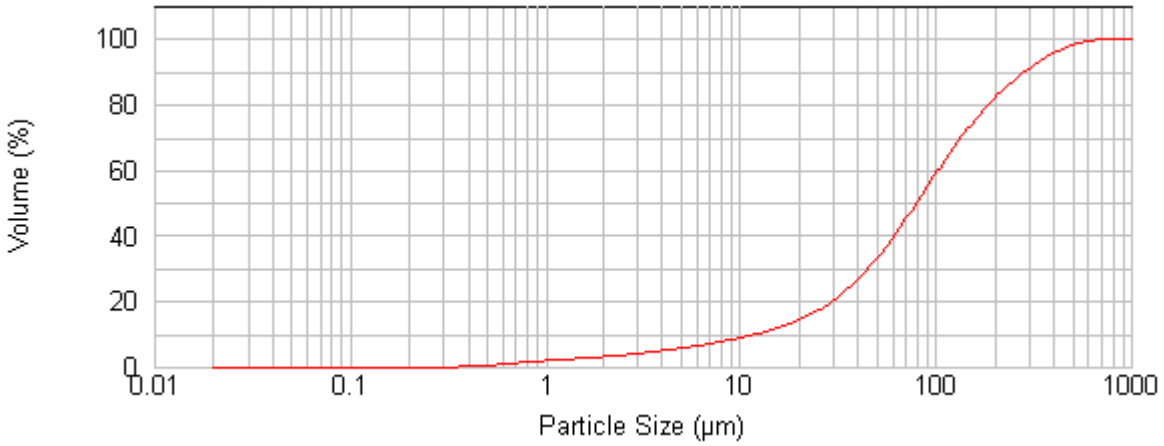

Figure 6–1 The particle size distribution of fine ferrochrome dust.

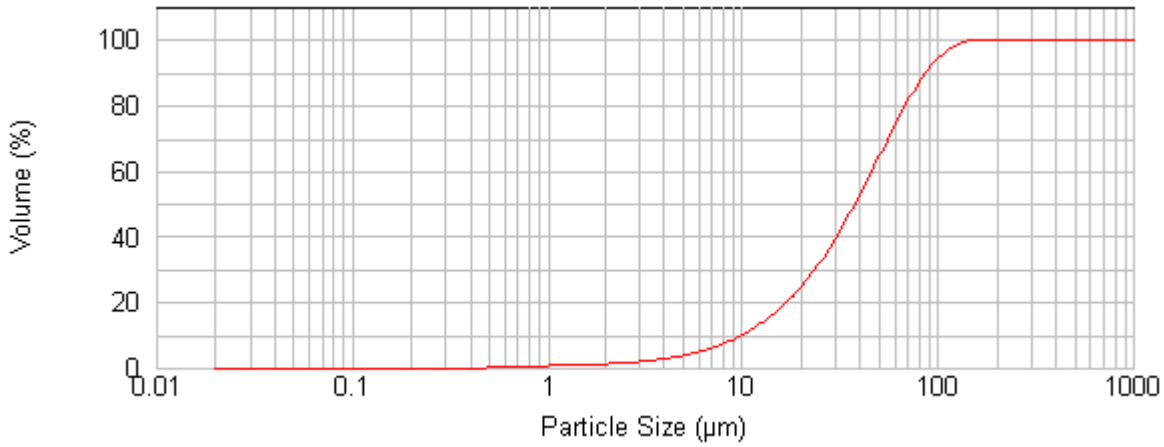

Figure 6–2 The particle size distribution of exfoliated vermiculite (VER 1).

6.1.2 Chemical and phase compositions of FCD and vermiculite

The chemical compositions of the FCD and exfoliated vermiculite in weight percentage of oxides are presented in Table 6–2. The FCD is mainly a SiO_2-Al_2O_3-Cr_2O_3-Fe_2O_3-MgO based material. It also contains a significant amount of CaO and ZnO, and trace amounts of Ni and V. The relatively high amount of Zn found in FCD can be associated with the volatility of this component during the smelting operation. The exfoliated vermiculite has silica as major constituent, but also contains a significant amount of magnesium oxide, iron oxides, and alumina.

Table 6–2 XRF analysis of FCD and exfoliated vermiculite.

Oxides	**FCD**	**VER 1**	**VER 2**	**VER 3**
SiO_2	19.58	40.94	39.90	39.30
Al_2O_3	11.52	9.78	8.45	8.00
Fe_2O_3	15.30	8.79	8.55	7.78
TiO_2	0.44	1.10	0.99	0.93
MgO	8.93	23.56	24.70	23.90
CaO	2.35	3.89	3.72	4.10
Na_2O	0.01	0.01	0.07	0.05
K_2O	1.00	4.83	5.12	4.70
MnO	0.26	0.07	0.06	0.06
P_2O_5	0.04	1.35	0.65	0.64
Cr_2O_3	20.40	0.04	0.04	0.03
NiO	0.10	0.02	0.03	0.02
V_2O_5	0.16	0.03	0.01	0.01
ZnO	3.95	0.01	0.01	0.01
Ba	0.01	0.05	0.05	0.05
LOI	14.29	5.19	7.97	10.20
Total	98.34	99.66	100.32	99.78

X-ray diffraction patterns shown in Figures 6–3 and II–1 (Appendix II) indicate that FCD has spinel ($MgAl_2O_4$), diopside ($CaMgSi_2O_6$), quartz (SiO_2), magnesiochromite ($MgCr_2O_4$) and forsterite (Mg_2SiO_4) as major phases. It also contains chromite ($FeCr_2O_4$), alpha iron (Fe), graphite (C) and cristobalite (SiO_2) particles. The XRD patterns of exfoliated vermiculite (VER 1) before and after adsorption are illustrated in Figures 6–4, II–2 and II–3 (Appendix II). The XRD patterns of the both samples before and after adsorption exhibit an alternation of the phases vermiculite $(Mg,Fe,Al)_3(Al,Si)_4O_{10}(OH)_2•4H_2O$, biotite $K(Fe,Mg)_3AlSi_3O_{10}(F,OH)_2$ and hydrobiotite $K(Mg,Fe)_3(Al,Fe)Si_3O_{10}(OH,F)_2]•[(Mg,Fe^{++},Al)_3(Si,Al)_4O_{10}(OH)_2•4(H_2O)$. The latter is an interstratification between vermiculite and biotite layers. The XRD patterns can be interpreted as follows: The material before adsorption contains more vermiculite, less intermediate phase (hydrobiotite) and possibly the same amount of biotite compared to the sample after adsorption. The decrease in vermiculite phase observed in Cr(VI)-loaded vermiculite may be explained by the major role of vermiculite in the adsorption process. No peak shifts are observed when the XRD patterns before and after

adsorption are compared. It can also be seen from the XRD patterns in Figures II–4 (Appendix II) that the crystalline peak at 2θ=7.2º corresponding to vermiculite decreases in intensity with milling time. After 5 and 10 minutes of grinding time, the resulted XRD patterns show only a halo around 2θ=7.2º. This is due to progressive amorphization and agglomeration of vermiculite particles which takes place with increasing of grinding time [82].

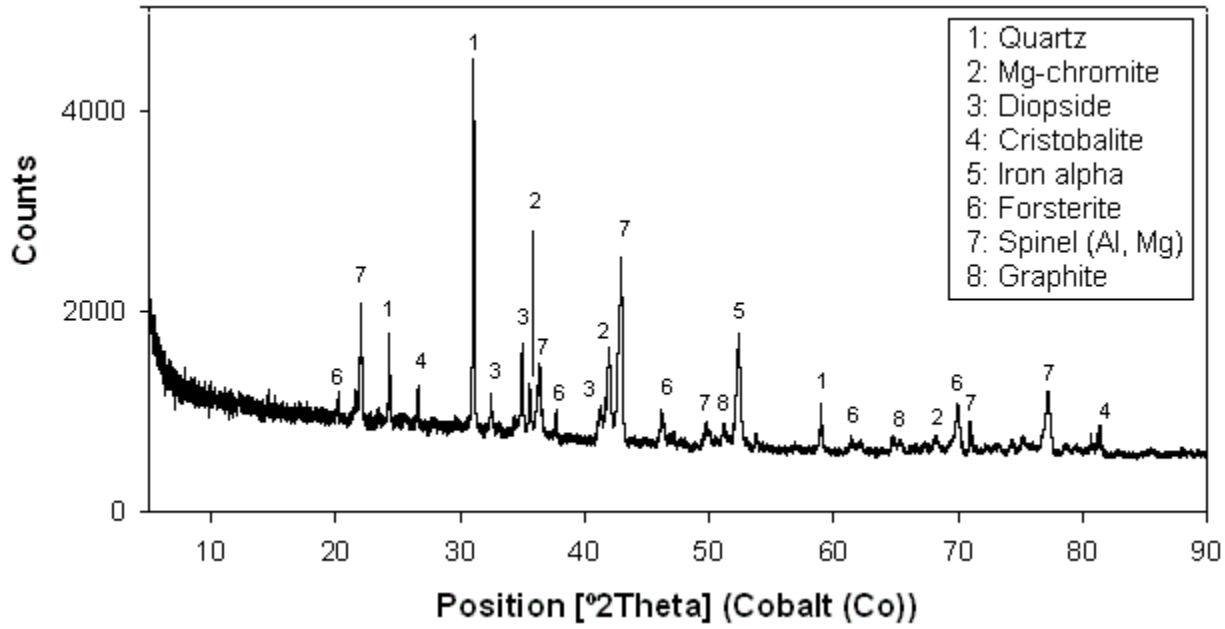

Figure 6–3 XRD pattern of the FCD.

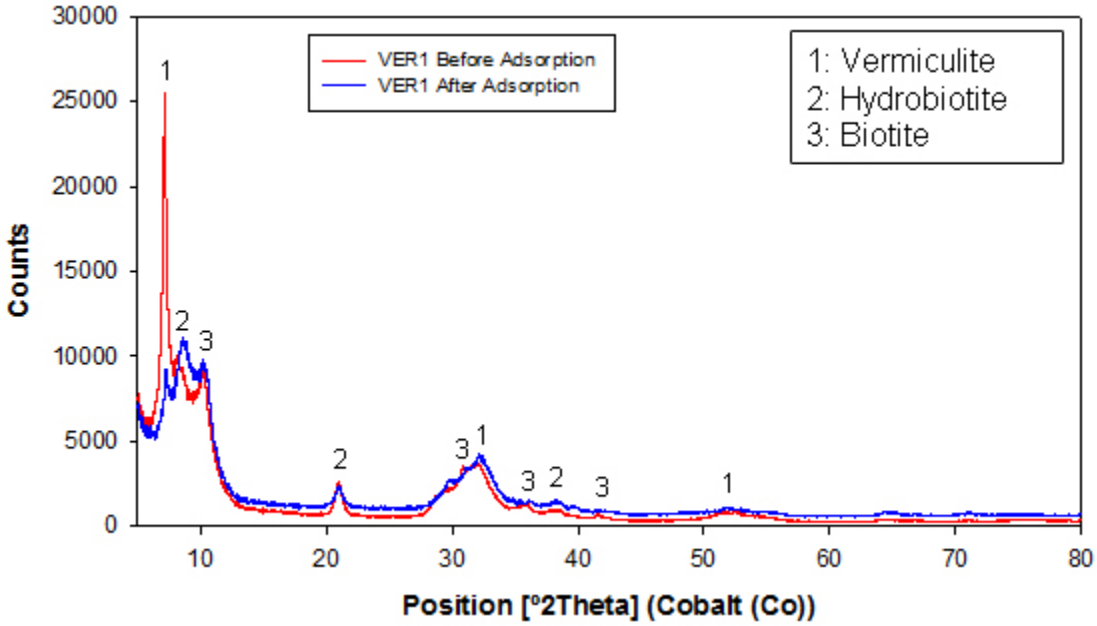

Figure 6–4 XRD pattern of vermiculite (VER 1).

The detailed XRD patterns illustrated in Appendix II (Figure II–2, Figure II–5 and Figure II–6) can be interpreted as follows: VER 1 and VER 2 contain more vermiculite, and less intermediate phase (hydrobiotite) compared to VER 3. VER 1 contains more biotite than VER 2 and VER 3. It can be concluded that VER 2 is more pure than VER 1 and VER 3. The latter is mainly composed of hydrobiotite. The significance of hydrobiotite in VER 3 is also confirmed by the high value of the Loss On Ignition value. The intermediate phase (hydrobiotite) as well as the vermiculite in VER 3 is presumably more crystalline than those of VER 1 and VER 2 (reflected by sharper peaks). The biotite of VER 2 seems more crystalline than the biotite in VER 1.

6.1.3 Microstructure of FCD and exfoliated vermiculite

The microstructure of the fine FCD and exfoliated vermiculite before and after adsorption are illustrated in Figures 6–5 and 6–6, respectively. FCD mainly consists of 1.8 of char particles, 38.8% of $(Mg,Fe,Al,Cr)_3O_4$ spinel phase (shiny bulky particles), 2.3% of iron, 4.9% of chromite ore, and the remainder is a glassy phase composed of approximately 68.2% of SiO_2, 10.3% of CaO and 21.5% of MgO. EDS analysis of the FCD indicate the presence of Si, Cr, Fe, Al and Mg in almost all the phases identified. Figures 6–6 (a) and (b) show that vermiculite before and after adsorption has an irregular and porous surface, which indicates high surface area. Vermiculite mainly consists of Si, Mg, Al and Fe, and also contains significant levels of Ca and K.

Fourier Transform Infrared (FT-IR) spectra of the adsorbent prior to and after adsorption are illustrated in Figure 6–7. In the adsorbent before adsorption, the broad band observed at 3494.9 cm^{-1} may be assigned to O–H stretching vibration of the hydroxyl groups including Si–OH and Al–OH. The peak at 1631.5 cm^{-1} is attributed to bending vibration of water molecules. The broad band observed at 1002.3 cm^{-1} is assigned to stretching vibration of the Si–O–Si group. The peaks observed at 678.8 cm^{-1} and 443.6 cm^{-1} are due to the deforming and bending modes of the Si–O bonds of the tetrahedral sheet, respectively. After adsorption, the peaks observed at 3494.9 and 1631.5 cm^{-1} shifted slightly to 3385.5 and 1635.4 cm^{-1}, respectively. These changes observed in

vibration frequency in the functional groups were attributed to Cr(VI) adsorption onto vermiculite.

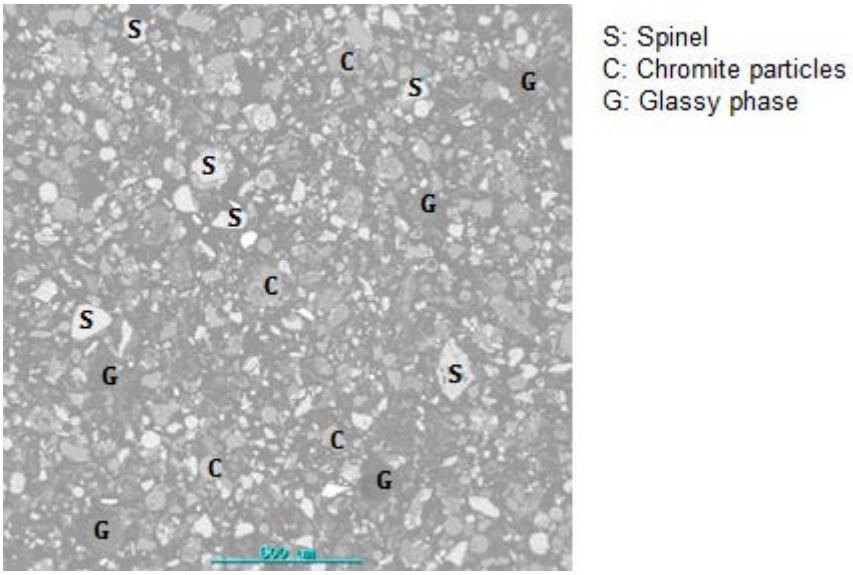

Figure 6–5 SEM micrograph of FCD.

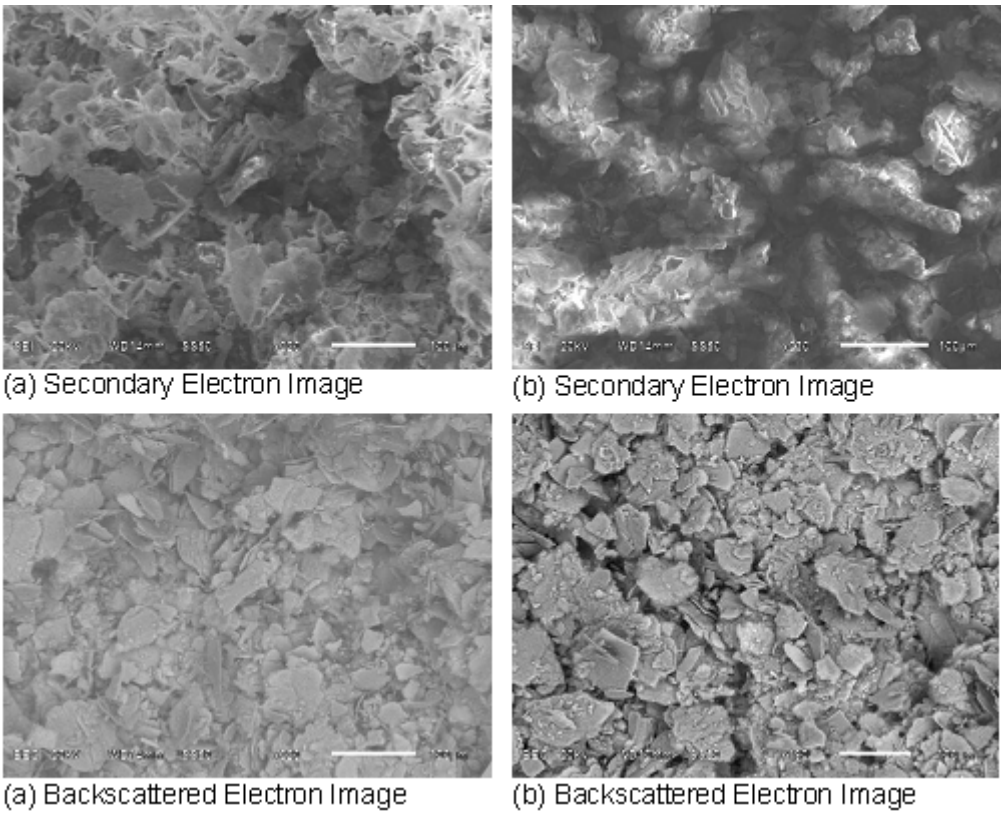

Figure 6–6 SEM micrographs of exfoliated vermiculite before (a) and after (b) adsorption.

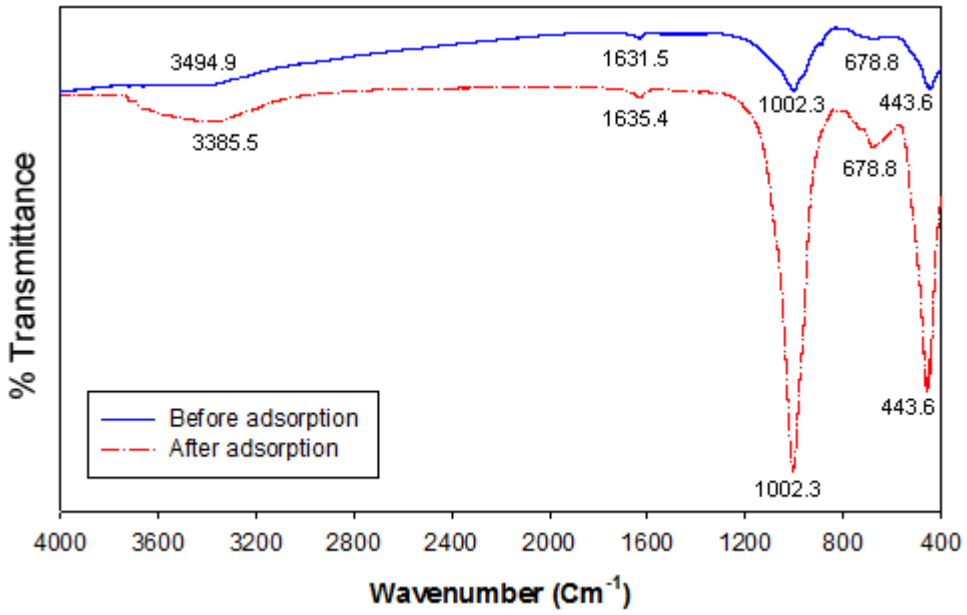

Figure 6–7 FT-IR spectra of exfoliated vermiculite before and after adsorption.

6.2 Leaching tests of FCD

The results of the ASTM and TCLP leaching tests on the FCD along with the statistical analysis of the generated pH and Cr(VI) measured concentration are presented in Table 6–3. It can be seen that the ASTM test generates an average basic pH of 9.07 while the TCLP test generates a slightly acidic pH of 4.43. Standard deviations of 0.23% and 3.29% were observed for the measurement of the pH for the ASTM and TCLP tests, respectively. For the measurement of Cr(VI) concentrations in the leachate, average values of 0.75 and 0.81 $mg.L^{-1}$ were obtained for the ASTM and TCLP tests, respectively. These values exceed the regulation limit applied in South Africa which is fixed at 0.02 $mg.L^{-1}$ of Cr (VI) in leachate from wastes. Standard deviations of 4.51% and 1.32% were found for the measurement of Cr(VI) concentrations using respectively the ASTM and TCLP tests.

Table 6–3 Leachability of Cr(VI) from FCD.

Method	FCD	Generated pH				Cr(VI) concentration (mg/l)			
		pH	Mean	Stdev	RSD (%)	Conc.	Mean	Stdev	RSD† (%)
ASTM	Replicate 1	9.05	9.07	0.02	0.23	0.74	0.75	0.03	4.51
	Replicate 2	9.06				0.78			
	Replicate 3	9.09				0.72			
TCLP	Replicate 1	4.57	4.43	0.15	3.29	0.80	0.81	0.01	1.32
	Replicate 2	4.45				0.81			
	Replicate 3	4.28				0.82			

† RSD: Relative Standard Deviation.

6.3 Effect of pH

The pH of an aqueous solution strongly affects the adsorption/desorption of heavy metals onto clay minerals [5,12]. Cr(VI) adsorption onto vermiculite was found to be pH-dependent with the most significant variations occurring in the range of pH 1.0 and pH 2.0 as shown in Figure 6–9. It can be seen from Figure 6–9 that the adsorption of Cr(VI) is high at lower pH, with a maximum removal efficiency of 98.4 % at pH between 1.0 and 2.0, which drastically decreases off with increasing pH. This is explained by the fact that in aqueous solution, the distribution of Cr(VI) species mainly depends on solution pH and Cr(VI) concentration as shown in Figure 6–8. The distribution diagram depicted in Figure 6–8 is based on the equilibrium constants shown below [11,21,83]:

$$H_2CrO_4 \overset{\log K = 0.382}{\leftrightarrow} HCrO_4^- \overset{\log K = -6.145}{\leftrightarrow} CrO_4^{2-}$$
$$HCrO_4^- \updownarrow \log K = 1.706 \; Cr_2O_7^{2-}$$

It can be observed from Figure 6–8 that: (1) in acidic pH, the predominant form of Cr(VI) is hydrochromate ($HCrO_4^-$) which is the product of the hydrolysis reaction of the dichromate ($Cr_2O_7^{2-}$) and chromate (CrO_4^{2-}). (2) in basic pH, the predominant forms of Cr(VI) are $Cr_2O_7^{2-}$ and CrO_4^{2-}.

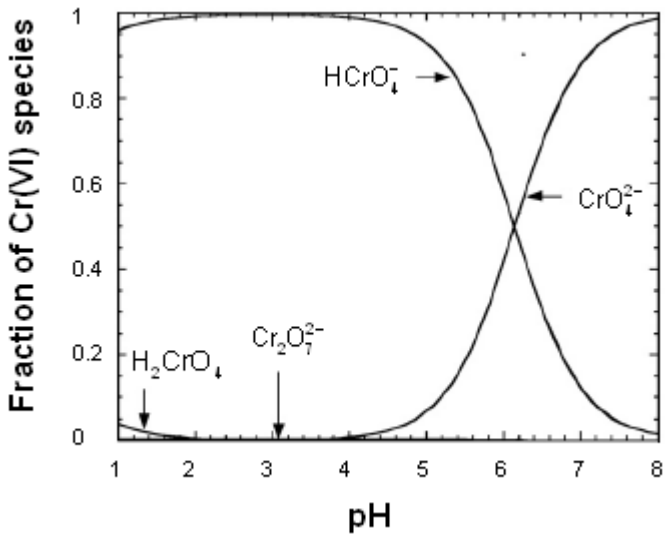

Figure 6–8 Distribution diagram of Cr(VI) species as function of pH [11,21]

High adsorption observed at low pH is presumably attributed to the large number of H^+ ions in solution, which in turn protonated the pH-dependent surface charge of vermiculite as follows:

$$\equiv Si - OH + H^+ \leftrightarrow \equiv Si - OH_2^+$$

$$\equiv Al - OH + H^+ \leftrightarrow \equiv Al - OH_2^+$$

Therefore, there is a high electrostatic attraction between hydrochromate ($HCrO_4^-$) and the protonated surface of vermiculite. A further decrease in pH was found to have an insignificant effect on removal efficiency. This can be explained by the fact that the adsorption reaction has reached equilibrium at pH 1.5. Hence, the equilibrium pH of 1.5 was taken as the optimal value for further adsorption studies. The decrease in adsorption at higher pH may be attributed to the fact that the overall surface charge on the adsorbent becomes negative due to the increase of OH^- activity as follows:

$$\equiv Si - OH + OH^- \leftrightarrow \equiv Si - O^- + H_2O$$

$$\equiv Al - OH + OH^- \leftrightarrow \equiv Al - O^- + H_2O$$

Knowing that the dominant species of Cr(VI) at alkaline pH are $Cr_2O_7^{2-}$ and CrO_4^{2-}, it is evident that these anions are poorly adsorbed on the surface of the adsorbent due to a repulsive electrostatic force between the adsorbate and adsorbent.

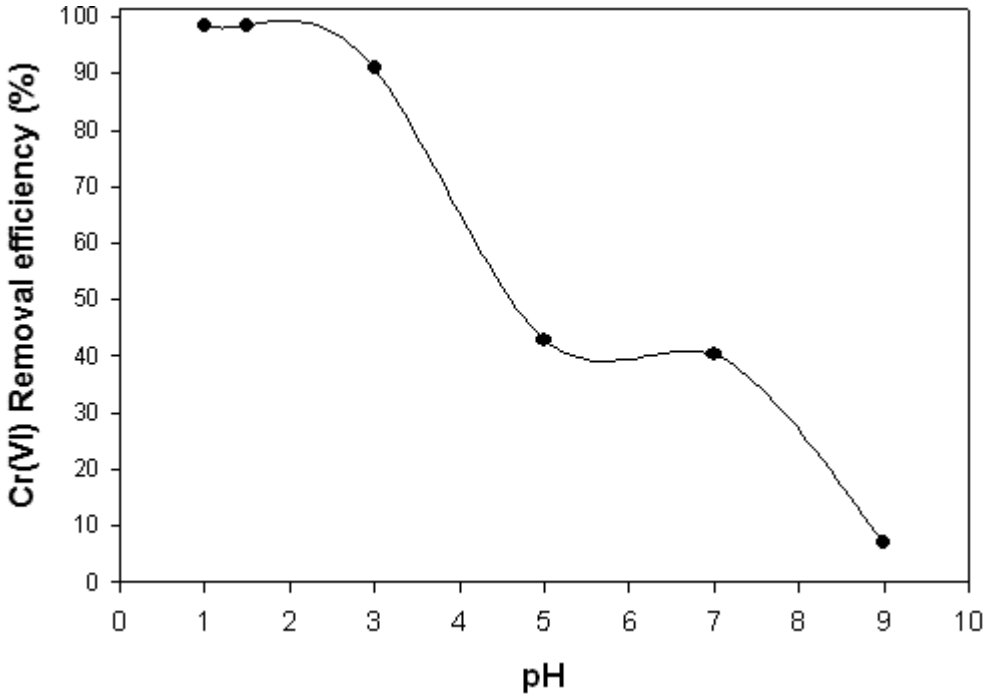

Figure 6–9 Effect of pH on Cr(VI) removal efficiency (adsorbent dosage 10 $g.L^{-1}$ and contact time 120 minutes).

6.4 Effect of adsorbent concentration with contact time

Adsorbent dosage and contact time are important parameters in the adsorption process. The effect of adsorbent concentration on removal efficiency was investigated at different contact times and initial pHs, ranging from 10 to 150 minutes and 1 to 9, respectively, and the relevant data are presented in Appendix III. The effect of adsorbent concentration with contact time on removal efficiency at pH 1.5, and the effect of adsorbent dosage on removal efficiency at pH 1.5 and 120 minutes of contact time are respectively shown in Figures 6–10 and 6–11. It is apparent from Figures 6–10 and 6–11 that an average removal efficiency enhancement of 1% was observed by increasing the contact time from 10 to 120 minutes and the adsorbent dosage from 2.5 to 10 $g.L^{-1}$. It has also been observed that the process was rapid in the initial stages and gradually

decreased and became constant after equilibrium was reached at about 2 hours of contact time and 10 $g.L^{-1}$ of adsorbent concentration. Further increase in contact time and adsorbent dosage had an insignificant effect on Cr(VI) uptake. According to Bansal *et al*. [11], this can be explained by the fact that the higher the dose of adsorbent in the solution, the greater the surface area, the greater the availability of active sites and the easier the adsorption of Cr(VI). However, the magnitude of uptake capacity decreased with increment in adsorbent dose due, probably, to overlapping of adsorption sites as a result of overcrowding of adsorbent particles.

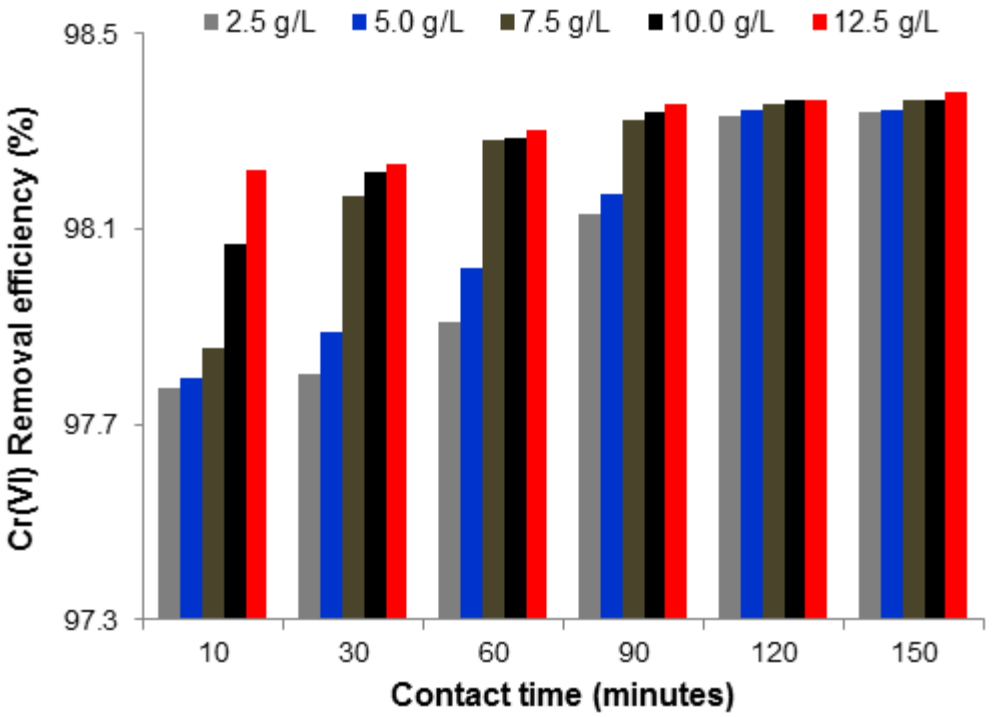

Figure 6–10 Effect of adsorbent concentration with contact time on Cr(VI) removal efficiency at pH 1.5.

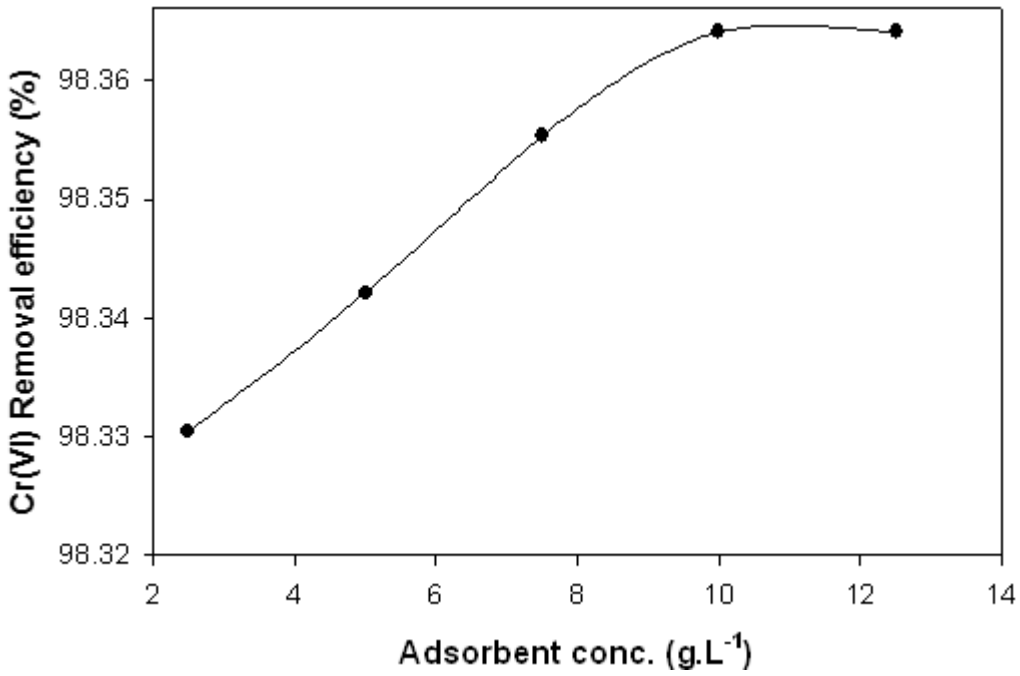

Figure 6–11 Effect of adsorbent dosage on Cr(VI) removal efficiency (pH 1.5 and contact time 120 minutes).

6.5 Effect of temperature

The effect of temperature on adsorption was investigated at temperature ranges from 20 to 80ºC at pH 1.5, 10 $g.L^{-1}$ of adsorbent concentration and 2 hours of contact time. Figure 6–12 shows that the adsorption of Cr(VI) onto vermiculite increases from 98.36 to 98.47 % with increasing temperature from 20 to 80ºC. Since this trend was observed in this study, the adsorption of Cr(VI) onto vermiculite is an endothermic process. This may be explained by the fact that, increasing temperature not only increases the active surface centers that are available for adsorption, but also the kinetic energy of the Cr(VI) compounds in solution as a result of higher mobility of ions [84]. An increase in temperature also decreases the activation energy for adsorption [66].

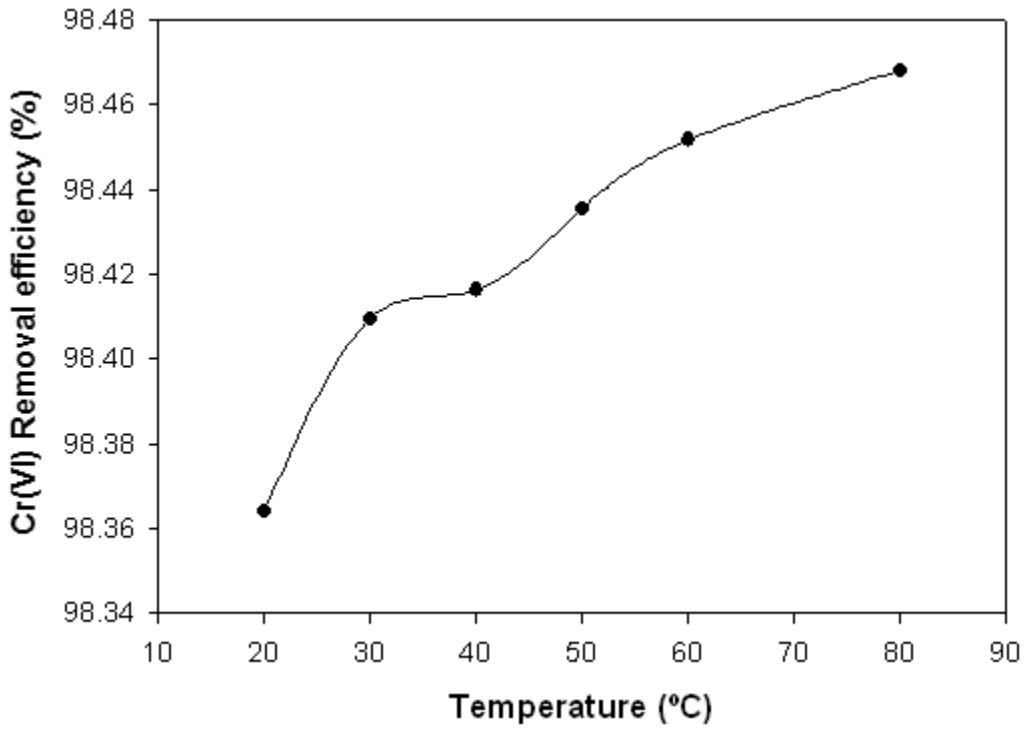

Figure 6–12 Effect of temperature on Cr(VI) removal efficiency (pH 1.5, adsorbent dosage 10 $g.L^{-1}$ and contact time 120 minutes).

6.6 Effect of particle size

The effect of particle size on adsorption of Cr(VI) onto vermiculite is depicted in Figure 6–13. It is evident from the experimental data that the removal efficiency decreases from 98.36 to 96.99 % with an increase in particle size from –75 to +600–1000 µm. It is known that the average particle size of the adsorbent is inversely proportional to its specific surface area [36,66]. Therefore, the relatively higher adsorption capacity with smaller adsorbent particle size may be attributed to the fact that small particle sizes not only yield larger surface areas, but also increase the number of broken bonds at crystal corners and edges [63].

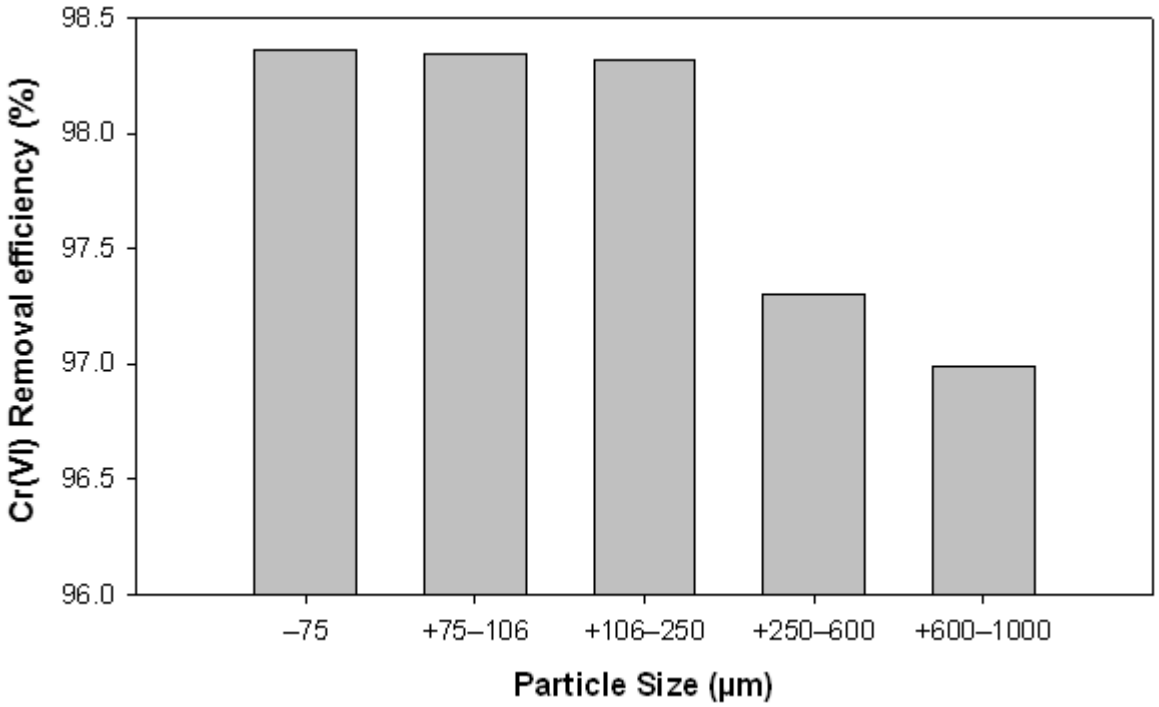

Figure 6–13 Effect of particle size on Cr(VI) removal efficiency (pH 1.5, adsorbent dosage 10 $g.L^{-1}$ and contact time 120 minutes).

6.7 Adsorption isotherms

To get a correct equilibrium relationship between the mass of solute adsorbed per unit mass of adsorbent, experimental data were fitted to equations (1), (2), (3) and (4), developed in Chapter 4, which represent the non-linear and linear forms of the Freundlich and Langmuir adsorption isotherms. The linear forms of the Freundlich and Langmuir plots are illustrated in Figures 6–14 and 6–15, respectively. Figure 6–16 represents the non-linear plots of the Freundlich and Langmuir isotherms along with the experimental data isotherm. Calculated adsorption parameters of linear, Freundlich and Langmuir models as well as their correlation coefficients are presented in Table 6–4. The maximum adsorption capacity q_m and Langmuir equilibrium constant K_L of vermiculite were found to be 23.26 $mg.g^{-1}$ and 0.15 $L.g^{-1}$, respectively. Constants related to the adsorption capacity K_F and adsorption intensity n were found to be 7.88 and 4.16, respectively. Since the value of 1/n is between 0 and 1, the adsorption of Cr(VI) onto vermiculite under the studied conditions was favourable [63].

Although the experimental data fitted both adsorption models, the high value of the Langmuir model correlation coefficient (R^2 = 0.996) indicated a strong correlation between the experimental equilibrium data isotherm and the Langmuir isotherm. Therefore, this finding suggests the existence of monolayer coverage of the adsorbate at the surface of the adsorbent [63,85].

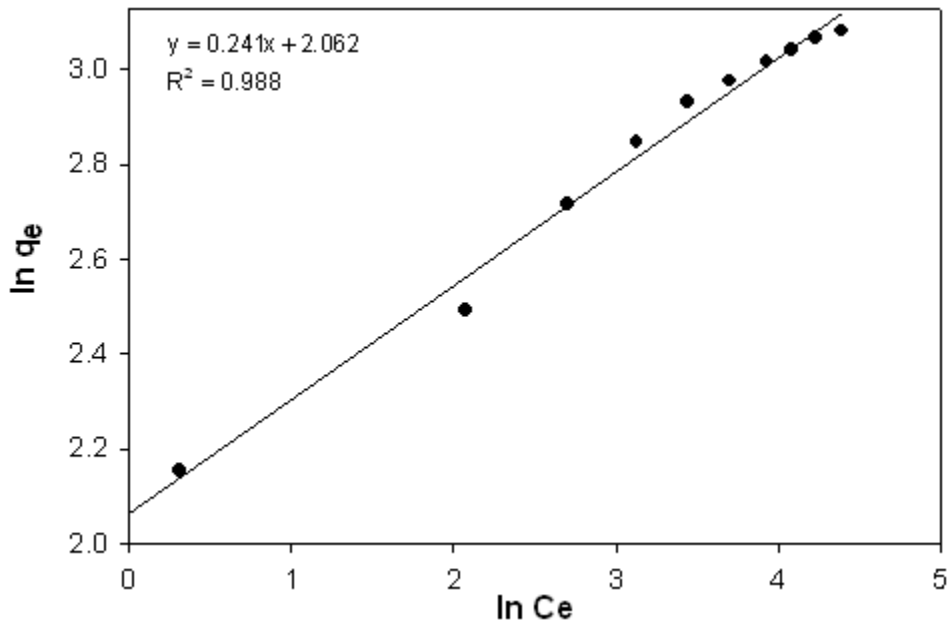

Figure 6–14 Linear plot for the Freundlich isotherm at optimum conditions for VER 1.

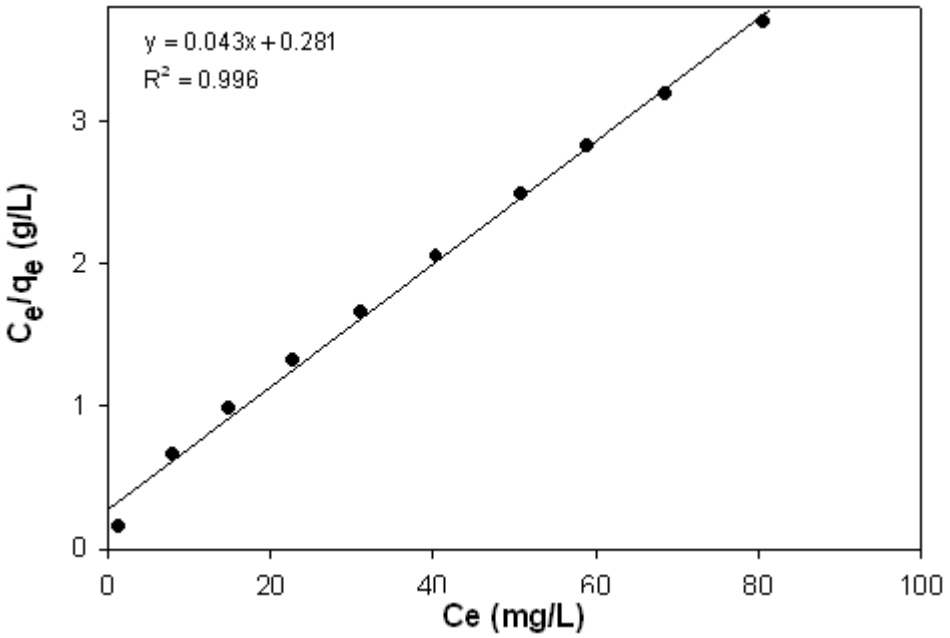

Figure 6–15 Linear plot for the Langmuir isotherm at optimum conditions for VER 1.

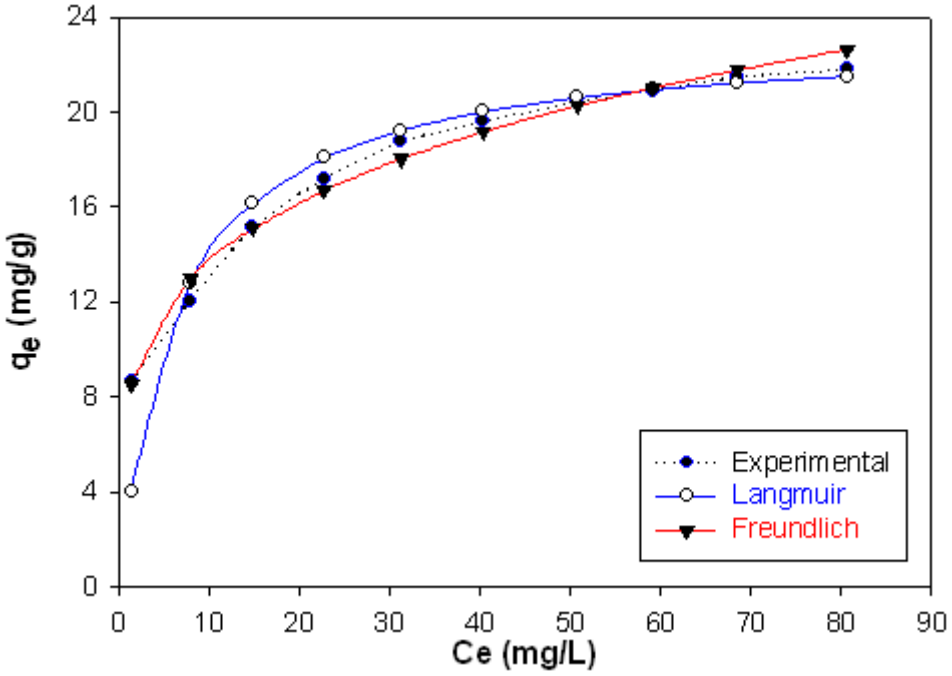

Figure 6–16 Non-linear isotherm plots of Cr(VI) adsorption data at optimum conditions for VER 1.

Table 6–4 The isotherm parameters and regression coefficients obtained for Cr(VI) adsorption data (pH 1.5, adsorbent dosage 10 $g.L^{-1}$ and contact time 120 minutes).

Langmuir isotherm			**Freundlich isotherm**		
q_m (mg/g)	K_L (L/mg)	R^2	K_F (L/g)	n	R^2
23.26	0.15	0.996	7.88	4.16	0.988

The favourability of the process was also confirmed by the separation factor R_L, expressed by equation (17) developed in Chapter 4. The R_L values for all tested initial Cr(VI) concentrations are between 0 and 1 as shown in Table 6–5. R_L values also revealed that the process tends to be irreversible for low Cr(VI) initial concentrations, and linear for high Cr(VI) initial concentrations.

Table 6–5 R_L values for Cr(VI) adsorption onto vermiculite.

C_0 ($mg.L^{-1}$)	10	20	30	40	50	60	70	80	90	100
R_L	0.39	0.25	0.18	0.14	0.12	0.01	0.09	0.08	0.07	0.06

6.8 Adsorption kinetics

For the two initial tested Cr(VI) concentrations (10 and 20 $mg.L^{-1}$), it was observed from Figures 6–17 and 6–18 that, firstly, the adsorption of Cr(VI) onto vermiculite is rapid in the initial stages, followed by a progressive uptake. After equilibrium has been reached, no significant change in uptake has been observed. Secondly, the removal efficiency at equilibrium decreased from 86.30 to 60.33% when the metal ion concentration was increased from 10 to 20 $mg.L^{-1}$, and thirdly, the uptake or amount of Cr(VI) adsorbed at equilibrium, increased from 8.63 to 12.07 $mg.g^{-1}$ when the Cr(VI) concentration increased from 10 to 20 $mg.L^{-1}$. Gupta and Babu [31] attributed the rapid adsorption observed within the initial stages of the process to the mechanism of Cr(VI) transfer to the functional sites which includes diffusion through the fluid film around the adsorbent particle and diffusion through the pores to the internal adsorption sites. In the initial stages of adsorption of Cr(VI), the concentration gradient between the film and the available pore sites is large, and hence the removal of Cr(VI) is faster. The rate of Cr(VI) removal decreases in the later stages of Cr(VI) adsorption as intra-particle diffusion becomes predominant and may be due to the slow pore diffusion of Cr(VI) into the bulk of the adsorbent. For the second observation, Bansal *et al*. [11] assumed that at low metal ion concentrations, the ratio of available surface to the initial Cr(VI) concentration is larger, so the removal is higher. However, in case of higher concentrations this ratio is low; hence the removal efficiency is also low. The increase of adsorption capacity by increasing metal ion concentration may be attributed to an increase in the rate of mass transfer due to a high driving force associated with the higher concentration difference.

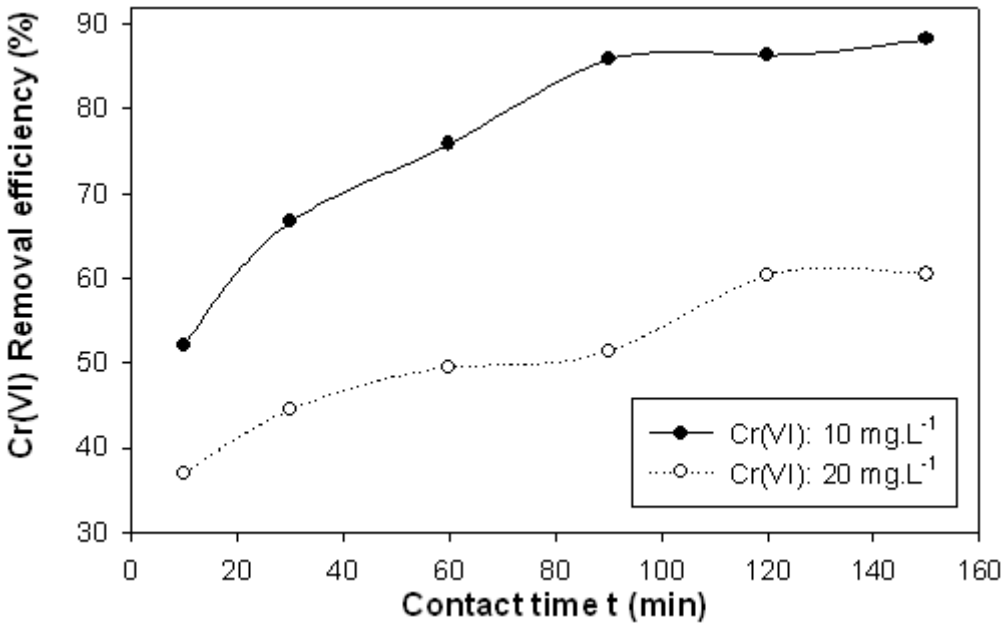

Figure 6–17 Effect of contact time on Cr(VI) removal efficiency (pH 1.5, adsorbent dosage 10 g.L^{-1}).

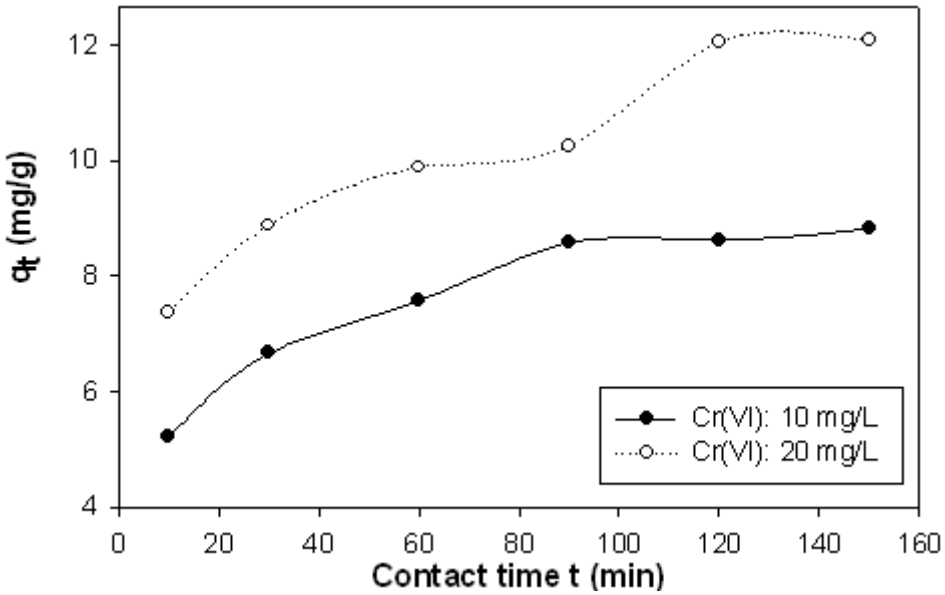

Figure 6–18 Effect of contact time on the amount of Cr(VI) adsorbed (pH 1.5, adsorbent dosage 10 g.L^{-1}).

Kinetic parameters including rate constants for the adsorption of Cr(VI) onto vermiculite were evaluated by means of the linear forms of the Lagergren equations (14) and (16) developed in Chapter 4. The values of the kinetic parameters along with their correlation

coefficients are presented in Table 6–6. It can be observed from the linear plots of the pseudo-first order and pseudo-second order equations depicted in Figures 6–19 and 6–20, respectively, and also from high values of regression coefficients for the two tested initial Cr(VI) concentrations that the experimental data are in good agreement with the pseudo-second order Lagergren equation.

The above findings reinforce the chemisorption phenomena of the process, which involves valence forces through sharing or exchange of electrons between adsorbent and adsorbate [22]. Hence, the overall mechanism is a reaction between functional surface groups present at the vermiculite crystal edges and hydrochromate ions in a surrounding solution, which form stable units. This process is presumably controlled by 3 steps: (1) the protonation of functional groups on the surface of the adsorbent; (2) the binding of $HCrO_4^-$ to the protonated groups present on the vermiculite surface; (3) the chemical bonding between $HCrO_4^-$ and adjacent functional groups of vermiculite. Bradl [64] explained this mechanism as a result of surface complexation with direct covalent bonds between the adsorbent surface and the adsorbing anion. The resulting stable surfaces are called inner-sphere complexes due to lack of water molecules interposed between the surface functional group and the bound ion. The coordinate-covalent bonding reactions are given below:

$$\equiv Si - OH_2^+ + HCrO_4^- \leftrightarrow \equiv Si - HCrO_4 + H_2O$$

$$\equiv Al - OH_2^+ + HCrO_4^- \leftrightarrow \equiv Al - HCrO_4 + H_2O$$

Table 6–6 The kinetic parameters evaluated for the adsorption of Cr(VI) onto vermiculite (pH 1.5, adsorbent dosage 10 $g.L^{-1}$ and contact time 120 minutes).

C_0 ($mg.L^{-1}$)	q_e exp. ($mg.g^{-1}$)	Pseudo-first order			Pseudo-second order		
		K_1	q_e	R^2	K_2	q_e	R^2
10	8.63	0.05	8.48	0.87	0.01	9.43	1.00
20	12.07	0.01	3.48	0.95	0.01	12.93	0.99

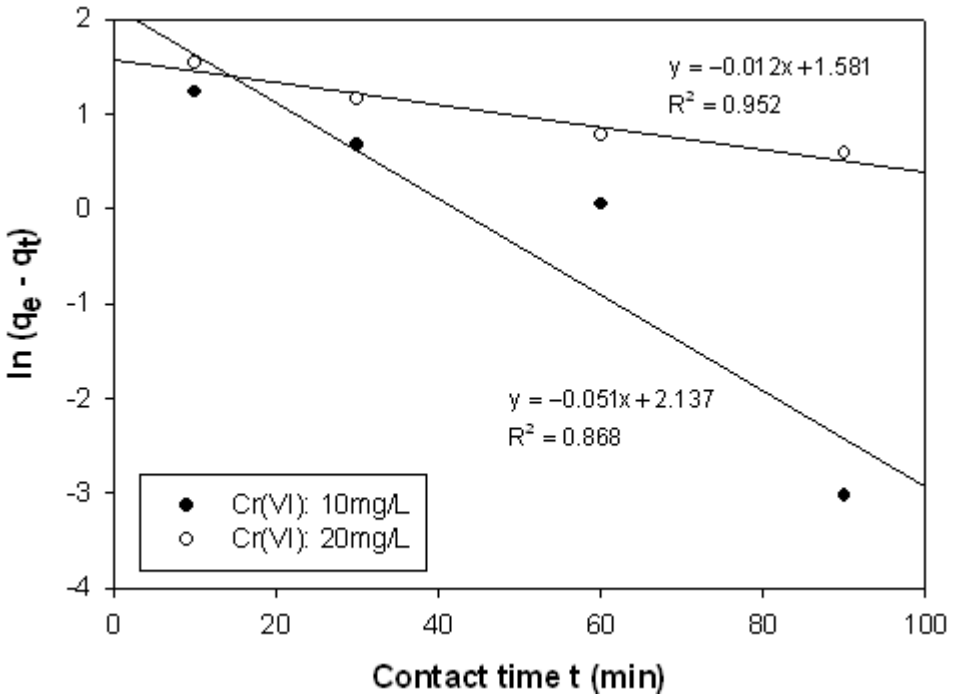

Figure 6–19 Linear plot for the pseudo-first order Lagergen equation (pH 1.5, adsorbent dosage 10 $g.L^{-1}$).

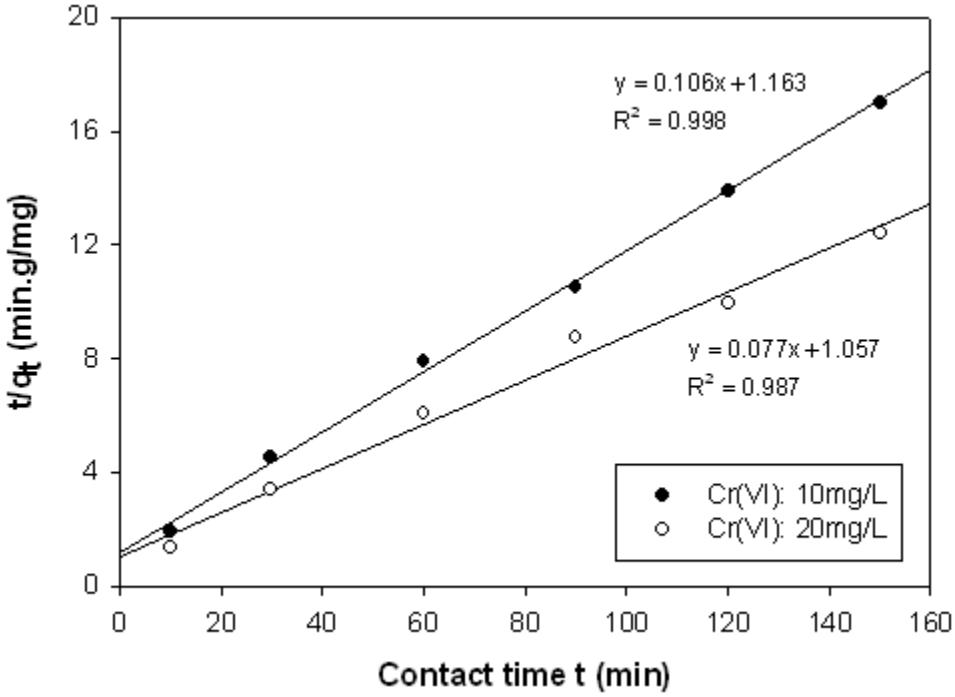

Figure 6–20 Linear plot for the pseudo-second order Lagergen equation (pH 1.5, adsorbent dosage 10 $g.L^{-1}$).

6.9 Adsorption thermodynamics

The adsorption free energy change ($\Delta G°$), enthalpy ($\Delta H°$) and entropy ($\Delta S°$) were evaluated from equations (11) and (12), respectively. $\Delta H°$ and $\Delta S°$ were calculated from the slope and intercept of the plot of Van't Hoff equation (1/T vs. ln K_C) illustrated in Figure 6–21. Values of thermodynamic parameters at different temperatures are represented in Table 6–7. The standard Gibbs free energy change was found to increase negatively with temperature which suggests the spontaneity of the adsorption process. The positive value of $\Delta H°$ and $\Delta S°$ suggest the endothermic nature and the feasibility of the process, respectively. The positive value of $\Delta S°$ also indicates the increased randomness at the adsorbent-solution interface [85,86].

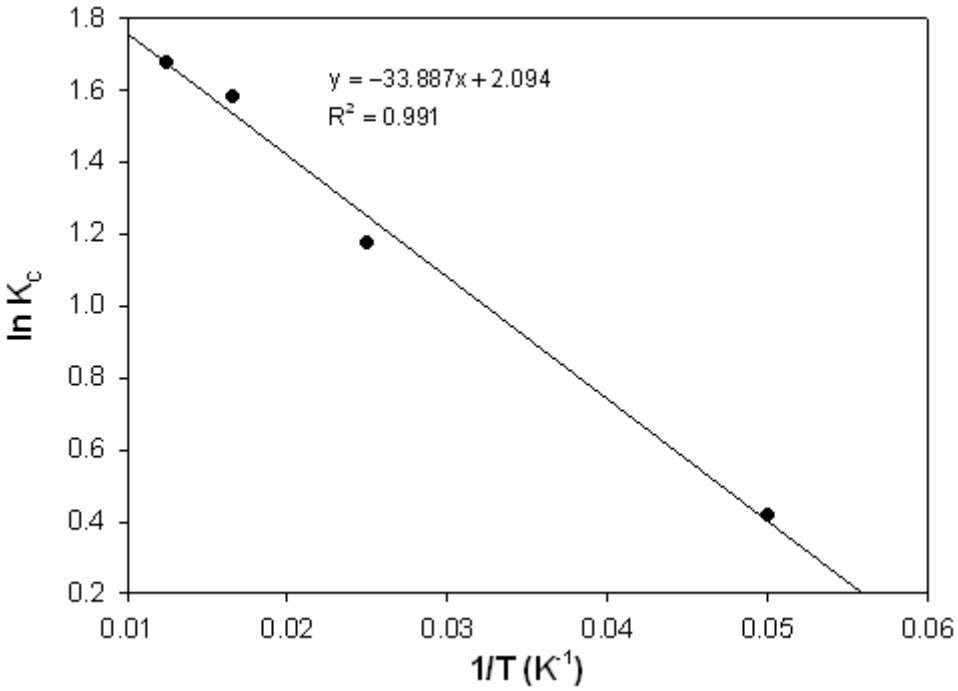

Figure 6–21 Van't Hoff plot for Cr(VI) adsorption onto vermiculite (pH 1.5, adsorbent dosage 10 $g.L^{-1}$ and contact time 120 minutes).

Table 6–7 The thermodynamic parameters for Cr(VI) adsorption onto vermiculite.

Temp (K)	ΔG°(J.mol^{-1})	ΔH°(J.mol^{-1})	ΔS°(J.mol^{-1}.K^{-1})
293	-1020.7	281.73	17.41
313	-3052.4		
333	-4374.1		
353	-4916.6		

6.10 Effect of phase composition on Cr(VI) uptake.

The three vermiculite samples of chemical and phase compositions mentioned in sub-section 6.1.2 were used in order to investigate the influence of phase composition on hexavalent chromium adsorption onto vermiculite. Linear plots of Langmuir isotherms corresponding to Cr(VI) adsorption onto VER 1, VER 2 and VER 3 along with Langmuir constants are shown in Figure 6–22 and Table 6–8, respectively. It can be seen from Table 6–8 that the maximum uptake of Cr(VI) onto the three exfoliated vermiculite samples slightly drops off with a decrease in concentration of the vermiculite phase. Therefore, it can be concluded that vermiculite phase is the major phase responsible for adsorption of Cr(VI) onto vermiculite.

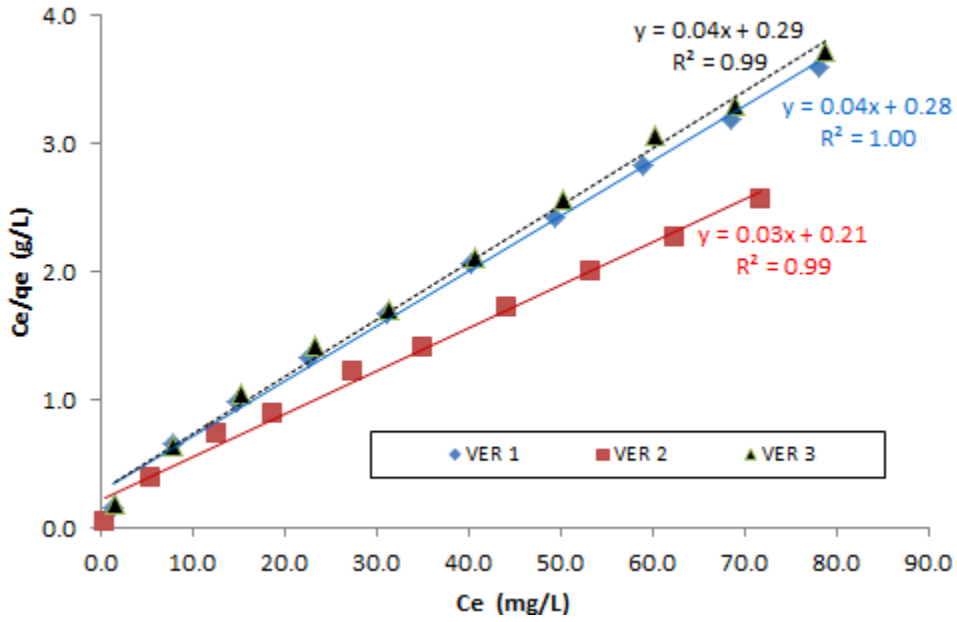

Figure 6–22 Linear plot for the Langmuir isotherm at optimum conditions for VER 1, VER 2 and VER 3.

Table 6–8 The isotherm parameters and regression coefficients obtained for Cr(VI) adsorption data (10 $g.L^{-1}$ of vermiculite at 20°C, pH 1.5 and 120 minutes).

Vermiculite Samples	q_m ($mg.g^{-1}$)	K_L ($L.mg^{-1}$)	R^2
VER 1	23.26	0.15	1.00
VER 2	29.91	0.16	0.99
VER 3	22.46	0.16	0.99

6.11 Leachability study

6.11.1 Using ASTM and TCLP

To assess if the treated FCD and the Cr(VI)-loaded vermiculite can safely be disposed of, Cr(VI) leachability from the two products was investigated by means of the Modified ASTM D 3987–85 (2004) and TCLP Method 1311 leaching tests for a period of 12 months. These Modified Leachate Extraction Procedures differ from the standard tests in that 5 g of solid sample were used instead of 70 and 100 g for ASTM and TCLP, respectively. The solid–liquid ratio was kept unchanged at 1:20.

The desorption study was conducted by preparing the Cr(VI)-loaded vermiculite and the treated FCD samples as follows:

Approximately 400 g of Cr(VI)-loaded vermiculite sample (SM T) were obtained after stabilization of PS 1, a pure solution having 1 $mg.L^{-1}$ of Cr(VI), by VER 1. The stabilization process was conducted by adding 50 g of VER 1 to 5 liters of PS 1. To get the desired amount of the SM 1, the stabilization process was run 9 times. The Cr(VI)-loaded vermiculite subsamples from each process were kept at room temperature for 30 days. Thereafter, the dry subsamples were mixed together and homogenized using the sampling method described in section 5.2. The homogenized Cr(VI)-loaded vermiculite sample (SM T) was kept at room temperature throughout the desorption study. At 30 day-intervals, three replicate samples under identical conditions and having 5 g each were taken from the same SM T stock, and subsequently leached for Cr(VI) desorption according to the Modified ASTM D 3987–85 (2004) and TCLP Method 1311 leaching tests.

As for the treated FCD, 140 g of the treated dust, derived from two ASTM leaching tests, were kept at room temperature in an open container for 30 days. Thereafter, the dry subsamples were mixed together and homogenized in the same way as for the Cr(VI)-loaded vermiculite. The homogenized treated FCD sample (FCD T) was kept at room temperature throughout the desorption study. The desorption study was conducted in the same way as for the Cr(VI)-loaded vermiculite, except that it was run at 6 month-intervals.

Results presented in Table 6–9 show that no additional Cr(VI) leached from FCD throughout the desorption study. As for the Cr(VI)-loaded vermiculite, monthly measurements over a 12 month period showed that the concentration of Cr(VI) in the leachate was below the regulation limit, and beyond 3 months, no additional Cr(VI) leached. The low degree of Cr(VI) desorption from the Cr(VI)-loaded vermiculite suggests the chemisorption of Cr(VI) onto the vermiculite surface.

Table 6–9 Results of Cr(VI) leaching from stabilized matrix.

Time (Days)	Cr(VI) Leached ($mg.L^{-1}$)			
	Treated Ferrochrome Dust		Cr(VI)–Loaded Vermiculite	
	ASTM	TCLP	ASTM	TCLP
30	(a)	(a)	0.012	0.013
60	–	–	0.012	0.014
90	–	–	(a)	(a)
120	–	–	(a)	(a)
150	–	–	(a)	(a)
180	–	–	(a)	(a)
210	(a)	(a)	(a)	(a)
240	–	–	(a)	(a)
270	–	–	(a)	(a)
300	–	–	(a)	(a)
330	–	–	(a)	(a)
360	(a)	(a)	(a)	(a)

(a) Below detection limit

6.11.2 Using Acid Rain Test

A concern was raised on the possibility of Cr(VI) desorption from the Stabilized Matrix in the presence of carbon dioxide and water. To address this concern, the Cr(VI)-loaded vermiculite was leached according to the Acid Rain Test. The Acid Rain Test procedure is based on the fact that carbon dioxide dissolves in rain water, to form carbonic acid. The carbonic acid could mobilize Cr(VI) from the Stabilized Matrix [81]. This method is similar to the TCLP Method 1311 leaching test, but instead of using TCLP solutions, the Acid Rain Test entails the extraction of a sample of waste with a saturated solution of carbonic acid called acid rain solution [81].

The experiments were run as follows: 5 g of the Cr(VI)-loaded vermiculite sample (VER 1) were added to 100 mL of acid rain solution and agitated continuously for 20 hours at room temperature (~23ºC). Thereafter, the slurry was filtered through a 0.45 µm Whatman Grade NC 45 (Cellulose Nitrate Membrane) filter paper, and the pH of the filtrate was measured immediately. An aliquot sample was taken from the filtrate for determination of Cr(VI) concentration.

Three Cr(VI)-loaded vermiculite samples labeled SM1, SM2 and SM3 were prepared as follows: the first sample was obtained after stabilization using a leachate from FCD, the second and the third using synthetically prepared Cr(VI) solutions having 1 and 10 $mg.L^{-1}$ of Cr(VI), respectively.

The Stabilized Matrices were kept at room temperature for 14 days before running the desorption test. Therefore, no long-term stabilization study was investigated during this test. It should be noted that an average pH of 5 was generated during this process for the three Cr(VI)-loaded vermiculite samples.

Results, in triplicate, presented in Table 6–10 show Cr(VI) desorption above the regulation limits applied in South Africa for all the studied samples. The desorption of Cr(VI) from SM is presumably due to the fact that chromate binding was depressed in the presence of dissolved inorganic carbon, which compete for adsorption site [87].

Table 6–10 Leachability of Cr(VI) from Stabilizing Matrix using Acid Rain Test

Sample	Replicate	Cr(VI) concentration (mg/l)				Cr(VI) desorption (%)	
		Conc.	Mean	Stdev	RSD† (%)	Desorption	Mean
SM1	Replicate 1	0.25	0.24	0.01	3.90	7.52	7.28
	Replicate 2	0.23				6.97	
	Replicate 3	0.24				7.36	
SM2	Replicate 1	0.26	0.25	0.01	3.37	5.98	5.78
	Replicate 2	0.25				5.74	
	Replicate 3	0.24				5.60	
SM3	Replicate 1	0.46	0.46	0.01	2.03	1.02	1.01
	Replicate 2	0.44				0.99	
	Replicate 3	0.46				1.03	

† RSD: Relative Standard Deviation.

6.12 Financial indications

Due to confidentiality reasons, information about the cost of the dust treatment process implemented at one of the local based companies cannot be disclosed. Therefore, the cost presented in Table 6–11 serves only as a general guide.

The stabilization process was run using the ASTM D 3987–85 (2004) ferrochrome dust leachate which was obtained by adding 70 g of FCD in 1.4 L of distilled water.

Knowing that 10 g of vermiculite is necessary for the stabilization of the amount of Cr(VI) (< 1 $mg.L^{-1}$) containing in 1 L of FCD, it is evident that 0.2 ton g of vermiculite will be necessary for the stabilization of 1 ton of FCD.

30 ml of HCl 32% is necessary to adjust the pH of 1 L of FCD leachate at 1.5, therefore 20 000 L of FCD leachate will need 600 L of HCl.

Table 6–11 Financial indications for Cr(VI) stabilization using vermiculite for 1 metric ton of FCD (electricity and water consumptions are not taken into account)

Material	Quantity	Unit Value ($)	Total Price ($)
Vermiculite	0.2 t	180/t [a]	36
HCl	600 L	6.6/L [b]	3,960
Total			**3,996**

[a] Average price of superfine grade (Mandoval SA)
[b] Merck SA

The average exchange rate is R7 per U.S. dollar.

CHAPTER 7: CONCLUSIONS AND RECOMMENDATIONS

7.1 Conclusions

This study proved that South African vermiculite can be used to remove Cr(VI) from fine ferrochrome dust after it is leached in aqueous solutions. Measurement over a 12 month period showed that no additional Cr(VI) leached from the treated ferrochrome dust. FCD can then safely be disposed of.

The adsorption process was found to be highly pH dependent. The optimum pH obtained for Cr(VI) adsorption onto vermiculite was found to be 1.5. The adsorption capacity is reduced with further increasing the pH. The adsorption increased with the increase in contact time and reached equilibrium after 2 hours. It was also observed that the adsorption of Cr(VI) onto vermiculite is rapid in the initial stages, followed by a progressive uptake. After equilibrium was reached, no significant change in uptake was observed. Increase in adsorbent dosage led to an increase in Cr(VI) adsorption. The optimum Cr(VI) uptake was obtained at an adsorbent dosage of 10 $g.L^{-1}$. The process was enhanced by decreasing the particle size of the adsorbent.

The stability of Cr(VI)-loaded vermiculite remained unchanged after 12 months, since the amounts of Cr(VI) leached from the stabilized matrix by both the ASTM and TCLP leaching methods were less than the regulation limits, and beyond 3 months, no additional Cr(VI) leached. The disadvantage of the stabilization of Cr(VI) using vermiculite is the desorption observed when leaching with the Acidic Rain solution; this desorption was found to be slightly above the regulation limits applied in South Africa. The measured concentration of Cr(VI) in each eluted sample showed that the amount of Cr(VI) leached was almost the same for the ASTM and TCLP tests, except for the Acid Rain Test which led to a high Cr(VI) desorption, presumably due to high concentration of inorganic carbon in solution.

XRD analysis of the adsorbent showed that the peak at $2\theta=7.2^{o}$, the major peak of the vermiculite phase, drastically decreased in intensity after adsorption. It was also

observed that the extent of Cr(VI) adsorption onto vermiculite slightly increases with an increase in concentration of the vermiculite phase; this suggests the major role of the vermiculite phase in the adsorption process. When the FT-IR spectra of the adsorbent prior to and after adsorption were compared, it was found that the peaks corresponding to the silanol (Si–OH) and aluminol (Al–OH) functional groups slightly shifted; which implies their involvement in the adsorption process.

The adsorption kinetic data fitted well the pseudo-second order model. The equilibrium data of Cr(VI) adsorption onto vermiculite were well described by both Langmuir and Freundlich isotherms, however, the Langmuir model indicated a strong positive relationship between the experimental equilibrium data and its related isotherm. The maximum adsorption capacity was found to be 23.26 $mg.g^{-1}$. The thermodynamic parameters evaluated suggested the spontaneous and endothermic nature of the adsorption process.

7.2 Recommendations for the future work

Exfoliated vermiculite is a highly efficient heat insulating material due to its low bulk density, high melting point and low thermal conductivity. It will be meaningful to investigate if the Cr(VI)-loaded vermiculite can safely be used as a lightweight heat insulator. The microstructure of the Cr(VI)-loaded vermiculite show that material has an irregular and high porous surface. The high porosity presented by Cr(VI)-loaded vermiculite provide an effective means of reducing the apparent density and improving the refractoriness of components manufactured [65]. Furthermore, Cr(VI)-loaded vermiculite, mainly composed of SiO_2, MgO, Al_2O_3 and Fe_2O_3 can expand at high temperature and forms high-melting phases such as mullite and spinel.

References

1 Barnhart, J., Occurence, used and properties of Chromium. *Regulatory Toxicology and Pharmacology* 26 (1997) S3–S7.

2 Palmer, C.D. and Wittbrodt, P.R., Processes Affecting the remediation of chromium-contaminated sites. *Environmental Health Perspectives* 92 (1991) 25–40.

3 International Chromium Development Association (ICDA), Statistical bulletin. Paris, France, 2009.

4 Papp, J.F., Chromium. *U.S. Geological Survey Minerals Year Book, 2007*. http://minerals.usgs.gov/minerals/pubs/commodity/chromium/myb1-2007-chrom.xls

5 Independent Environmental Technical Evaluation Group (IETEG), Chromium(VI) Handbook. CRC Press, Florida, USA, 2005.

6 ICDA, Health Safety and Environment Guidelines for Chromium. Paris, France, 2007.

7 Maine, C.F., Smit, J.P. and Giesekke, E.W. Report to the Water Research Commission on the project "*Solid Stabilization of Soluble Waste in the Ferro-alloy Industry*", 2000.

8 Ma, G. and Garbers-Craig, A.M., Cr (VI)-Containing Electric Furnace Dust and filter cake: characteristics, Formation, Leachability and Stabilization. University of Pretoria, Pretoria, Republic of South Africa, 2006.

9 Pillay, K., Blottnitz, H. von and Petersen, J., Ageing of chromium(III)-bearing slag and its relation to the atmospheric oxidation of solid chromium(III)-oxide in the presence of calcium oxide. *Chemosphere* 52 (2003) 1771–1779.

10 Pagana, A.E., Sklari, S.D., Kikkinides, E.S. and Zaspalis, V.T., Microporous ceramic membrane technology heart the removal of Arsenic Chromium and ions from contaminated water. *Microporous and Mesoporous Materials* 110 (2008) 150–156.

11 Bansal, M., Singha, D. and Garg, V.K., A comparative study for the removal of hexavalent chromium from aqueous solution by agriculture wastes carbons. *Journal of Hazardous Materials* 171 (2009) 83–92.

12 Fonseca, M.G. da, Oliveira, M.M. de and Arakaki, L.N.H., Removal of cadmium, zinc, manganese and chromium cations from aqueous solution by a clay mineral. *Journal of Hazardous Materials* B137 (2006) 288–292.

13 Bhattacharya, A.K., Naiya, T.K., Mandal, S.N. and Das, S.K., Adsorption, kinetics and equilibrium studies on removal of Cr(VI) from aqueous solutions using different low-cost adsorbents. *Chemical Engineering Journal* 137 (2008) 529–541.

14 Laforest, G. and Duchesne, J., Evaluation of the degree of Cr ions immobilization by different binders. *Cement and Concrete Research* 35 (2004) 1173–1177.

15 Laforest, G. and Duchesne, J., Immobilization of chromium (VI) evaluated by binding isotherms for ground granulated blast furnace slag and Ordinary Portland Cement. *Cement and Concrete Research* 35 (2005) 2322–2332.

16 Bailey, S.E., Olin, T.J., Bricka, R.M. and Adrian, D., A review of potentially low-cost sorbents for heavy metals. *Water Research* 33 (1999) 2469–2479.

17 US Environmental Protection Agency, In situ treatment of soil and groundwater contaminated with chromium. EPA/625/R-00/005, October 2000.

18 Fonseca, M.G. da, Oliveira, M.M. de, Arakaki, L.N.H., Espinola, J.G.P. and Airoldi, C., Natural vermiculite as an exchanger support for heavy cations in aqueous solutions. *Journal of Colloid and Interface Science* 285 (2005) 50–55.

19 Emsley, J., "Chromium". Nature's Building Blocks: An A-Z Guide to the Elements. Oxford University Press, Oxford, UK, 2001, pp. 495–498.

20 Calder, L.M., Chromium in the Natural and Human Environments. *Advances in Environmental Science and Technology* 20 (1988) 215–229.

21 Weng, C.H., Sharma, Y.C. and Chu, S.H., Adsorption of Cr(VI) from aqueous solutions by spent activated clay. *Journal of Hazardous Materials* 155 (2008) 65–75.

22 Namasivayam, C. and Sureshkumar, M.V., Removal of chromium(VI) from water and wastewater using surfactant modified coconut coir pith as a biosorbent. *Bioresource Technology* 99 (2008) 2218–2225.

23 Bartlett, R.J., Chromium cycling in soils and water: links, gaps and methods. *Environmental Health Perspectives* 92 (1991) 17–24.

24 Torres, R.A., Removing Hexavalent Chromium from Subsurface Waters with Anion-Exchange Resin, Lawrence Livermore National Laboratory, UCRL-ID-114369, 1995.

25 King, T. and Rytuba, J.J., AVIRIS and field imaging spectroscopy of mineral and vegetation distribution in the coast range mercury mineral belt, California. *Geol. Soc. Am. Abstr. Programs* 32 (1999) 6, A–70.

26 Kaczynski, S.E. and Kleber, R.J., Aqueous trivalent chromium photoproduction in natural waters. *Environ. Sci. Technol*. 27 (1993) 1572–1576.

27 Babel, S. and Kurniawan, T.A., Low-cost adsorbents for heavy metals uptake from contaminated water: a review. *Journal of Hazardous Materials* B97 (2003) 219–243.

28 Rao, M., Parwate, A.V. and Bhole, A.G., Removal of Cr^{6+} and Ni^{2+} from aqueous solution using bagasse and fly ash. *Waste Management* 22 (2002) 821–830.

29 Qian, G., Yang, X., Dong, S., Zhou, J., Sun, Y., Xu, Y. and Liu, Q., Stabilization of chromium-bearing electroplating sludge with MSWI fly ash-based Friedel matrices. *Journal of Hazardous Materials* 165 (2009) 955–960.

30 Sharma, D.C. and Forster, C.F., Continuous adsorption and desorption of chromium ions by sphagnum moss peat. *Process Biochem* 30 (1995) 293–298.

31 Gupa, S. and Babu, B.V., Utilization of waste product (tamarind seeds) for the removal of Cr(VI) from aqueous solutions: Equilibrium, kinetics, and regeneration studies. *Journal of Environmental Management* 90 (2009) 3013–3022.

32 Uysal, M. and Irfan, A., Removal of Cr(VI) from industrial wastewaters by adsorption. Part I: Determination of optimum conditions. *Journal of Hazardous Materials* 149 (2007) 482–491.

33 Baral, S.S., Das, S.N., and Rath, P., Hexavalent chromium removal from aqueous solution by adsorption on treated sawdust. *Biochemical Engineering Journal* 31 (2006) 216–222.

34 http://www.galleries.com/minerals/silicate/clays.htm

35 Skipper, N.T., Soper, A.K., McConnell, J.D.C. and Refson, K., The structure of interlayer water in hydrated 2:1 clay. *Chemical Physics Letters* 166 (1990) 141–145.

36 Bergaya, F., Theng, B.K.G. and Lagaly, G., Handbook of Clay Science. 1st edition, Elsevier, Oxford, United Kingdom, 2006.

37 A. Kabata-Pendias, *Soil–plant transfer of trace elements—an environmental issue*. Geoderma 122 (2004) 143–149.

38 Kraepiel, A.M.L, Keller, K. and Morel, F.M.M., A Model for Metal Adsorption on Montmorillonite. *Journal of Colloid and Interface Science* 210 (1999) 43–54.

39 Abollino, O., Aceto, M., Malandrino, M., Sarzanini, C. and Mentasti, E., Adsorption of heavy metals on Na-montmorillonite. Effect of pH and organic substances. Water Research 37 (2003) 1619–1627.

40 Krishna, B.S., Murty, D.S.R., Jaiprakash, B.S., Thermodynamics of chromium(VI) anionic species sorption onto surfactant-modified montmorillonite. *Journal Colloid Interf. Sci*. 229 (2000) 230–236.

41 US Environmental Protection Agency (USPEA), Feasibility for Identifying Mineralogical and Geochemical Tracers for Vermiculite Ore Deposits. EPA/910/R-01/002, February 2001.

42 Schneider, R.M., Cavalin, C.F., Barros, M.A.S.D. and Tavares, C.R.G., Adsorption of chromium ions in activated carbon. *Chemical Engineering Journal* 132 (2007) 355–362.

43 Khezami, L. and Capart, R., Removal of chromium(VI) from aqueous solution by activated carbons: Kinetic and equilibrium studies. *Journal of Hazardous Materials* 123 (2005) 223–231.

44 Baral, S.S., Dasa, S.N., Rath, P. and Chaudhury, G.R., Chromium(VI) removal by calcined bauxite. *Biochemical Engineering Journal* 34 (2007) 69–75.

45 Sharma, Y.C., Singh, B., Agrawal, A. and Weng, C.H., Removal of chromium by riverbed sand from water and wastewater: Effect of important parameters. *Journal of Hazardous Materials* 151 (2008) 789–793.

46 Barros, M. and Arroyo, P.A., Thermodynamics of the Exchange Processes between K^{+}, Ca^{2+} and Cr^{3+} in Zeolite NaA. *Adsorption* 10 (2004) 227–235.

47 Mulligan, C.N., Yong, R.N. and Gibbs, B.F., Remediation technologies for metal-contaminated soils and groundwater: an evaluation. *Engineering Geology* 60 (2001) 193–207.

48 Cheung, K.H. and Gu, J-D., Mechanism of hexavalent chromium detoxification by microorganisms and bioremediation application potential: A review. *International Biodeterioration & Biodegradation* 59 (2007) 8–15.

49 Selley, R.C., Robin, L., Cocks, M. and Plimer, I.R., Encyclopedia Of Geology. Elsevier, Oxford, UK, 2005.

50 Mungasavalli, D.P., Viraraghavan, T. and Jin, Y-C., Biosorption of chromium from aqueous solutions by pretreated Aspergillus niger: Batch and column studies. *Colloids and Surfaces A: Physicochem. Eng. Aspects* 301 (2007) 214–223).

51 http://www.alibaba.com

52 Potter, M.J., *U.S. Geological Survey Minerals Year Book, 2007.* http://minerals.usgs.gov/minerals/pubs/commodity/vermiculite/myb1-2006-vermi.xls

53 Crangle, R.D. Jr, Vermiculite. *U.S. Geological Survey Minerals Year Book, 2008*. http://minerals.usgs.gov/minerals/pubs/commodity/vermiculite/myb1-2007-vermi.xls

54 http://www.vermiculite.org/papers.htm

55 Badger, S.R. and Kneller W.A., The characterization and formation of electric arc furnace (EAF) dusts, *Electric Furnace Conference Proceedings*, ISS, Chicago, 1997, pp. 95–98.

56 Huber, J.C., Rocabois, P., Faral, M., Birat, J.P., Patisson, F. and Ablitzer, D., The formation of EAF dust, *Electric Furnace Conference Proceedings,* ISS, Orlando, 2000, pp. 171–181.

57 Delhaes, C., Hauck, A. and Neuschutz, D., Mechanisms of dust generation in a stainless steelmaking converter, *Steel Research*. 64 (1993) 22–27.

58 Ohno, T., Ono, S. and Okajima, M., Experimental results on dust formation by small melting furnace, *Transactions ISIJ*. 26 (1986) pp. B–312.

59 Eksteen, J.J., Frank, S.J. and Reuter, M.A., Dynamic structures in variance based data reconciliation adjustments for a chromite smelting furnace, *Minerals Engineering*, 15 (2002) 931–943.

60 Correspondances with Xstrata Lynderberg Plant workers.

61 http://www.ecodose.co.za/

62 Addison, J., Vermiculite: A Review of the Mineralogy and Health Effects of Vermiculite Exploitation. *Regulatory Toxicology and Pharmacology* 21 (1995) 397–405.

63 Langmuir, D., Aqueous Environmental Geochemistry. Prentice Hall, NJ, USA, 1997.

64 Bradl, H.B., Adsorption of heavy metal ions on soils and soils constituents. *Journal of Colloid and Interface Science* 277 (2004) 1–18.

65 Suvorov, S.A. and Skurikhin, V.V., Vermiculite – A Promising Material For High-Temperature Heat Insulators. *Refractories and Industrial Ceramics*, Vol. 44, No. 3, 2003.

66 Inglezakis, V.J. and Poulopoulos, S.G., Adsorption, Ion Exchange and Catalysis: Design of Operations and Environmental Applications. Elsevier, Oxford, UK, 2005.

67 http://www.frtr.gov/matrix2/section4/4-44.html

68 Sarı, A., Tuzen, M. and Soylak, M., Adsorption of Pb(II) and Cr(III) from aqueous solution on Celtek clay. *Journal of Hazardous Materials* 144 (2007) 41–46.

69 Lyman, W.J., Reehl, W.F. and Rosenblatt, D.H., Handbook of Chemical Property Estimation Methods. Environmental Behavior of Organic Compounds. McGraw-Hill, New York, 1982.

70 Harland, C.E., Ion Exchange: Theory and Practice. 2nd ed. The Royal Society of Chemistry, Cambridge, UK, 1994.

71 Hamadi, N.K., Chen, X.D., Farid, M.M. and Lu, M.G.Q., Adsorption kinetics for the removal of chromium(VI) from aqueous solution by adsorbents derived from used tyres and sawdust. *Chemical Engineering Journal* 84 (2001) 95–105.

72 Gerlach, R.W., Dobb, D.E., Raab, G.A. and Nocerino, J.M., Gy sampling theory in environmental studies. *J. Chemometrics* 16 (2002) 321–328.

73 Petersen, L., Dahl, C.K. and Esbensen, K.H., Representative mass reduction in sampling–a critical survey of techniques and hardware. *Chemometrics and Intelligent Laboratory Systems* 74 (2004) 95–114.

74 American Society for Testing and Materials, *Standard Test Method for Screening Apparent Specific Gravity and Bulk Density of Waste*. Method D 5057–90 (Reapproved 2006), ASTM, PA, USA.

75 American Society for Testing and Materials, *Standard Test Method for Screening of pH in Waste*. Method D 4980–89 (Reapproved 2003), ASTM, PA, USA.

76 INTERNATIONAL ATOMIC ENERGY AGENCY, Field Estimation of Soil Water Content: A Practical Guide to Methods, Instrumentation and Sensor Technology. IAEA, Austria, Vienna, 2008.

77 Naiker, O. and Riley, T., Xstrata Alloys in Profile. *South African Institute of Mining and Metallurgy, Johannesburg*, 5-8 March 2006, p. 297–305.

78 Gillman, G.P. and Sumpter, E.A., Modification to the compulsive exchange method for measuring exchange characteristics of soils. *Aust. J. Soil Res*. 24 (1986) 61–66.

79 American Society for Testing and Materials, *Standard Test Method for Shake Extraction of Solid Waste with Water*. Method D 3987–85 (Reapproved 2004), ASTM, PA, USA.

80 US Environmental Protection Agency (USPEA), *Toxicity Characteristic Leaching Procedure (Method 1311 Revision 0, Jul. 1992)*. EPA, July 1992.

81 Department of Water Affairs and Forestry (DWAF), Minimum Requirements for the Handling, Classification and Disposal of Hazardous Waste. 2nd Ed. Johannesburg, Republic of South Africa, 1998.

82 Perez-Maqueda, L.A., Jimenez de Haro, Poyato, Perez-Rodrıguez, J.L., Comparative study of ground and sonicated vermiculite. *Journal of Materials Science*. 39 (2004) 5347–5351.

83 Wang, X.S., Tang, Y.P. and Tao, S.R., kinetics, equilibrium and thermodynamic study on removal of Cr (VI) from aqueous solutions using low-cost adsorbent Alligator weed. *Chemical Engineering Journal* 148 (2009) 217–225.

84 Liu, Y., Xiao, D. and Li, H., Kinetics and thermodynamics of lead (II) adsorption on vermiculite. *Separation Science and Technology* 42 (2007) 185–202.

85 Nityanandi, D. and Subbhuraam, C.V., Kinetics and thermodynamics of adsorption of Cr(VI) from aqueous solution using puresorbe. *Journal of Hazardous Materials* 170 (2009) 876–882.

86 Debnath, S. and Ghosh, U.C., Kinetics, isotherm and thermodynamics for Cr(III) and Cr(VI) adsorption from aqueous solutions by crystalline hydrous titanium oxide. J. *Chem. Thermodynamics* 40 (2008) 67–77.

87 Zachara, J.M., Ainsworth, C.C., Cowan, C.E., and Resch, C.T. “Adsorption of Chromate by Subsurface Soil Horizons.” *Soil Science Society American Journal* 53 (1989) 418–428.

Appendixes

Appendix I Calibration curves for Cr(VI) determination using the UV/Vis Spectrometer

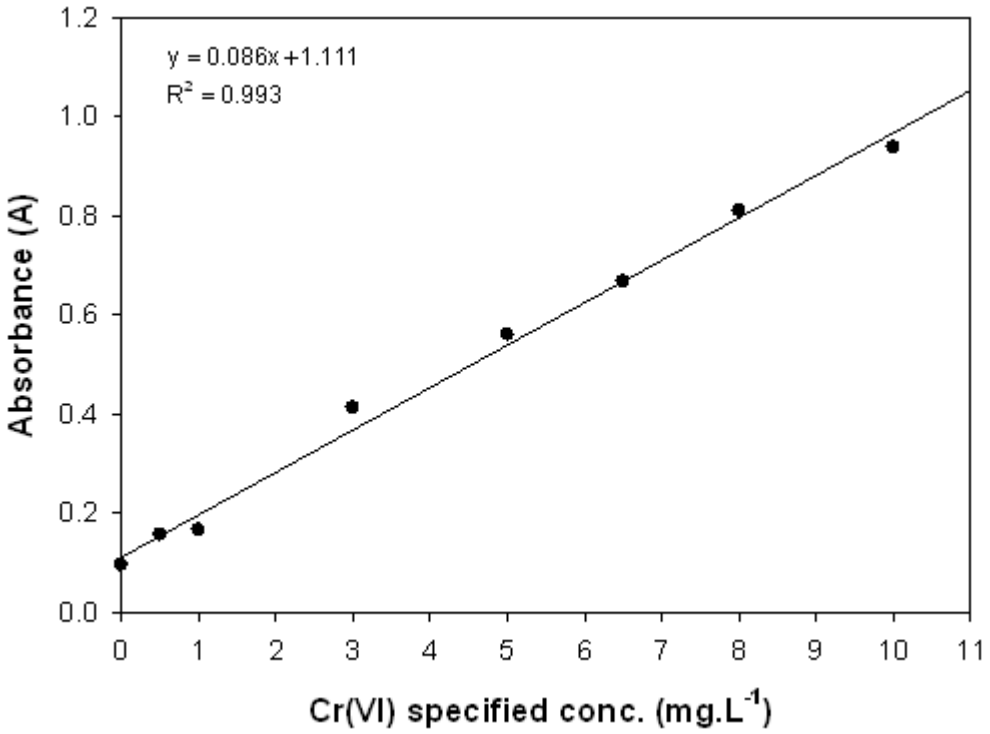

Figure I–1 Calibration Set 1: Cr(VI) conc. : 0.50 – 10.00 $mg.L^{-1}$

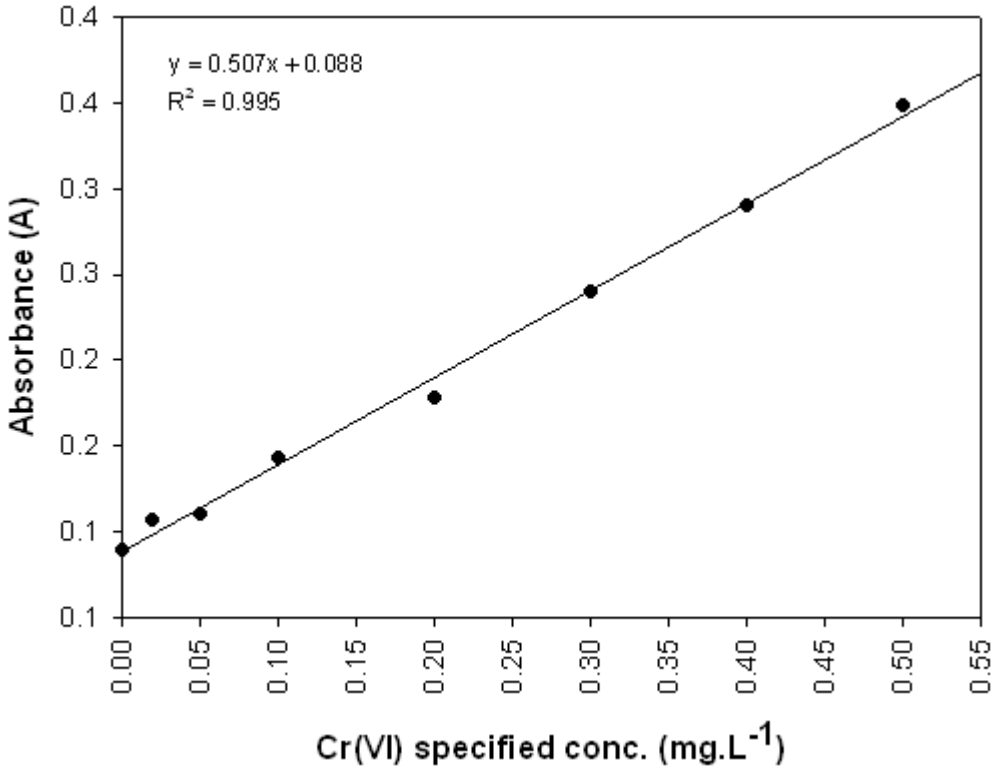

Figure I–2 Calibration Set 2: Cr(VI) conc. : 0.02 – 0.50 $mg.L^{-1}$

Appendix II XRD Patterns

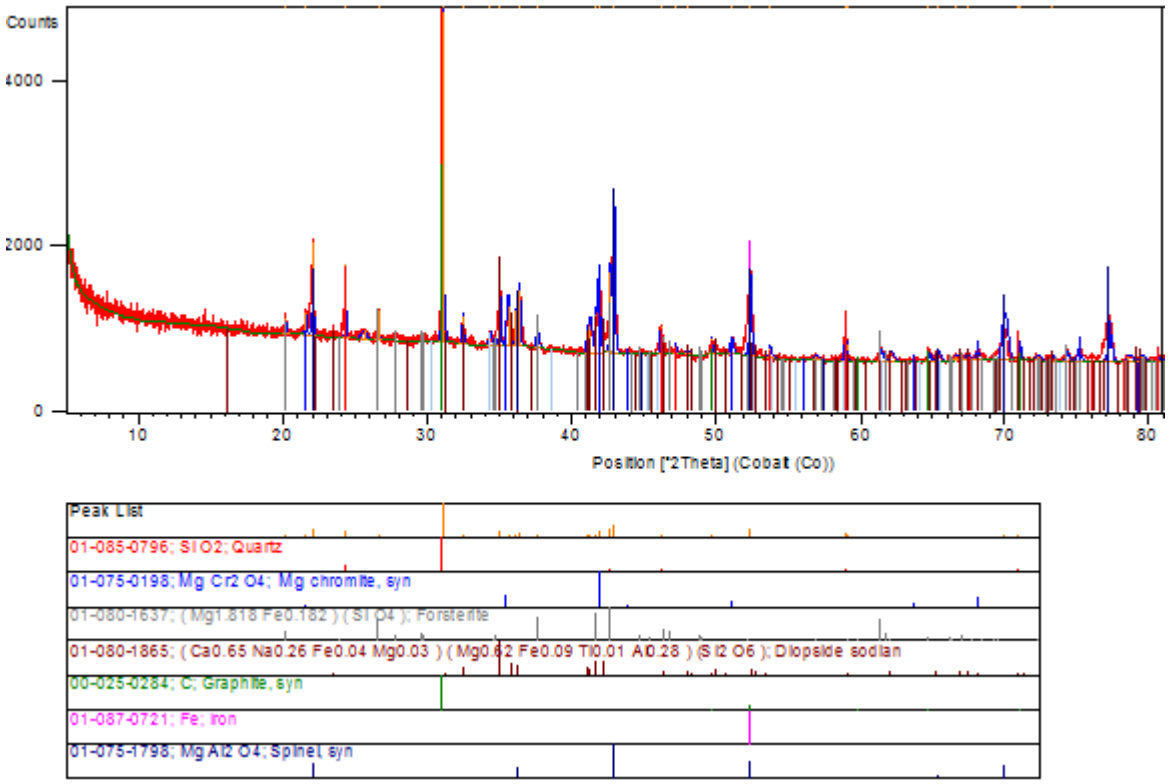

Figure II–1 XRD pattern of the FCD

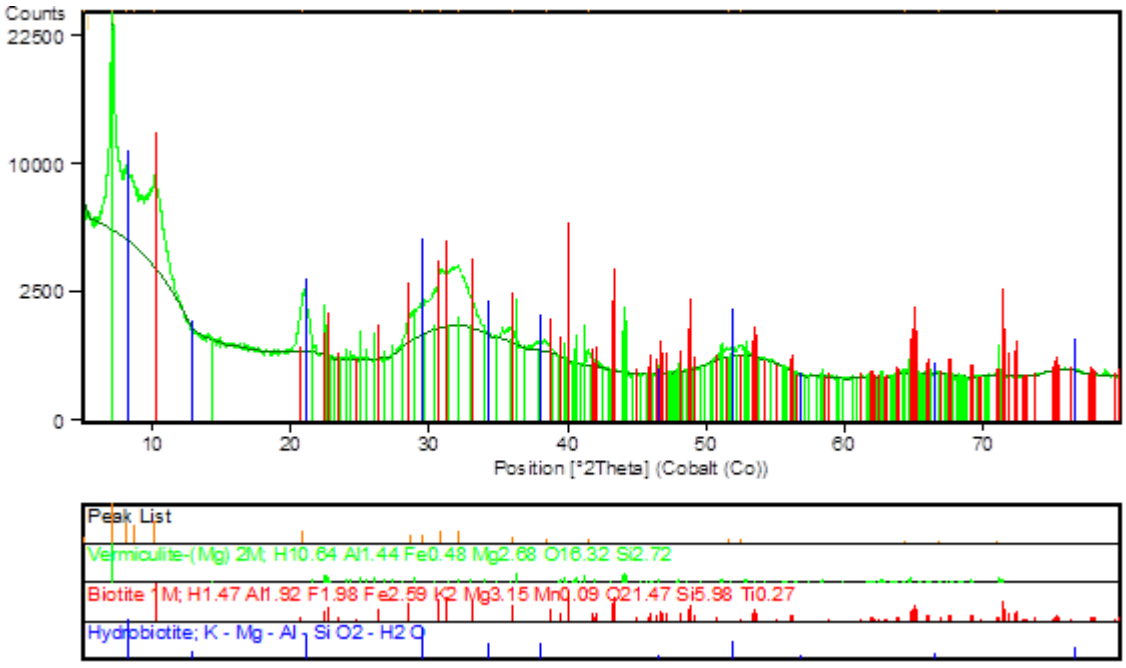

Figure II–2 XRD pattern of vermiculite (VER 1)

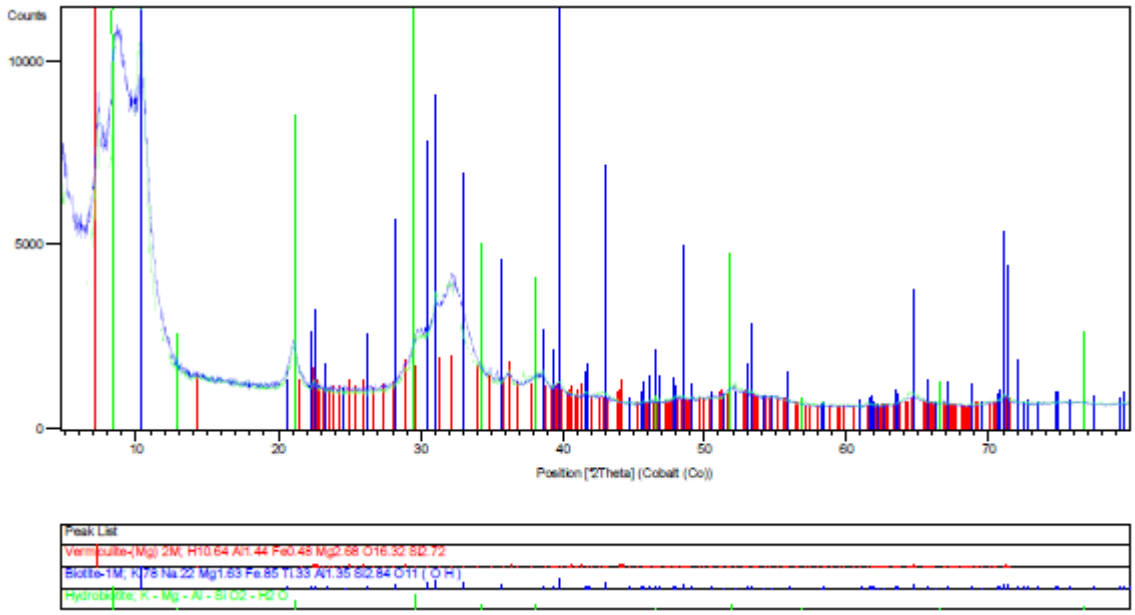

Figure II–3 XRD pattern of vermiculite (VER 1) after adsorption

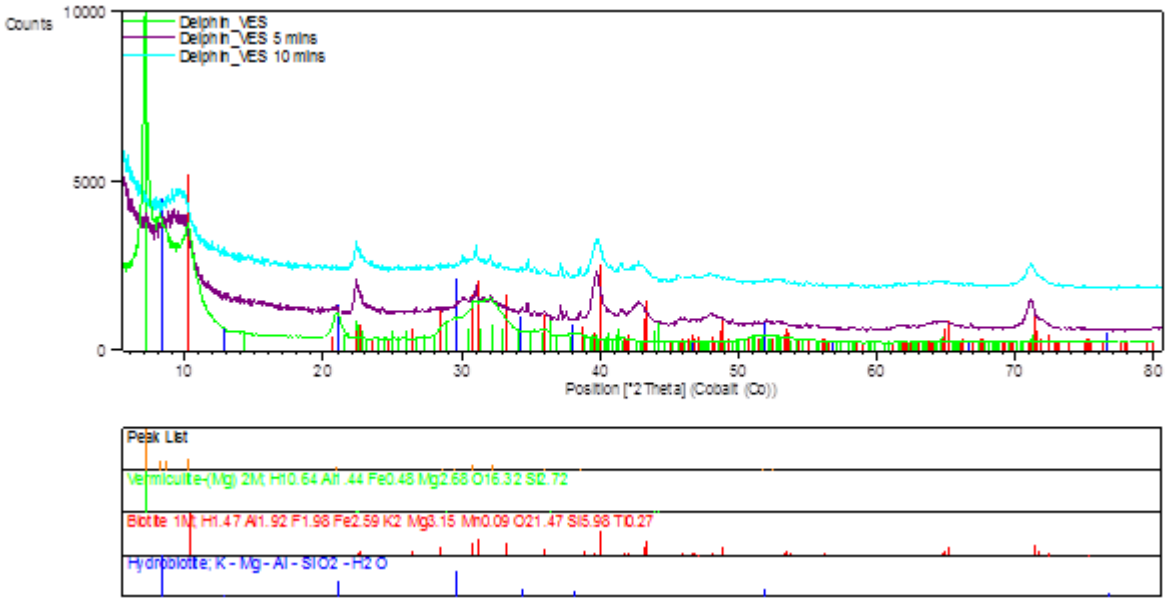

Figure II–4 XRD patterns of VER 1 at different milling times

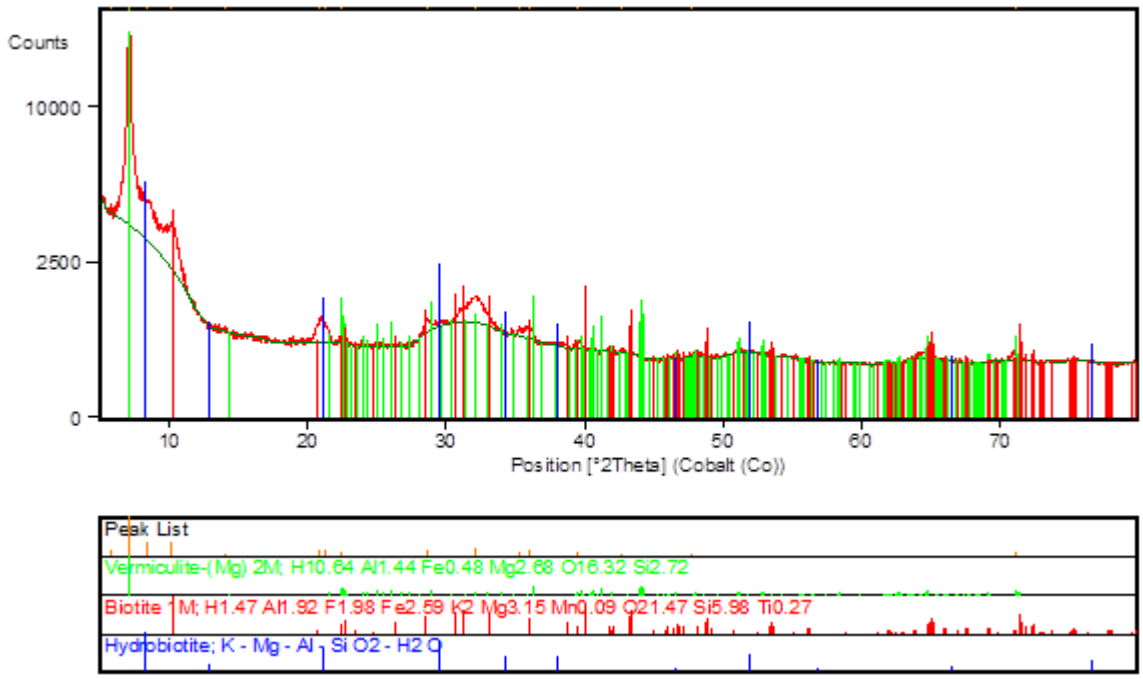

Figure II–5 XRD pattern of vermiculite (VER 2)

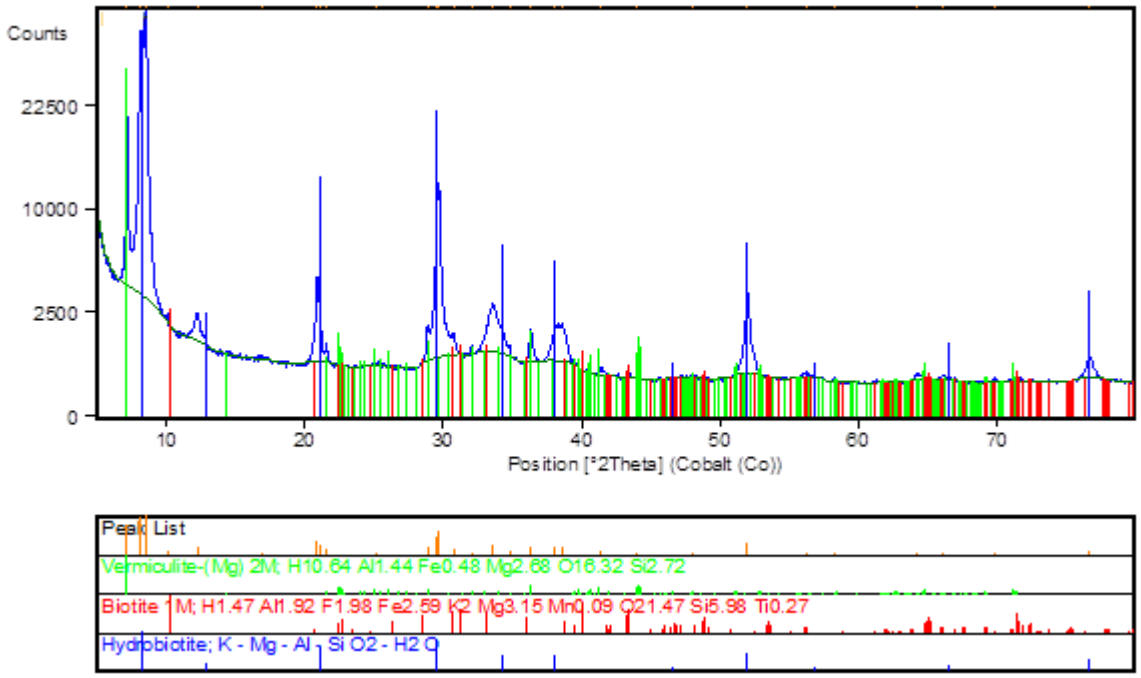

Figure II–6 XRD pattern of vermiculite (VER 3)

Appendix III Effects of operating parameters on removal efficiency

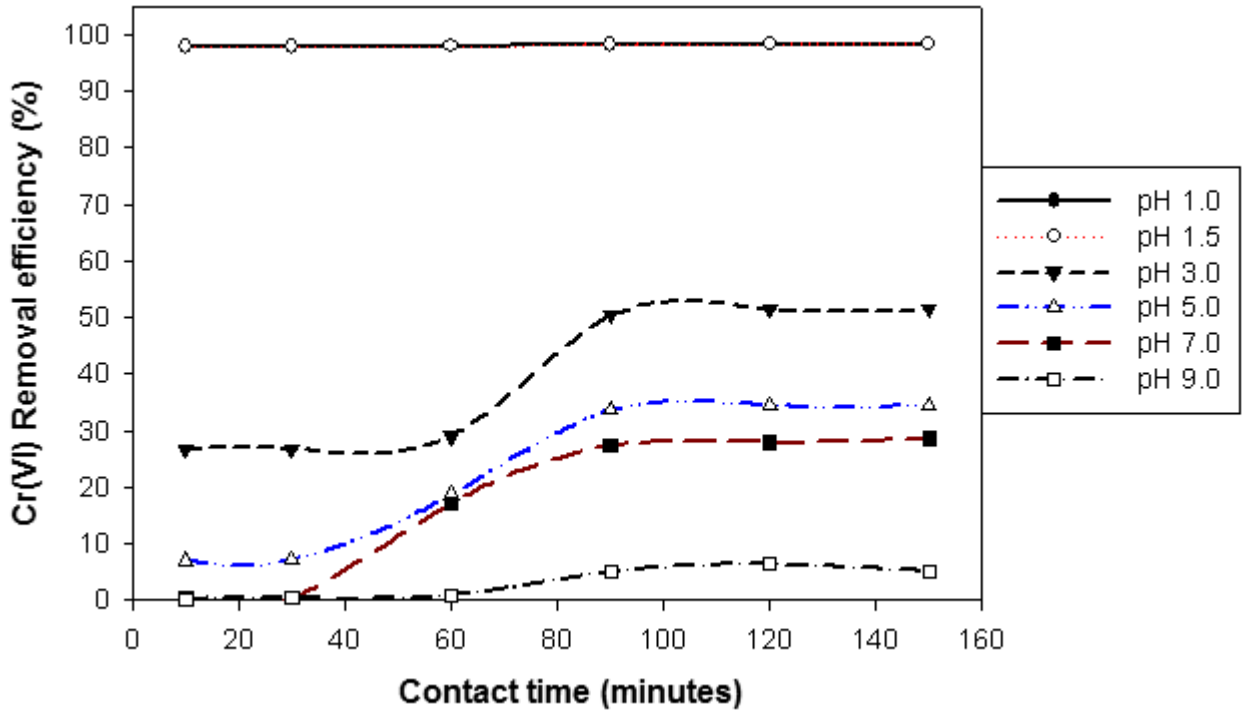

Figure III–1 Effect of pH and contact time on removal efficiency (adsorbent concentration: 2.5 $g.L^{-1}$).

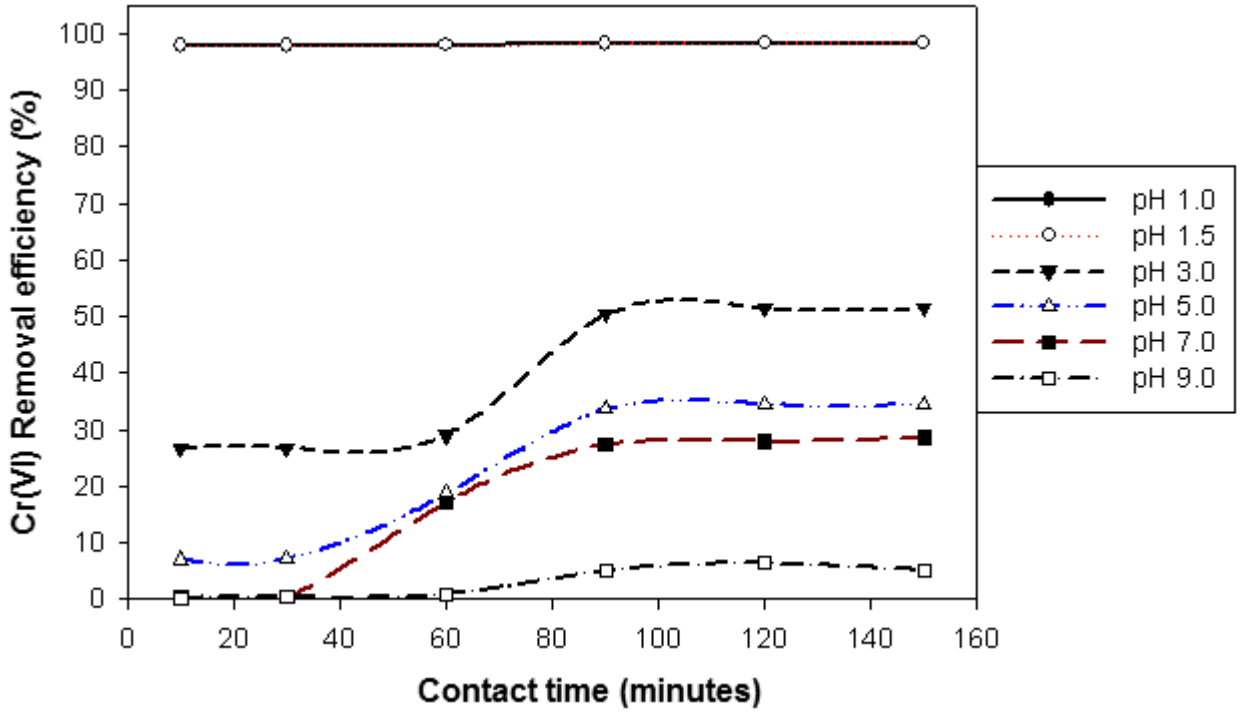

Figure III–2 Effect of pH and contact time on removal efficiency (adsorbent concentration: 5.0 $g.L^{-1}$).

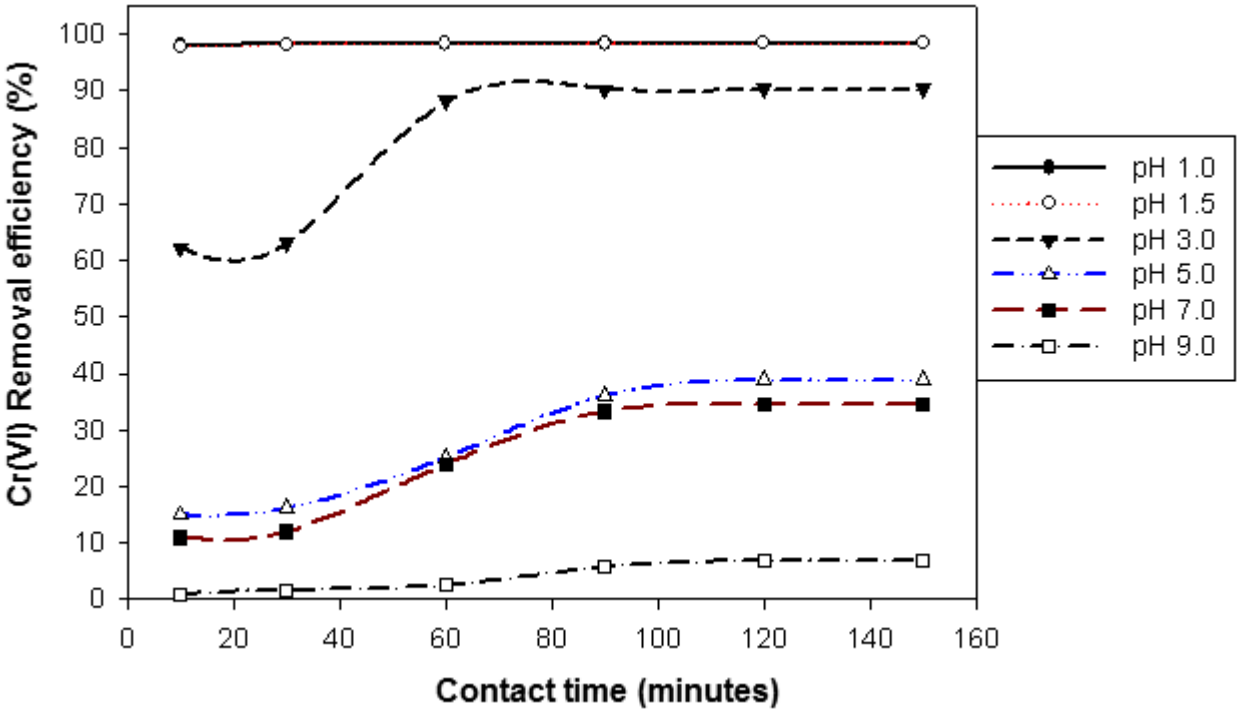

Figure III–3 Effect of pH and contact time on removal efficiency (adsorbent concentration: 7.5 $g.L^{-1}$).

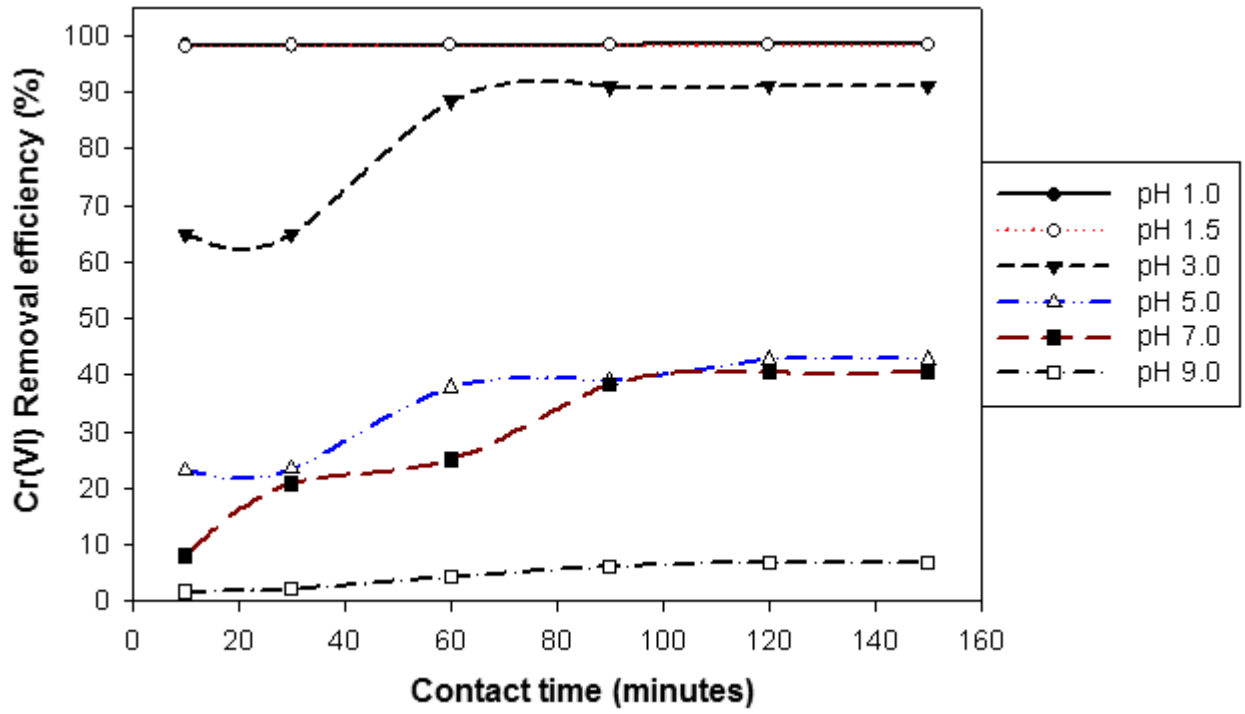

Figure III–4 Effect of pH and contact time on removal efficiency (adsorbent concentration: 10.0 $g.L^{-1}$).

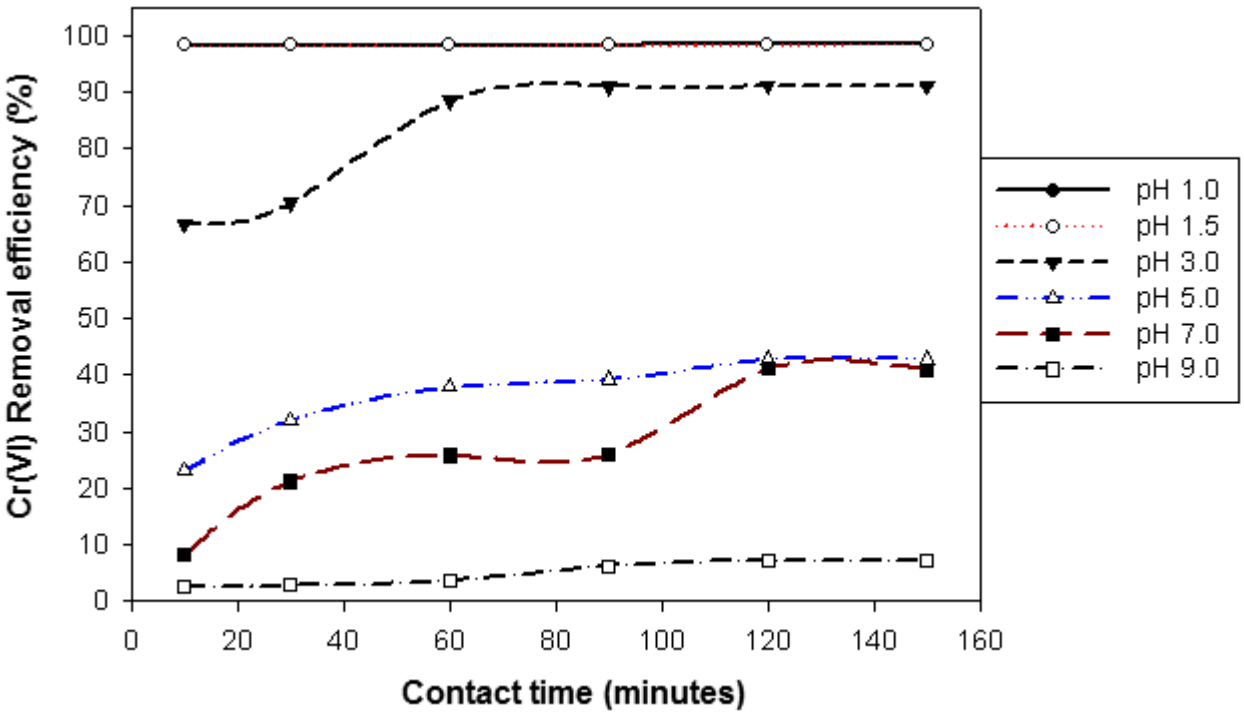

Figure III–5 Effect of pH and contact time on removal efficiency (adsorbent concentration: 12.5 $g.L^{-1}$).

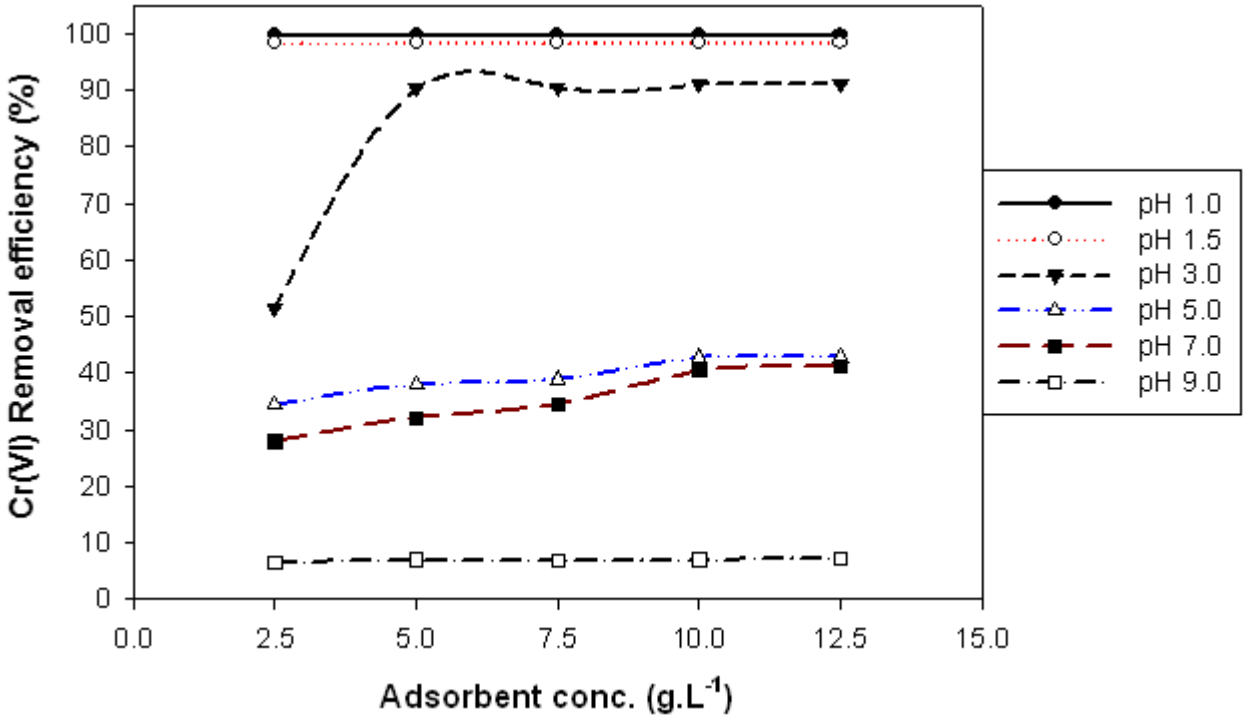

Figure III–6 Effect of adsorbent dosage on removal efficiency at different pH (contact time: 120 min).

Appendix IV Experiment Details

Table IV–1 Freundlich and Langmuir Isotherms data for Cr(VI) adsorption onto vermiculite. pH 1.5, adsorbent dosage 10 $g.L^{-1}$ and contact time 120 minutes.

Initial Cr(VI) conc. ($mg.L^{-1}$)	Equilibrium Cr(VI) conc.		Non-linear			Linear		
			Experimental	Langmuir	Freundlich	Langmuir	Freundlich	
	C_e ($mg.L^{-1}$)	Stdev	q_e ($mg.g^{-1}$)	q_e ($mg.g^{-1}$)	q_e ($mg.g^{-1}$)	C_e/q_e ($g.L^{-1}$)	ln C_e	ln q_e
10.00	1.370	0.015	8.630	4.034	8.495	0.159	0.315	2.155
20.00	7.935	0.231	12.065	12.760	12.964	0.658	2.071	2.490
30.00	14.884	0.068	15.116	16.166	15.083	0.985	2.700	2.716
40.00	22.785	0.048	17.215	18.077	16.710	1.324	3.126	2.846
50.00	31.242	0.118	18.758	19.237	18.029	1.666	3.442	2.932
60.00	40.386	0.088	19.614	20.020	19.178	2.059	3.698	2.976
70.00	49.550	0.087	20.450	20.549	20.145	2.423	3.903	3.018
80.00	59.072	0.344	20.928	20.942	21.016	2.823	4.079	3.041
90.00	68.522	0.536	21.478	21.233	21.780	3.190	4.227	3.067
100.00	78.203	0.070	21.797	21.464	22.483	3.588	4.359	3.082

Table IV–2 Kinetic data for Cr(VI) adsorption onto vermiculite. pH 1.5, adsorbent dosage 10 $g.L^{-1}$ and temperature 20°C.

Time (min)	Cr(VI) Uptake ($mg.g^{-1}$)		Pseudo-1st order		Pseudo-2nd order		Removal Effic. (%)	
	10mg/L	20mg/L	10mg/L	20mg/L	10mg/L	20mg/L	10mg/L	20mg/L
	q_t	q_t	$\ln(q_e - q_t)$	$\ln(q_e - q_t)$	t/q_t	t/q_t		
10	5.200	7.365	1.233	1.548	1.923	1.358	52.002	36.824
30	6.662	8.884	0.677	1.157	4.503	3.377	66.620	44.420
60	7.579	9.891	0.050	0.776	7.917	6.066	75.785	49.457
90	8.581	10.266	-3.024	0.587	10.488	8.767	85.815	51.328
120	8.630	12.065	–	–	13.905	9.946	86.301	60.325
150	8.818	12.089	–	–	17.010	12.408	88.182	60.444

Table IV–3 Thermodynamic data for Cr(VI) adsorption onto vermiculite. pH 1.5, adsorbent dosage 10 $g.L^{-1}$ and contact time 120 minutes.

Temp. (K)	T^{-1} (K^{-1})	q_e ($mg.g^{-1}$)	C_e ($mg.L^{-1}$)	Stdev	K_C	ΔG°(J/mol)	ln K_C	ΔH°(J/mol)	ΔS°(J/mol.K)
293	0.05	12.06	7.94	0.23	1.52	-1020.72	0.42	281.73	17.41
313	0.03	15.27	4.73	0.11	3.23	-3052.40	1.17		
333	0.02	16.58	3.42	0.03	4.85	-4374.10	1.58		
353	0.01	16.85	3.15	0.05	5.34	-4916.57	1.68		